**TECHNICAL REPORT STANDARD PAGE**

| 1. Report No. **FHWA/LA.09/449** | 2. Government Accession No. | 3. Recipient's Catalog No. |
|---|---|---|
| 4. Title and Subtitle<br>**Calibration of Resistance Factors Needed in the LRFD Design of Driven Piles** | 5. Report Date<br>**May 2009**<br>6. Performing Organization Code | |
| 7. Author(s)<br>**Murad Y. Abu-Farsakh, Sungmin Yoon, and Ching Tsai** | 8. Performing Organization Report No.<br>**449** | |
| 9. Performing Organization Name and Address<br>**Louisiana Transportation Research Center**<br>**4101 Gourrier Avenue**<br>**Baton Rouge, LA 70808** | 10. Work Unit No.<br>11. Contract or Grant No.<br>**LTRC Number: 07-2GT**<br>**State Project Number: 736-99-1408** | |
| 12. Sponsoring Agency Name and Address<br>**Louisiana Transportation Research Center**<br>**4101 Gourrier Avenue**<br>**Baton Rouge, LA 70808** | 13. Type of Report and Period Covered<br>**Final Report**<br>**November 2006–May 2009**<br>14. Sponsoring Agency Code | |

15. Supplementary Notes
**Conducted in Cooperation with the U.S. Department of Transportation, Federal Highway Administration**

16. Abstract

This research project presents the calibration of resistance factors for the Load and Resistance Factor Design (LRFD) method of driven piles driven into Louisiana soils based on reliability theory. Fifty-three square Precast-Prestressed-Concrete (PPC) piles that were tested to failure were included in this investigation. The predictions of pile resistances were based on static analysis ($\alpha$-method for clay and Nordlund method for sand), three direct CPT methods [Schmertmann method, De Ruiter and Beringen method, and Bustamante and Gianeselli (LCPC) method], and the average of the three CPT methods. Also, dynamic measurements with signal matching analysis of pile resistances using the Case Pile Wave Analysis Program (CAPWAP), which is based on the measured force and velocity signals obtained near the pile top during driving, were calibrated. The Davisson and modified Davisson interpretation methods were used to determine measured ultimate load carrying resistances from pile load tests. The predicted ultimate pile resistances obtained using the different prediction methods were compared with measured resistances determined from pile load tests. Statistical analyses were carried out to evaluate the capability of the prediction design methods to estimate measured ultimate pile resistance of driven piles. The results showed that the static method over-predicts pile resistance, while the dynamic measurement with signal matching analysis [CAPWAP-EOD (end of drive) and 14 days BOR (beginning of restrike)] under-predicts pile resistance. Among the three direct CPT methods, the De Ruiter and Beringen method was the most consistent prediction method with the lowest COV. Reliability based analyses using the First Order Second Moment (FOSM) method, the First Order Reliability Method (FORM), and the Monte Carlo (MC) simulation method were also conducted to calibrate the resistance factors ($\phi$) for the investigated pile design methods. The resistance factors with the target reliability ($\beta_T$) of 2.33 for the different design methods were determined and compared with American Association of State Highway and Transportation Officials (AASHTO) recommendation values. In addition, the evaluation of different design methods was performed.

| 17. Key Words | 18. Distribution Statement | | |
|---|---|---|---|
| **LRFD, Reliability Analysis, CPT, Static Analysis, Driven Pile capacity, Static load test.** | **Unrestricted. This document is available through the National Technical Information Service, Springfield, VA 21161.** | | |
| 19. Security Classif. (of this report)<br>**Unclassified** | 20. Security Classif. (of this page)<br>**Unclassified** | 21. No. of Pages<br>**122** | 22. Price |

# Calibration of Resistance Factors Needed in the LRFD Design of Driven Piles

by

Murad Y. Abu-Farsakh, Ph.D., P.E.
Sungmin Yoon, Ph.D., P.E.

and

Ching Tsai, Ph.D., P.E.

Louisiana Transportation Research Center
4101 Gourrier Avenue
Baton Rouge, LA 70808

LTRC Project No. 07-2GT
State Project No. 736-99-1408

conducted for

Louisiana Department of Transportation and Development
Louisiana Transportation Research Center



May 2009

# ABSTRACT

This research project presents the calibration of resistance factors for the Load and Resistance Factor Design (LRFD) method of driven piles driven into Louisiana soils based on reliability theory. Fifty-three square Precast-Prestressed-Concrete (PPC) piles that were tested to failure were included in this investigation. The predictions of pile resistances were based on static analysis ($\alpha$-method for clay and Nordlund method for sand), three direct CPT methods [Schmertmann method, De Ruiter and Beringen method, and Bustamante and Gianeselli (LCPC) method], and the average of the three CPT methods. Also, dynamic measurements with signal matching analysis of pile resistances using the Case Pile Wave Analysis Program (CAPWAP), which is based on the measured force and velocity signals obtained near the pile top during driving, were calibrated. The Davisson and modified Davisson interpretation methods were used to determine measured ultimate load carrying resistances from pile load tests. The predicted ultimate pile resistances obtained using the different prediction methods were compared with measured resistances determined from pile load tests. Statistical analyses were carried out to evaluate the capability of the prediction design methods to estimate measured ultimate pile resistance of driven piles. The results showed that the static method over-predicts pile resistance, while the dynamic measurement with signal matching analysis [CAPWAP-EOD (end of drive) and 14 days BOR (beginning of restrike)] under-predicts pile resistance. Among the three direct CPT methods, the De Ruiter and Beringen method was the most consistent prediction method with the lowest COV. Reliability based analyses using the First Order Second Moment (FOSM) method, the First Order Reliability Method (FORM), and the Monte Carlo (MC) simulation method were also conducted to calibrate the resistance factors ($\phi$) for the investigated pile design methods. The resistance factors with the target reliability ($\beta_T$) of 2.33 for the different design methods were determined and compared with American Association of State Highway and Transportation Officials **(**AASHTO) recommendation values. In addition, the evaluation of different design methods was performed.

# ACKNOWLEDGMENTS

This research project was funded by the Louisiana Department of Transportation and Development (LADOTD) and the Louisiana Transportation Research Center (LTRC). The comments and suggestions of Mark Morvant, P.E. and Zhongjie Zhang, P.E., Ph.D. of LTRC are gratefully acknowledged.

# IMPLEMENTATION STATEMENT

The Federal Highway Administration and AASHTO set a transition date of October 1, 2007 after which all new federal-funded bridges shall be designed using the LRFD design method. The LRFD Code is the first attempt by AASHTO to establish a National Bridge Code addressing geotechnical design for bridges. This fact calls for the establishment of a local calibration that takes into account the geology of Louisiana. This research project aims at calibrating resistance factors associated with different pile design methods used by engineers designing bridges for LADOTD. Reliability indexes and corresponding resistance factors for different pile design methods are recommended and ready for immediate implementation. Engineers designing bridges for Louisiana should use the recommended resistance factors in lieu of factors shown in Section 10 of the LRFD Code. As experience is gained in the application of LRFD to design, the role of past successful allowable stress design (ASD) practices will become less important, and the advantage of the LRFD design can be fully addressed by achieving consistent levels of reliability in the design of both superstructures and foundations. In addition, calibration efforts in this research are documented so that the calibration results become a heritage for future users of LADOTD and thereby enhance future LRFD research and development. One project will be selected to perform a cost/benefit analysis by comparing the design results obtained by using the related indexes and resistance factors obtained in this research and those recommended by the AASHTO LRFD Bridge Design Specifications (2007) and ASD Design.

# TABLE OF CONTENTS

ABSTRACT ..... iii
ACKNOWLEDGMENTS ..... v
IMPLEMENTATION STATEMENT ..... vii
TABLE OF CONTENTS ..... ix
LIST OF TABLES ..... ix
LIST OF FIGURES ..... xiiii
INTRODUCTION ..... 1
OBJECTIVE ..... 3
SCOPE ..... 5
BACKGROUND ..... 7
Predication of Ultimate Pile Resistance ..... 7
Static Methods ..... 7
Direct CPT Methods ..... 13
Dynamic Measurement with Signal Matching Analysis (CAPWAP) ..... 18
LRFD Calibration Using Reliability Theory ..... 19
LRFD Calibration via WSD ..... 21
Statistical Characterization of the Data Collected ..... 22
First Order Second Moment (FOSM) Method ..... 23
First Order Reliability Method (FORM) ..... 24
Monte Carlo Simulation Method ..... 27
METHODOLOGY ..... 29
Collecting of Pile Load Test Database ..... 29
Compilation of Pile Load Test Reports ..... 30
Ultimate Capacity of Piles from Load Test ..... 31
Soil Identification and Classification ..... 32
DISCUSSION OF RESULTS ..... 35
Predicted versus Measured Ultimate Pile Resistances ..... 35
LRFD Calibration ..... 55
CONCLUSIONS ..... 69
RECOMMENDATIONS ..... 71
ACRONYMS, ABBREVIATIONS, AND SYMBOLS ..... 73
REFERENCES ..... 75
APPENDIX ..... 79
Summary of Geotechnical Data for the State Projects Investigated ..... 79

# LIST OF TABLES

Table 1 $K_\delta$ for non-tapered piles *[19]* ..... 11
Table 2 Friction coefficient, $k_s$ (from Bustamante and Gianeselli, *[16]*) ..... 16
Table 3 Summary of the characteristics of the investigated piles..... 31
Table 4 Results of the analysis conducted on square precast prestressed concrete piles driven into Louisiana soils..... 37-50
Table 5 Evaluation summary of the different prediction methods ..... 51
Table 6 Resistance Factors ($\phi$) for Driven Piles ($\beta_T = 2.33$)..... 67

# LIST OF FIGURES


Figure 1 $\alpha$ factors for driven piles in clay *[19]* ..... 9
Figure 2 Chart for bearing capacity factor N'q *[19]* ..... 10
Figure 3 Correction factors ($C_f$) for coefficient of lateral stress ($K_\delta$) *[19]* ..... 12
Figure 4 Average cone tip resistance ($q_{c,avg}$) in Schmertmann *[14]* method ..... 15
Figure 5 General features of Louisiana Pile Design by Cone Penetration Test (LPD-CPT) program (www.ltrc.lsu.edu/downloads.html) ..... 17
Figure 6 Probability density functions for load effect and resistance ..... 20
Figure 7 Approximate locations of the investigated piles ..... 30
Figure 8 Estimation of ultimate bearing resistance using Davisson *[39]* method after Salgado *[41]* ..... 32
Figure 9 Typical summary of geotechnical data for a tested pile ..... 33
Figure 10 $R_m$ versus $R_p$ (Static method) ..... 51
Figure 11 $R_m$ versus $R_p$ (Schmertmann method) ..... 52
Figure 12 $R_m$ versus $R_p$ (LCPC method) ..... 52
Figure 13 $R_m$ versus $R_p$ (De Ruiter method) ..... 53
Figure 14 $R_m$ versus $R_p$ (CPT - Average method) ..... 53
Figure 15 $R_m$ versus $R_p$ (CAPWAP-EOD) ..... 54
Figure 16 $R_m$ versus $R_p$ (CAPWAP-14 days BOR) ..... 54
Figure 17 Histogram and PDF of resistance bias factors (Static method) ..... 56
Figure 18 Histogram and PDF of resistance bias factors (Schmertmann method) ..... 57
Figure 19 Histogram and PDF of resistance bias factors (LCPC method) ..... 57
Figure 20 Histogram and PDF of resistance bias factors (De Ruiter method) ..... 58
Figure 21 Histogram and PDF of resistance bias factors (CPT - Average method) ..... 58
Figure 22 Histogram and PDF of resistance bias factors (CAPWAP-EOD) ..... 59
Figure 23 Histogram and PDF of resistance bias factors (CAPWAP-14 days BOR) ..... 59
Figure 24 Cumulative distribution function (CDF) of bias values (Static method) ..... 60
Figure 25 Cumulative distribution function (CDF) of bias values (Schmertmann method) ..... 60
Figure 26 Cumulative distribution function (CDF) of bias values (LCPC method) ..... 61
Figure 27 Cumulative distribution function (CDF) of bias values (De Ruiter method) ..... 61
Figure 28 Cumulative distribution function (CDF) of bias values (CPT-Average method) 62
Figure 29 Cumulative distribution function (CDF) of bias values (CAPWAP-EOD) ..... 62
Figure 30 Cumulative distribution function (CDF) of bias values (CAPWAP-14 days BOR). 63
Figure 31 Resistance factors for different reliability indexes (Static method) ..... 63
Figure 32 Resistance factors for different reliability indexes (Schmertmann method) ..... 64

Figure 33 Figure 26 Resistance factors for different reliability indexes (LCPC method) ..... 64
Figure 34 Resistance factors for different reliability indexes (De Ruiter method) ..... 65
Figure 35 Resistance factors for different reliability indexes (CPT - Average method)..... 65
Figure 36 Resistance factors for different reliability indexes (CAPWAP-EOD)..... 66
Figure 37 Resistance factors for different reliability indexes (CAPWAP-14 days BOR)..... 66

# INTRODUCTION

The allowable stress design (ASD) method had been used in the design of bridges, which involves applying a factor of safety (FS). FS, defined as the fraction of the ultimate geotechnical pile resistance, that is traditionally known as pile capacity, over the allowable design load, accounts for uncertainties in the applied loads and soil resistance. The magnitude of FS has been empirically developed over time depending on the importance of the structure, the confidence levels of material properties, and the design methodology. However this approach suffers from the disadvantage that the uncertainties of the different sources of load and resistance are combined together in a single factor. Consequently, ASD may lead to a design with a different level of safety for similar structures. The LRFD method aims at separating uncertainties of load effect from uncertainties of resistance and then applying statistical theory to ensure the same level of structure safety.

The Bridge Design Specifications published by the American Association of Highway and Transportation Officials (AASHTO) has introduced the LRFD method to account for uncertainties associated with estimated loads and resistances *[1], [2]*. Since then, bridge superstructures have been designed using the LRFD method in most U.S. states. However, the LRFD method for design of bridge foundation is progressively gaining its prevalence; while the ASD method is still used for the bridge foundation design in practice. This can lead to inconsistent levels of reliability between superstructures and substructures. In an effort to maintain a consistent level of reliability, the Federal Highway Administration (FHWA) and AASHTO a mandated a date of October 1, 2007 after which all federal-funded new bridges including substructures shall be designed using the LRFD method. Accordingly, significant research efforts have been directed to implement the LRFD design methodology in bridge substructure and establish and to calibrate the proper resistance factors, which will be explained in greater detail in a later section, for local soil conditions in compliance with this mandate *[3], [4], [5], [6], [7], [8], [9], [10]*.

The current AASHTO design specification recommends resistance factors, $\phi$, for single driven piles in axial compression ranging from 0.10 to 0.65, depending on the design method *[11]*. However, the existing resistance factors are recommended based on a pile load test—a soil database that was collected from sites that do not necessary reflect Louisiana soils or design practice. For example, the driven pile database used in the existing AASHTO design specification is based on the data gathered by Florida DOT and FHWA *[12], [13]*. Therefore, the resistance factors recommended by the existing AASHTO Code need to be verified before being applied to local soil condition and design practice. Direct application of the

AASHTO resistance factors without calibration may result in over-conservative or unsafe design. When local experience and databases are available, the AASHTO recommends calibrating the resistance factor, $\phi$, using reliability analyses to produce an overall reliability level that is consistent with local practice.

Several methods have been developed and used in geotechnical engineering practice to estimate ultimate axial bearing resistance of driven piles. This includes static pile load tests, statnamic pile load tests, traditional static analysis, dynamic analysis, and static analysis using the results of in-situ testing such as the Cone Penetration Test (CPT). Static analyses based on soil properties obtained from borings and laboratory tests have been the main method used in practice by LADOTD engineers. However, the application of CPT in predicting ultimate bearing resistance of piles has increased over the last two decades due to the similarity between the cone penetrometer and the pile in which the cone can be considered as a model pile (e.g., *[14], [15], [16],* and *[17]*). The CPT is a simple, fast, repeatable, and cost effective in-situ test that can provide continuous subsurface soundings with depth. The measured CPT data (tip resistance, $q_c$; sleeve friction, $f_s$; and porewater pressure, u) can be effectively utilized for many geotechnical engineering applications including the prediction of ultimate pile resistance. Compared with traditional static design, CPT design methods can provide more economical estimations of the ultimate pile resistance. In addition, the dynamic measurement with signal matching analysis using CAPWAP is also gaining popularity due to its simplicity and economical advantage. Although the dynamic measurement with signal matching analysis cannot be a substitute of pile design analysis, it is mainly used for pile drivability and usually helps in verifying the pile design resistance.

In this research project, design methods used by LADOTD were calibrated based on data collected in Louisiana. For each design method, target reliability values and corresponding resistance factors were developed depending on availability of test data.

# OBJECTIVE

The objective of this research project is to calibrate resistance factors for different pile design methods needed in LRFD design of driven piles based on the Louisiana pile load test soil database, and LADOTD experience. The findings of this research effort will help Louisiana geotechnical engineers begin implementing the LRFD design methodology for the design of all driven piles in future Louisiana projects as mandated by AASHTO.

# SCOPE

To achieve the objective of this study, reliability based analyses were performed on different design methods used by LADOTD for the estimation of axial load resistance of driven piles in soft Louisiana soils. A database of 53 precast-prestressed-concrete (PPC) piles of different lengths and sizes that were loaded to failure were investigated in this study. Statistical analyses were conducted to evaluate different pile design methods, including the static design method ($\alpha$-method and Nordlund method), three different direct CPT design methods: [Schmertmann method, De Ruiter and Beringen method, and Bustamante and Gianeselli (LCPC) method], CAPWAP method. The target reliability ($\beta_T$) of 2.33 was selected. In addition, reliability analyses based on the FOSM, FORM, and MC simulation method were conducted to calibrate resistance factors ($\phi$) for different design methods needed in the LRFD design of single piles.

# BACKGROUND

## Predication of Ultimate Pile Resistance

The ultimate axial resistance ($Q_u$) of a driven pile consists of the end bearing resistance ($Q_b$) and the skin frictional resistance ($Q_s$). The ultimate pile resistance can be calculated using the following equation:

$$Q_u = Q_b + Q_s = q_b . A_b + \sum_{i=1}^{n} f_i A_{si} \quad (1)$$

where, $q_b$ is the unit tip bearing resistance, $A_b$ is the cross section area of the pile tip, $f_i$ is the average unit skin friction of the soil layer i, $A_{si}$ is the area of the pile shaft area interfacing with layer i, and n is the number of soil layers along the pile shaft. In clayey stratigraphies, the shaft frictional resistance dominates in many cases, while in sandy stratigraphies, the end bearing resistance can contribute to more than 50 percent of the ultimate pile resistance. Since Louisiana soils are mainly clay and silty clay deposits, the side friction ($Q_s$) is dominant in the total ultimate bearing resistance ($Q_u$) compared to the end bearing resistance ($Q_b$).

### Static Methods

**α–Tomlinson Method.** The α–method is based on total stress analysis. For a soil with an angle of internal friction, $\phi = 0$, or in total stress analysis, the ultimate skin resistance per unit area of the pile can be calculated as follows *[18]*:

$$f = \alpha S_u \quad (2)$$

where, α is an empirical adhesion coefficient, and $S_u$ is the undrained shear strength. In this research study, α values suggested by Tomlinson are used *[18]*. Figure 1 shows the α values versus the undrained shear strength ($S_u$).

The skin friction resistance ($Q_s$) is as follows:

$$Q_s = \int_0^L f \, C_d \, dz \quad (3)$$

where, L is length of the pile in contact with soil, and $C_d$ is the effective perimeter of the pile.

The pile tip resistance ($Q_b$) is calculated as follows:

$$Q_b = A_b \, S_u \, N_c \tag{4}$$

where, $A_b$ is the cross sectional area of the pile, and $N_c$ of 9 is used in this study as recommended by FHWA *[19]*.

**Nordlund Method.** In sand, the pile tip resistance ($Q_b$) can be calculated as:

$$Q_b = A_b . \bar{q} . \alpha . N_q^{'} \tag{5}$$

where, $\bar{q}$ is the effective vertical stress at tip level, $\alpha$ is a dimensionless correction factor, and $N'_q$ is a bearing resistance factor varying with $\phi$. In this research, the values proposed by Thurman are used for calculation *[20]*. Figure 2 presents the bearing resistance factor ($N'_q$) versus the friction angle ($\phi$).

The skin friction resistance ($Q_s$) was evaluated using the equation proposed by Nordlund in this research as follows *[21], [22]*:

$$Q_s = \int_0^L K_\delta \; C_f \overline{P}_D \sin(\delta) . C_d \, dz \tag{6}$$

where, $K_\delta$ is a coefficient of lateral stress, $C_f$ is a correction factor, $\overline{P}_D$ is the effective overburden pressure, $\delta$ is the pile-soil friction angle, and $C_d$ is the effective pile perimeter. Table 1 and Figure 3 present the coefficient of lateral stress ($K_\delta$) and the correction factor ($C_f$), respectively.

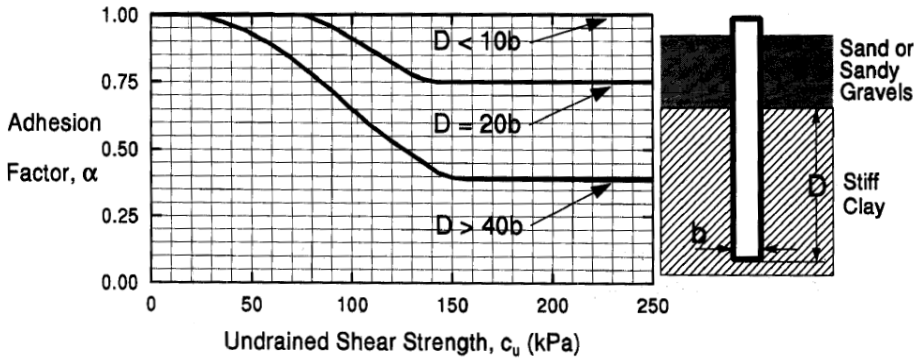


**(a) Sand layer over stiff clay layer**

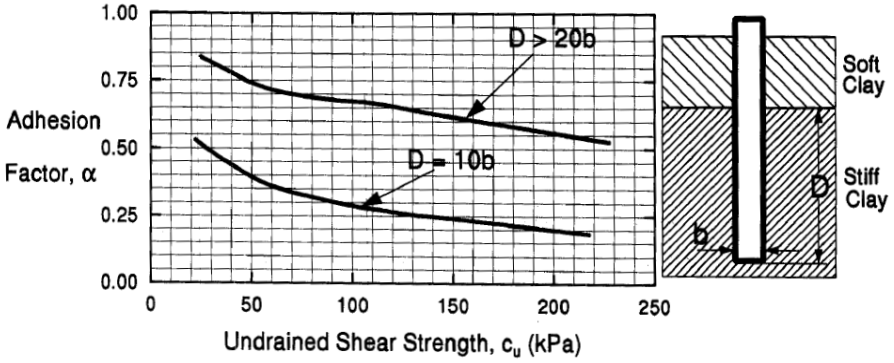


**(b) Soft clay layer over stiff clay layer**

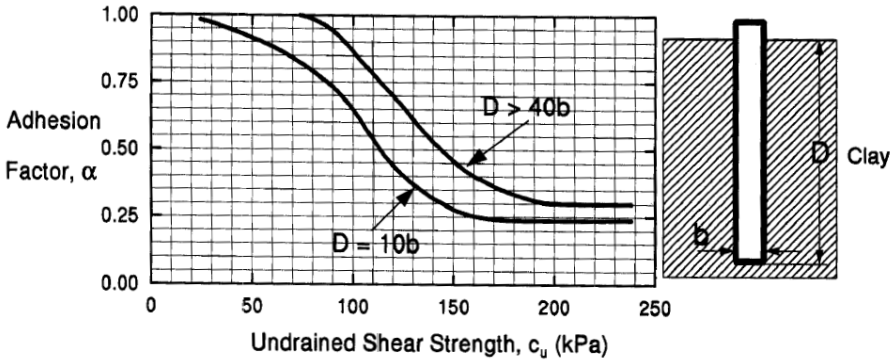


**(c) Clay layer only**

**Figure 1**
**α factors for driven piles in clay *[19]***

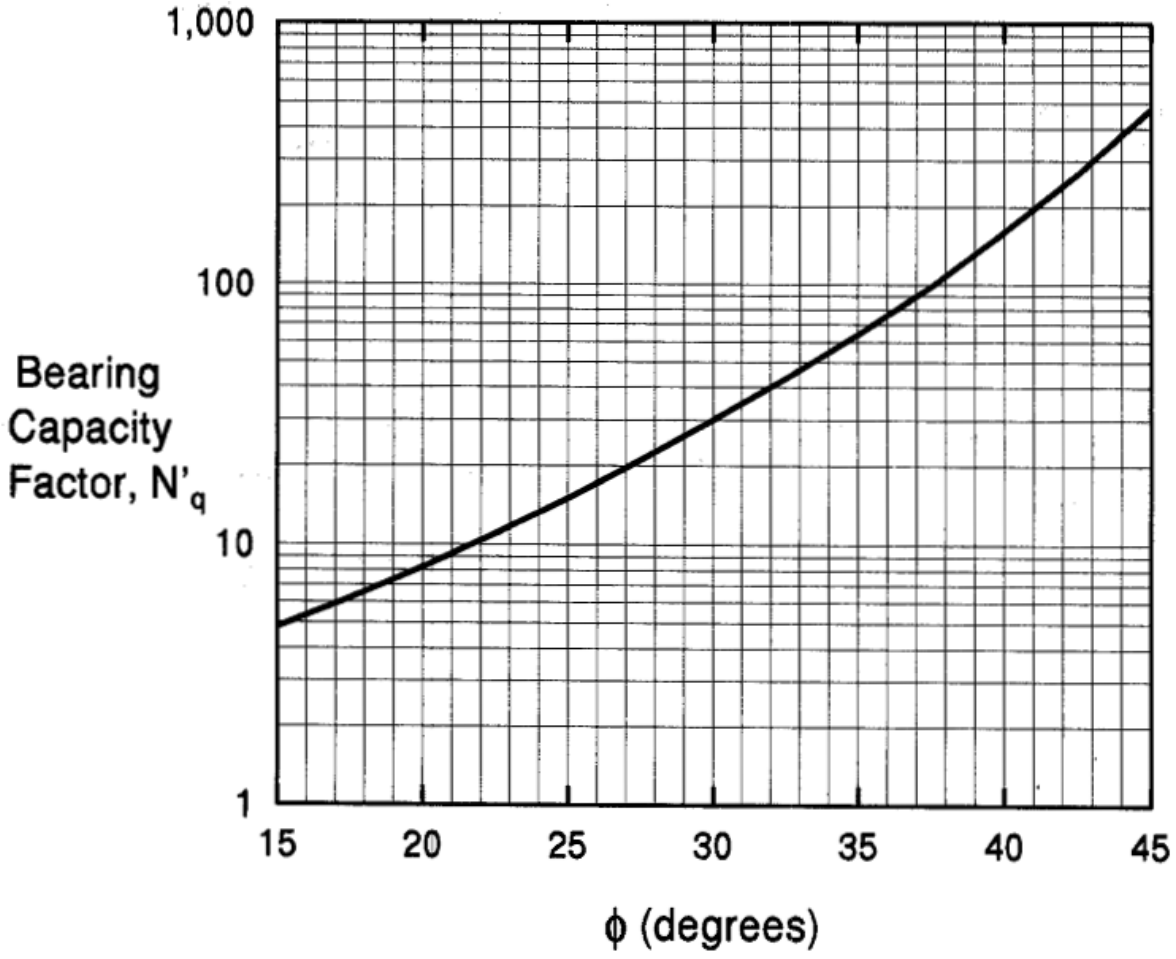


**Figure 2**
**Chart for bearing capacity factor N'q** ***[19]***

**Table 1**
**$K_\delta$ for non-tapered piles *[19]***

| $\phi$ | Volume of soil displaced per unit length ($ft^3/ft$) | | | | | | | | |
|---|---|---|---|---|---|---|---|---|---|
| | **0.1** | **0.3** | **0.5** | **0.7** | **1.0** | **3.0** | **5.0** | **7.0** | **10.0** |
| 25 | 0.70 | 0.77 | 0.80 | 0.83 | 0.85 | 0.92 | 0.95 | 0.98 | 1.00 |
| 26 | 0.73 | 0.82 | 0.86 | 0.88 | 0.91 | 1.00 | 1.04 | 1.06 | 1.09 |
| 27 | 0.76 | 0.86 | 0.91 | 0.94 | 0.97 | 1.07 | 1.12 | 1.15 | 1.18 |
| 28 | 0.79 | 0.90 | 0.96 | 0.99 | 1.03 | 1.14 | 1.2 | 1.23 | 1.27 |
| 29 | 0.82 | 0.95 | 1.01 | 1.05 | 1.09 | 1.22 | 1.28 | 1.32 | 1.36 |
| 30 | 0.85 | 0.99 | 1.06 | 1.10 | 1.15 | 1.29 | 1.36 | 1.40 | 1.45 |
| 31 | 0.91 | 1.08 | 1.16 | 1.21 | 1.27 | 1.44 | 1.52 | 1.57 | 1.63 |
| 32 | 0.97 | 1.17 | 1.26 | 1.32 | 1.39 | 1.59 | 1.68 | 1.74 | 1.81 |
| 33 | 1.03 | 1.26 | 1.37 | 1.44 | 1.51 | 1.74 | 1.85 | 1.92 | 1.99 |
| 34 | 1.09 | 1.35 | 1.47 | 1.55 | 1.63 | 1.89 | 2.01 | 2.09 | 2.17 |
| 35 | 1.15 | 1.44 | 1.57 | 1.66 | 1.75 | 2.04 | 2.17 | 2.26 | 2.35 |
| 36 | 1.26 | 1.61 | 1.78 | 1.89 | 2.00 | 2.35 | 2.52 | 2.63 | 2.74 |
| 37 | 1.37 | 1.79 | 1.99 | 2.11 | 2.25 | 2.67 | 2.87 | 2.99 | 3.13 |
| 38 | 1.48 | 1.97 | 2.19 | 2.34 | 2.50 | 2.99 | 3.21 | 3.36 | 3.52 |
| 39 | 1.59 | 2.14 | 2.40 | 2.57 | 2.75 | 3.30 | 3.56 | 3.73 | 3.91 |
| 40 | 1.70 | 2.32 | 2.61 | 2.80 | 3.00 | 3.62 | 3.91 | 4.10 | 4.30 |

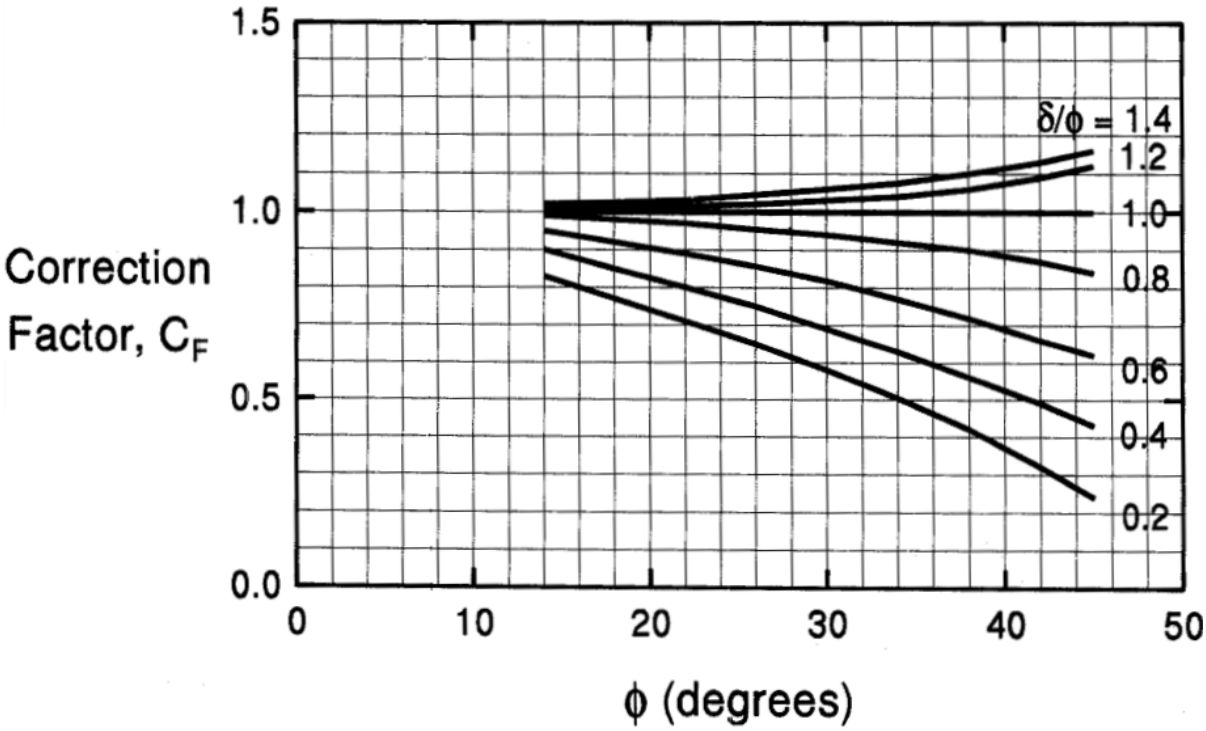


**Figure 3**
**Correction factors ($C_f$) for coefficient of lateral stress ($K_\delta$)** ***[19]***

## Direct CPT Methods

There are two main approaches in the estimation of pile resistance using CPT data, the indirect method and the direct method. In the indirect method, CPT data ($q_c$ and $f_s$) is used to estimate the soil strength parameters, such as the undrained shear strength ($S_u$) and the angle of internal friction ($\phi$), to predict pile resistance. While in the direct method, the unit end bearing resistance ($q_b$) of the pile is evaluated from the $q_c$, and the unit skin friction (f) of the pile is evaluated from either $f_s$ or $q_c$ profiles. It is believed that the direct method is more suitable in engineering practices *[17]*.

In the direct CPT methods, the pile resistance is predicted using a pile tip resistance ($Q_b$) and the skin friction resistance ($Q_s$), which can be expressed as the following equations:

$$Q_b = q_b A_b = (c_b . q_{c,avg}) . A_b \tag{7}$$

$$Q_s = \sum f_i . A_{si} = \sum \alpha_c f_{si} A_{si} \tag{8}$$

or

$$Q_s = \sum f_i . A_{si} = \sum (c_s . q_{ci}) . A_{si} \tag{9}$$

where $q_b$ is the unit end bearing resistance, $q_c$ is the cone tip resistance, $q_{c,avg}$ is the average cone tip resistance in the zone above and below the pile tip, $f_i$ is the unit skin friction, $f_{si}$ is the sleeve friction, $c_b$ is the correlation coefficient of tip resistance, $\alpha_c$ is the reduction factor, $c_s$ is the correlation coefficient of friction resistance, $A_b$ is the pile tip area, and $A_{si}$ is the pile surface area of each layer.

**Schmertmann Method.** Schmertmann proposed a direct CPT method based on model and full scale pile tests *[14]*. To estimate the pile tip resistance ($Q_b$), the average cone tip resistance ($q_{c,avg}$) is obtained in the zone ranging from 8D above to 0.7D-4D below the pile tip (see Figure 4). Schmertmann suggested a $c_b$ of 1.0 for sand and 0.6 for clay. The unit skin friction is calculated from the sleeve friction ($f_s$) using an $\alpha_c$ value of 0.2 to 1.25 for clayey soil. A maximum $f_s$ of 1.25 tsf is proposed.

**De Ruiter and Beringen Method.** The De Ruiter and Beringen method is known as the European method *[15]*. It is based on experience from offshore piles tested in the North Sea. In sand, unit tip resistance ($q_b$) is obtained similarly to the Schmertmann method *[14]*. The unit skin friction (f) for the compression piles is the minimum among $f_s$, $q_{c(side)}/300$, and 0.2 tsf. In clay, the unit tip resistance ($q_b$) is determined from the conventional bearing resistance theory as follows:

$$q_b = N_c S_u(\text{tip}) \tag{10}$$

$$S_u(\text{tip}) = \frac{q_c(\text{tip})}{N_k} \tag{11}$$

where, $N_c$ is the bearing resistance factor, and $N_k$ is the cone factor ranging from 15 to 20 depending on soil type and pile type. The unit skin friction (f) can be obtained from:

$$f = \beta\, S_u(\text{side}) \tag{12}$$

where $\beta$ is the adhesion factor and $\beta$ =1 for normally consolidated (NC) clay and 0.5 for overconsolidated (OC) clay.

**Bustamante and Gianeselli Method (LCPC Method).** Bustamante and Gianeselli method is known as the French method or the LCPC (Laboratoire Central des Ponts et Chaussees) method *[16]*. In this method, both unit tip resistance ($q_b$) and unit skin friction (f) are calculated from cone tip resistance ($q_c$). Average cone tip resistance ($q_{c,avg}$) is obtained in the zone ranging 1.5 D above and below the pile tip. A correlation coefficient of the tip resistance ($c_b$) from 0.15 to 0.6 was proposed for different soil types and installation procedures based on the empirical correlation ($c_b$ = 0.6 for piles driven into clay and silt and $c_b$ = 0.375 for piles driven into sand and gravel).

The unit skin friction (f) is obtained from cone tip resistance ($q_c$) and the correlation coefficient of friction resistance ($k_s$) as follows:

$$f = \frac{q_{eq}(\text{side})}{k_s} \tag{13}$$

where, $q_{eq}$(side) is the equivalent cone tip resistance of the soil layer, and $k_s$ is an empirical friction coefficient that varies from 30 to 150 depending on soil type, pile type, and installation procedure given in Table 2.

In this study, ultimate pile resistance was calculated using the Louisiana Pile Design by Cone Penetration Test (LPD-CPT) program developed by Louisiana Transportation Research Center. The program is capable of soil classification based on the probabilistic region estimation method proposed by Zhang and Tumay and provides the profile of the ultimate pile resistances with soil depth *[24]*. The ultimate pile resistances are predicted using the Schmertmann Method, De Ruiter and Beringen Method, LCPC Method, and the average of three CPT methods *[14], [15]*, *[16]*. Figure 5 presents the general features of the LPD-CPT program. The program is available for free downloading at the LTRC Web site (www.ltrc.lsu.edu/downloads.html).

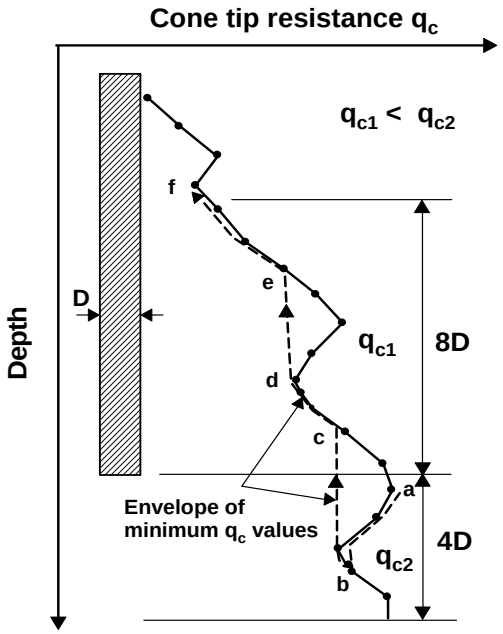


**Figure 4**
**Average cone tip resistance ($q_{c,avg}$) in Schmertmann *[14]* method**
**(from Abu-Farsakh and Titi *[23]*)**

**Table 2**
**Friction coefficient, $k_s$ (from Bustamante and Gianeselli, *[16]*)**

| Nature of Soil | $q_c$ (MPa) | $k_s$ |
|---|---|---|
| Soft clay and mud | < 1 | 30 |
| Soft chalk | ≤ 5 | 100 |
| Silt and loose sand | ≤ 5 | 60 |
| Moderately compact clay | 1 to 5 | 40 |
| Moderately compact sand and gravel | 5 to 12 | 100 |
| Compact to stiff clay and compact silt | > 5 | 60 |
| Weathered to fragment chalk | > 5 | 60 |
| Compact to very compact sand and gravel | > 12 | 150 |

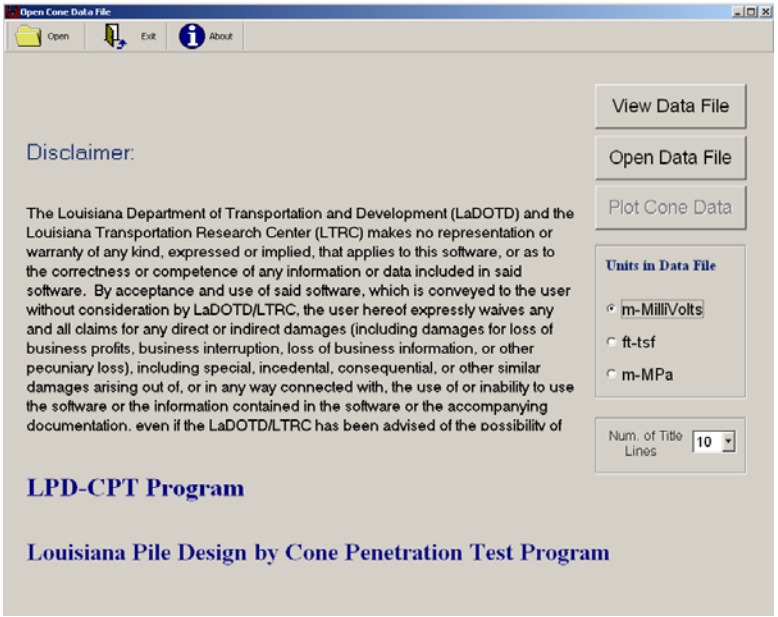


**(a) Data input screen**

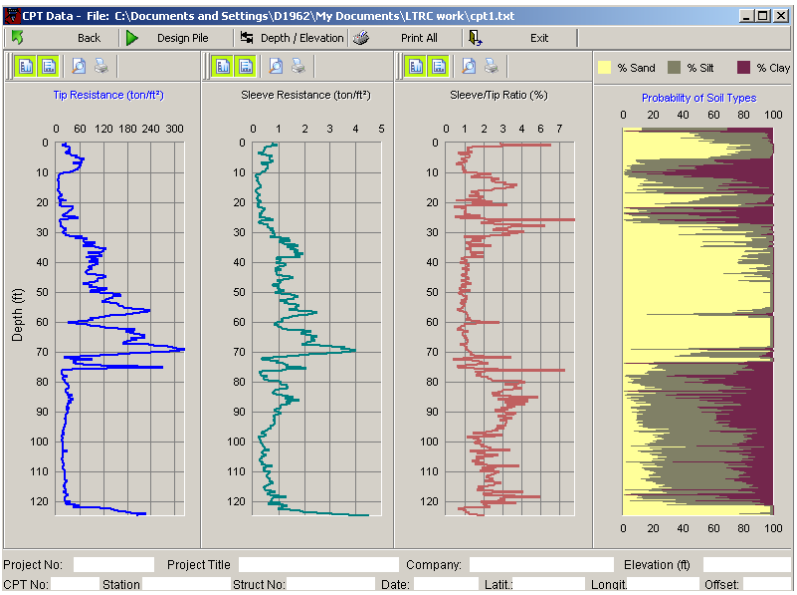


**(b) CPT profiles and soil classification**

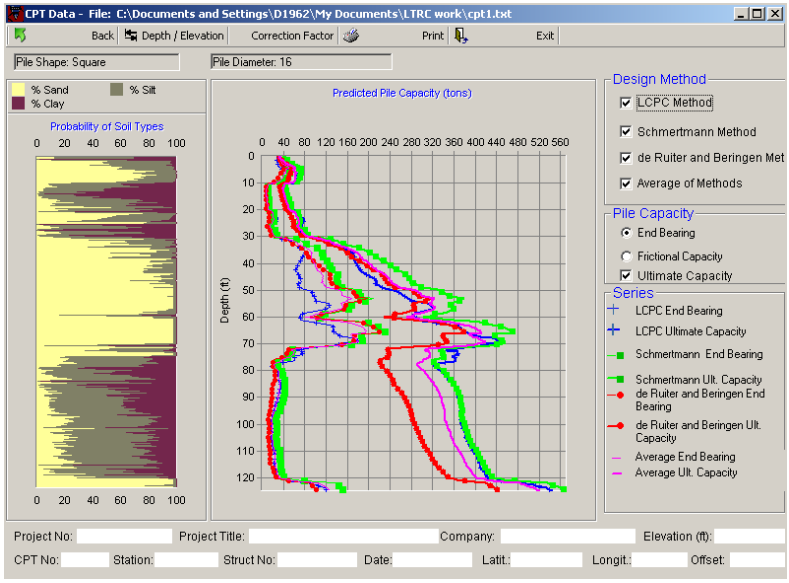


**(c) Soil classification and predicted pile resistance**

**Figure 5**
**General features of Louisiana Pile Design by Cone Penetration Test (LPD-CPT) program (www.ltrc.lsu.edu/downloads.html)**

**Dynamic Measurement with Signal Matching Analysis (CAPWAP)**

The evaluation of static capacity from pile driving is based on the concept that the driving operation includes failure in the pile-soil system in which a very fast load test is carried out under each blow. There are two main methods to estimate the ultimate capacity of driven piles on the basis of dynamic driving resistance. One method is using pile driving formulas (i.e., dynamic equations) and the second is wave-equation analysis. Dynamic equations predict total resistance based on work done by the pile during penetration. Wave equation methods are based on a numerical solution of the one-dimensional wave equation. Stress-wave propagation in a pile during driving can be described by the following one-dimensional wave equation modified by Paikowsky and Whitman to include frictional resistance along the pile *[25]*:

$$E_P \frac{\partial^2 u}{\partial^2 x^2} - \frac{S_P}{A_P} f_S = \rho_P \frac{\partial^2 u}{\partial t^2} \tag{14}$$

where, $E_P$ is the modulus of elasticity, $\rho_p$ is the unit density of the pile material, u(x,t) = longitudinal displacement of infinitesimal segment, $f_s$ = frictional stress along the pile, $A_p$ is the pile area, and $S_p$ is the pile circumference.

The numerical solution uses mathematical models for the pile and the pile-soil system. The wave equation formulation is used in two general ways: pre-driving analysis and post-driving analysis. When the one-dimensional wave equation solution is used for pre-driving analysis, the driving system is also modeled. Post-driving analyses use the measured force signal (calculated from strain readings) and the measured velocity signal (integrated from acceleration readings) obtained near the pile top during driving. At that point the velocity signal is used as a boundary condition while varying the parameters describing soil resistance in order to match calculated and measured force signals. These parameters include the side and tip quake, side and tip damping, pile shaft resistance, and pile tip resistance. Additional parameters may be used to describe soil resistance and rebound ratio for unloading different from that of loading. Iterations are performed by changing soil-model variables for each pile in contact with soil until the best match between force signals is obtained. The results of these analyses are assumed to represent the actual distribution of the ultimate static resistance of the pile. The procedure was first suggested by Goble et al., using the computer program CAPWAP *[26]*.

## LRFD Calibration Using Reliability Theory

The uncertainties of load effect and resistance are attributed to various sources and their levels of uncertainties are wide in range. Generally, resistance has higher uncertainty compared to the load effect *[3]*. Figure 6 shows the probability density functions for the load effect and resistance. Failure can be defined as load exceeding resistance, and probability of failure is related to the shaded area where two probability density functions overlap. In traditional allowable stress design (ASD), the mean factor of safety is the fraction of the mean resistance over the mean load effect. The mean safety factor for the resistance with lower uncertainty (solid curve) and resistance with higher uncertainty (dotted curve) is unchanged. Whereas in LRFD, the larger variability in resistance effect (dotted curve) will lead to a larger probability of failure, which is represented as a larger overlapped area. Accordingly, it is very important to incorporate with the uncertainties in the foundation design by using reliability based theory.

The LRFD method intends to separate uncertainties of load effect from uncertainties of resistance and then apply the statistical theory to ensure the same level of structure safety. To achieve this level of safety, load and resistance factors should be calibrated. This process is performed using measured data to derive statistical parameters characteristic of design methods and determine the magnitude of load and resistance factors needed to obtain acceptable margins of safety. There are mainly two procedures for LRFD calibration: (1) LRFD calibration to achieve consistency with traditional safety factors in ASD but not with target reliability when data is not available and (2) LRFD calibration using reliability theory *[27]*. When the LRFD design code is calibrated, local experience should be included for several reasons. First, different states have different soil deposition and foundation designers have developed well-established design methods which implicitly incorporate past experience. Such experience can result in cost saving designs but is not included in the existing AASHTO LRFD code, which was developed based on limited databases from other geological origins or stress histories *[11]*. Under this situation, if the design is performed by the existing code, such experience will be lost, which will cause either over conservative or unsafe design. Instead, if the calibration is performed by including local experience, cost saving designs can be obtained. This calibration can be performed by simply fitting the ASD to LRFD to achieve at least the same cost efficiency. Second, load tests are usually conducted to verify the design loads to evaluate the actual response of the pile under loading and to establish local load test databases. If these local databases are included, the uncertainties are reduced and design is expected to be improved.

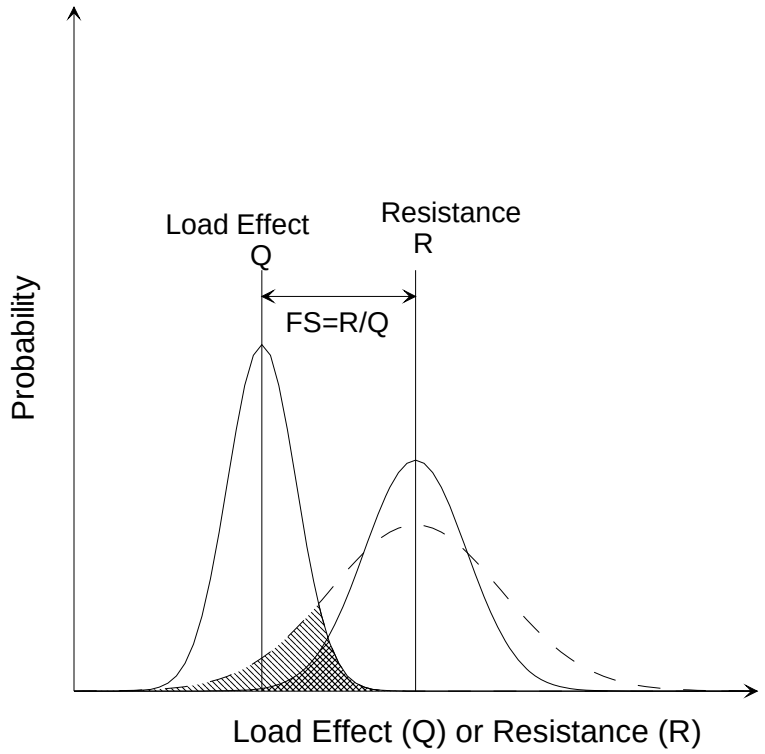


**Figure 6**
**Probability density functions for load effect and resistance**

**LRFD Calibration via WSD**

When there is not sufficient statistical data available for a statistical theory based calibration, calibration through fitting to the ASD method can be used *[28]*:

$$\phi = \frac{\gamma_D \frac{Q_D}{Q_L} + \gamma_L}{FS(\frac{Q_D}{Q_L} + 1)} \tag{15}$$

where, $\phi$ is the resistance factor; $Q_D$ and $Q_L$ are the dead load and live load, respectively; $\gamma_D$ and $\gamma_L$ are the load factors for dead load and live load, respectively; and $FS$ is the factor of safety.

Using equation (15), the resistance factors that need to be used in the LRFD method can be calculated to obtain a level of safety equal to that of the ASD method. This process provides the engineer with a visualization of uncertainty rather than the lumped single factor of safety in ASD. However, using the resistance factor obtained by fitting to the ASD method is not likely to improve the reliability of the design. Improved design can only be achieved when resistance factors are evaluated directly through statistical data based on reliability theory, rather than through calibration with existing factors of safety in ASD *[29]*. Thus, there is no difference in the design between the LRFD and ASD methods if the resistance factor is calibrated via ASD.

Ultimate pile resistances for the same site obtained by using different design methods show some variation depending on its reliability. Therefore, resistance factors ($\phi$) associated with different design methods should reflect its accuracy in predicting the ultimate bearing resistance of piles. In this research, resistance factors ($\phi$) were determined for the static design methods ($\alpha$–Tomlinson method for clay and Nordlund method for sand), three direct CPT methods (Schmertmann method, De Ruiter and Beringen method, and LCPC method), the average of three CPT methods, and the dynamic measurement with signal matching analysis method (CAPWAP).

**Statistical Characterization of the Data Collected**

To perform an LRFD calibration, the performance limit state equations must first be determined. Two limit states that are usually checked in the design of piles are the ultimate limit state (ULS) or the strength limit state and the serviceability limit state (SLS). Both limit states designs are carried out to satisfy the following criteria *[30]*:

Ultimate limit state (ULS): Factored resistance $\geq$ Factored load effects

Serviceability limit state (SLS): Deformation $\leq$ Tolerable deformation to remain serviceable

It is usually considered that the design of deep foundations is controlled by the ultimate limit state. Therefore, in the following discussion, only the ultimate limit state is considered. The following basic equation is recommended to represent limit states design by AASHTO *[11]*:

$$\phi R_n \geq \sum \eta . \gamma_i . Q_i \tag{16}$$

where, $\phi$ is the Resistance factor, $R_n$ is the Nominal resistance, and $\eta$ is the Load modifier to account for effects of ductility, redundancy, and operational importance. The value of $\eta$ usually is 1.00. $Q_i$ is the Load effect, and $\gamma_i$ is the Load factor.

Most driven piles develop both skin and toe resistances, but the percentage of skin or toe resistance to total resistance is not constant. Therefore, it is not possible to provide a fixed correlation between the three resistance factors (skin, toe, and total resistances). In this research, only the resistance for total resistance was calibrated. Thus, it should be noted that the same resistance factors for skin and end bearing are assumed, and the calibrated resistance factors are valid only for the ranges of pile dimensions (length and diameter) that employed in this study.

Considering the load combination of dead load and live load for AASHTO Strength I case, the performance limit equation is as follows *[31]*:

$$\phi R_n = \gamma_{\mathrm{D}} Q_D + \gamma_{\mathrm{L}} Q_L \tag{17}$$

The loads applied to piles are traditionally based on superstructure analysis, whereas actual load transfer to substructure, which is actually a pile-superstructure interaction problem, is poorly researched. Most researchers employ the load statistics and the load factors from

AASHTO LRFD specifications, which were originally recommended by Nowak, to make pile foundation design consistent with the bridge superstructure design *[9]*. For example, Zhang et al., Kim et al., and McVay et al., selected the statistical parameters of dead and live loads, which were used in the AASHTO LRFD specifications as follows *[31], [32], [33]*:

$$\gamma_L = 1.75 \quad \lambda_L = 1.15 \quad \mathrm{COV_L} = 0.18$$
$$\gamma_D = 1.25 \quad \lambda_D = 1.08 \quad \mathrm{COV_D} = 0.13$$

where, $\lambda_D$ and $\lambda_L$ are the load bias factors (mean ratio of measured over predicted value) for the dead load and live load, respectively. $\mathrm{COV_D}$ and $\mathrm{COV_L}$ are the coefficient of variation values for the dead load and live load, respectively.

The $Q_D/Q_L$ is the dead load to live load ratio which varies depending on the span length *[34]*. In this research, a $Q_D/Q_L$ of 3 is used for calibration.

The resistance statistics were calculated in terms of the bias factors. The bias factor is defined as the ratio of the measured pile resistance over the predicted pile resistance, i.e.:

$$\lambda_R = \frac{R_m}{R_p} \tag{18}$$

where, $R_m$ is the measured resistance and $R_p$ is the predicted (nominal resistance = $R_n$).

**First Order Second Moment (FOSM) Method**

Since FOSM is easy to use and valid for preliminary analyses, it was initially used in this study for calibration of resistance factors of driven piles. In the FOSM method, limit state function is linearized by expanding the Taylor series expansion about the mean value of the variable. Since only the mean and the variance are used in the expansion, it is called First (Mean) Order Second (variance) Moment. For the lognormal distribution of resistance and load statistics, Barker et al. derived the following relation for calculating the reliability index, β *[35]*:

$$\beta = \frac{\ln\left[\lambda_R \mathrm{FS}\left(\frac{Q_D/Q_L + 1}{\lambda_D Q_D/Q_L + \lambda_L}\right)\sqrt{\frac{1+\mathrm{COV}_\mathrm{R}^2+\mathrm{COV}_\mathrm{D}^2+\mathrm{COV}_\mathrm{L}^2}{1+\mathrm{COV}_\mathrm{R}^2}}\right]}{\sqrt{\ln\left[\left(1+\mathrm{COV}_\mathrm{R}^2\right)\left(1+\mathrm{COV}_\mathrm{D}^2+\mathrm{COV}_\mathrm{L}^2\right)\right]}} \qquad (19)$$

For LRFD, this equation is modified by replacing overall factor of safety (FS) by partial factor of safety and then rearranging to express relation to resistance factor ($\phi$) as follows:

$$\phi = \frac{\lambda_R\left(\gamma_D \frac{Q_D}{Q_L} + \gamma_L\right)\sqrt{\frac{1+\mathrm{COV}_\mathrm{D}^2+\mathrm{COV}_\mathrm{L}^2}{1+\mathrm{COV}_\mathrm{R}^2}}}{\left(\lambda_D \frac{Q_D}{Q_L} + \lambda_L\right)\exp\left(\beta_T\sqrt{\ln\left[\left(1+\mathrm{COV}_\mathrm{R}^2\right)\left(1+\mathrm{COV}_\mathrm{D}^2+\mathrm{COV}_\mathrm{L}^2\right)\right]}\right)} \qquad (20)$$

When statistical data is available, the calibration can be performed based on reliability theory. The design based on the resistance factors obtained from this process is expected to be better than ASD and fully achieved the advantages of the LRFD method. If both the resistances and the load are log-normally distributed and the performance limit state design equation is linear, the First Order Second Moment method can be used to obtain the reliability index. Unfortunately, for deep foundations, under some conditions, neither the loads nor the resistance are normally or log-normally distributed, and sometimes the design equation may be nonlinear. Therefore, advance reliability theory based methods are needed. In this study, FORM and the Monte Carlo simulation were also used with FOSM for the LRFD calibration of pile design methods *[36], [37]*.

**First Order Reliability Method (FORM)**

Hasofer and Lind proposed a modified reliability index that did not exhibit the invariance problem *[36]*. The "correction" is to evaluate the limit state function at a point known as the "design point" instead of the mean values. The design point is a point on the failure surface g = 0. Since the design point is generally not known in advance, an iteration technique must be used to solve the reliability index. Detailed procedure regarding FORM can be found in Nowak and Collins *[37]*. Only information on the means and the standard deviations of the

resistances and the loads are needed while detailed information on the type of distribution for each random variable are not needed.

FORM is an analytical scheme that is used to approximate probability integral when basic variables have strictly increasing continuous joint cumulative distribution function (CDF).

Steps for FORM using the Rackwitz-Fiessler method *[38]*:

1. Define limit state function, $g(x_1, x_2, x_3....)$.

   The limit state function for LRFD is developed as follows:

$$Q = Q_D + Q_L = \lambda_D Q_D + \lambda_L Q_L \tag{21}$$

$$\varphi R = \gamma_D Q_D + \gamma_L Q_L \tag{22}$$

   from (21) and (22)

$$\text{g(R.L)} = \left( \frac{\gamma_D Q_D + \gamma_L Q_L}{\varphi} \right) \lambda_R - (\lambda_D Q_D + \lambda_L Q_L) = 0 \tag{23}$$

   Now the specified live load to dead load ratio,$(Q_L/Q_D)$ equation (23) can be rearranged as:

$$\text{g(R.L)} = \left( \frac{\gamma_D + \gamma_L * \kappa}{\varphi} \right) \lambda_R - (\lambda_D + \lambda_L * \kappa) = 0 \tag{24}$$

   where, $\kappa = \dfrac{Q_L}{Q_D}$

2. Assuming initial design point ($x_i$*), mean values are a reasonable choice for most cases. In this case, initial design values for dead load and live load ($x_2$ and $x_3$) assumed and that for resistance ($x_1$) is determined by equating the limit state function equal to zero. Also for lognormal variables equivalent normal parameters are then determined as:

$$\mu^e{}_x = x^* - \sigma^e{}_x \left[ \Phi^{-1}(F_x(x)) \right] \tag{25}$$

$$\sigma^{e}_{x} = \frac{1}{fx(x^*)}\varphi\left[\frac{x^* - \mu^{e}x}{\sigma^{e}x}\right] = \frac{1}{fx(x^*)}\varphi\left[\Phi^{-1}(F_x(x^*)\right] \quad (26)$$

where, $\phi$ and $\Phi$ denotes the mass probability density function (PDF) and the cumulative distribution function (CDF) for normal distribution, respectively.

3. Corresponding to the design point x*, the reduced variable is found as:

$$z^*_i = \frac{x^* - {}_x \mu^{e} x_i}{\sigma^{e} x_i} \quad (27)$$

4. Partial derivatives of the limit state function is found at the design point and vector G is defined as:

$$G = \begin{Bmatrix} G1 \\ G2 \\ G3 \end{Bmatrix} \text{ where, } G_i = -\frac{\partial g}{\partial Zi}\bigg| \text{ at design point } = -\frac{\partial g}{\partial Xi}\bigg| * (\sigma^{e} x_i) \text{ at design point} \quad (28)$$

$$\beta = \frac{\{G\}^T \{z^*\}}{\sqrt{\{G\}^T \{G\}}} \text{ where, } \{z^*\} = \begin{Bmatrix} z^*_1 \\ z^*_2 \\ z^*_3 \end{Bmatrix} \quad (29)$$

$$\alpha = \frac{\{G\}}{\sqrt{\{G\}^T \{G\}}} \quad (30)$$

5. The new design point is determined in the reduced variable as:

$$z^*_i = \alpha_i \beta \quad (31)$$

$$x^*_i = \mu^{e}_{xi} + z_i \sigma^{e}_{xi} \quad (32)$$

Also at this step, the new design point for resistance ($x_1$) is determined by inserting new design values for loads ($x_2$ and $x_3$) into the g function. With new design points, steps from 1 to 5 are followed. The process is repeated until $\beta$ and the design point converges. In this study, the excel sheet was used to get the FOSM solution with the "Goal seek" function for given load and resistance statistics. Iterations for FORM is done using the "SOLVER" tool.

**Monte Carlo Simulation Method**

For more complicated limit state functions, the application of the general statistical method for the calculation of the reliability index is either extremely difficult or impossible. Under this circumstance, the Monte Carlo simulation provides the only feasible way to determine the reliability index or the probability of failure. The procedures of the Monte Carlo simulation are described in the following paragraphs.

First, simulated values of the random variables in the limit state equation are generated. These values are then used to simulate values of the limit state function itself. Finally, the simulated values of the limit state function are plotted on normal probability paper. The probability of failure can be found by reading the probability value at the location where the plotted data curve intersects a vertical line passing through the origin. If there are too few data points and the plotted curve does not intersect the vertical axis, the plotted curve can be extrapolated.

The Monte Carlo method is a technique by which a random number generator is used to extrapolate CDF values for each random variable. Extrapolation of CDF makes estimating β possible; otherwise, a limited quantity of data would restrict the reliable estimate of β. Once the reliability index, β, is estimated, the probability of failure can be estimated by assuming the distribution of g(x). The steps of the Monte Carlo simulation method are as follows;

1. Generate random numbers for each set of variables. Here there are three variables (resistance, dead load and live load bias factor), so three sets of random variable have to be generated independently for each one. The number of simulations required is found using the following equation:

$$N = \frac{1 - P_{true}}{V_p^{\,2} * (P_{true})} \tag{33}$$

where, $P_{true}$ is the lowest magnitude of probability that is to be determined using Monte Carlo, and $V_p$ is the desired coefficient of variation of the simulation result. To estimate a probability as low as $10^{-2}$ and keep variance under 10 percent, the number of points to be generated in the Monte-Carlo simulation is 9900.

For each lognormal variable, the sample value $x_i$ is estimated as:

$$x^*_i = \exp(\mu_{lnx} + z_i \sigma_{lnx}) \tag{34}$$

where, $\sigma^2_{\ln x} = \ln(V^2_x + 1)$ and $\mu_{\ln x} = \ln(\mu x) - \frac{1}{2}\sigma^2_{\ln x}$

In the previous expressions, $\mu_{x,}$ and $V_x$ are the arithmetic mean and variance of x, respectively, and $\mu_{lnx}$ and $\sigma_{lnx}$ are the equivalent lognormal mean and standard deviation [mean and standard deviation of ln(x)] and $z_i$ = NORMSINV(RAND()) is the random standard normal variable generated using the EXCEL function.

2. Define the limit state function. This is done in step 1 for FORM.

3. Find the number of cases where $g(x_i) \leq 0$. The probability of failure is then defined as:

$$Pf = \frac{\text{count}(g \leq 0)}{N} \tag{35}$$

and reliability index $\beta$ is estimated as:

$$\beta = \Phi^{-1}(Pf) \tag{36}$$

# METHODOLOGY

As discussed earlier, the objective of this research study is to calibrate resistance factors for different pile design methods needed in the LRFD design of driven piles based on the Louisiana database and experience. A total of 53 pile load tests, their corresponding borings and CPT tests were identified and collected from LADOTD files. The collected pile load test data, soil properties, and CPT profiles were compiled and analyzed. This section describes the methodology of collecting, compiling, and analyzing the pile load test reports.

## Collecting of Pile Load Test Database

The LADOTD practice for pile load tests is mainly to validate and verify the pile capacity estimates based on a selected design method/procedure. If the tested pile fails to provide the required support for design loads, more piles will be added to increase the load carrying capacity and/or increase the lengths of the driven piles. The reports of all pile load tests conducted in Louisiana projects are available in the general files section at LADOTD headquarters in Baton Rouge. In this study, pile load test reports were obtained from the pavement and geotechnical design section at LADOTD.

The research team carefully reviewed and evaluated the collected pile load test reports from LADOTD for potential inclusion in the current research. The criterion for including a pile load test case in the analysis was based on the availability of proper documentation on pile data (installation and testing), pile failed during loading, adequate subsurface exploration and soil testing from borings, CPT soundings, and site location. If a pile load test report was found to be satisfactory, the report was then considered for inclusion in this study.

The pile load test database used for calibration was established by conducting an extensive search in LADOTD's project files. Only PPC piles that have been tested to failure and include adequate soil information were included in this study. The use of PPC piles is more economical in Louisiana where the driving of piles is not a problem. A total of 53 pile load tests met this criterion. Figure 7 presents a map of Louisiana with locations of the test piles that were investigated in this research. A summary of the characteristics of the investigated piles is presented in Table 3.

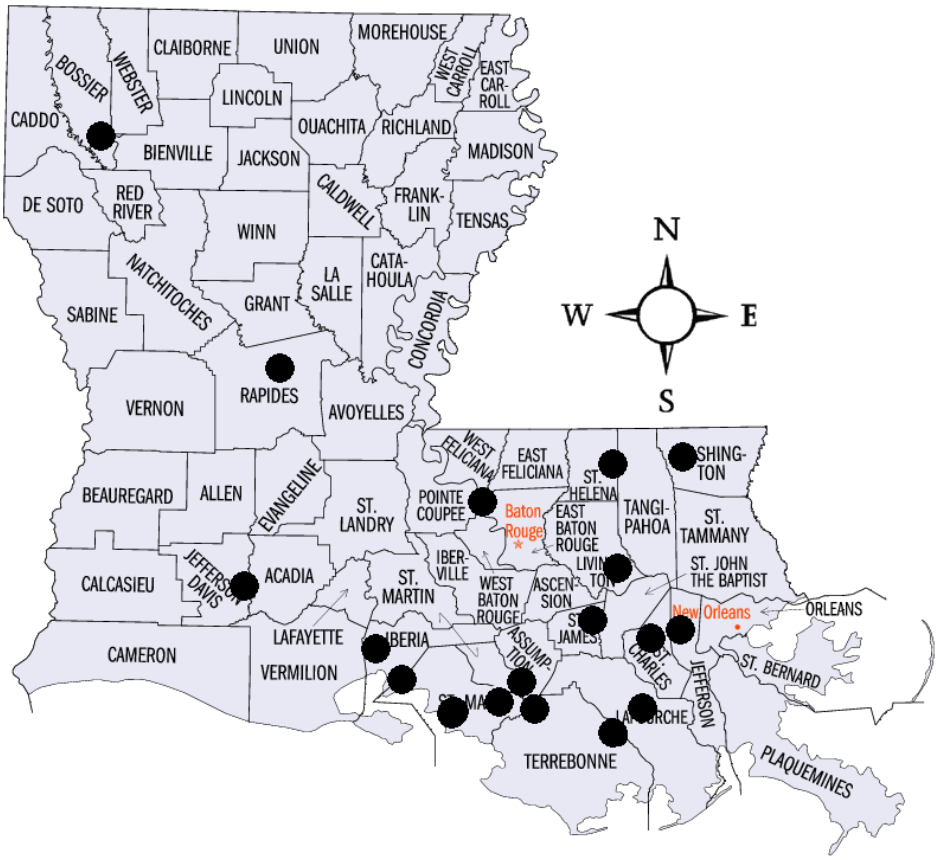


**Figure 7**
**Approximate locations of the investigated piles**

## Compilation of Pile Load Test Reports

The data on the selected pile load test reports were compiled. The information and data regarding the project, soil stratification and properties, pile characteristics, load test data, CPT profiles, dynamic test data, etc. were processed and transferred from each load test report to tables, forms, and graphs. Some of the CPT soundings were obtained in digital format. The remainder of the CPT profiles were scanned using a high resolution scanner and then were converted to a digital format using the automated digitizing software UN-SCAN-IT. The following data and information were collected and compiled for each pile load test report.

The site data provide the necessary information to identify the location of the project. The site identification used herein is the Louisiana state project number. For example, the site ID 005-05-0065 is the state project number for St. Louis Canal Bridge.

**Table 3**
**Summary of the characteristics of the investigated piles**

| Square PPC Pile Size | Pile Type | | Predominant Soil Type | | |
|---|---|---|---|---|---|
| | Friction | End-Bearing | Cohesive | Cohesionless | Limit of Information |
| 14" | 22 | 0 | 19 | 3 | 0 |
| 16" | 5 | 0 | 3 | 0 | 2 |
| 18" | 2 | 0 | 1 | 1 | 0 |
| 24" | 9 | 1 | 7 | 3 | 0 |
| 30" | 13 | 1 | 9 | 5 | 0 |
| Total | 51 | 2 | 39 | 12 | 2 |

The soil data consist of information on the soil boring location (station number), soil stratigraphy, unit weight, Atterberg limits, laboratory testing (shear strength, physical properties, etc.), and in-situ test results (e.g., SPT for cohesionless soil).

The foundation data consist of pile characteristics (pile ID, material type, cross-section, total length, and embedded length), installation data (location of the pile, date of driving, driving record, hammer type, etc.), and pile load test (date of loading, applied load with time, pile head movement, pile failure under testing, etc.).

The cone penetration soundings include test location (station number), date, cone tip resistance, and sleeve friction profiles with depth.

## Ultimate Capacity of Piles from Load Test

The measured ultimate pile resistance ($Q_u$) was interpreted from the load-deformation curve using the Davisson method for piles with a size less than 24 inches and the modified Davisson method proposed by Kyfor et al. for piles exceeding a size of 24 inches *[39], [40]*.

In the Davisson method, the ultimate bearing resistance is determined from the intersection between a load-settlement curve and a straight line with a slope of L/AE and an initial settlement intercept of 0.15 + D/120 (in.) [(L: pile length, A: cross-sectional area of the pile, E: Young's modulus of the pile, and D: pile diameter (in.)]. Figure 8 illustrates a sample load-deformation test analysis using the Davisson method. In addition to load test results, all other relevant information such as soil borings, pile driving logs, and CPT data were also collected. Figure 9 shows a typical summary of geotechnical data for a tested pile. The summary of geotechnical data for all projects investigated in this research is presented in the Appendix.

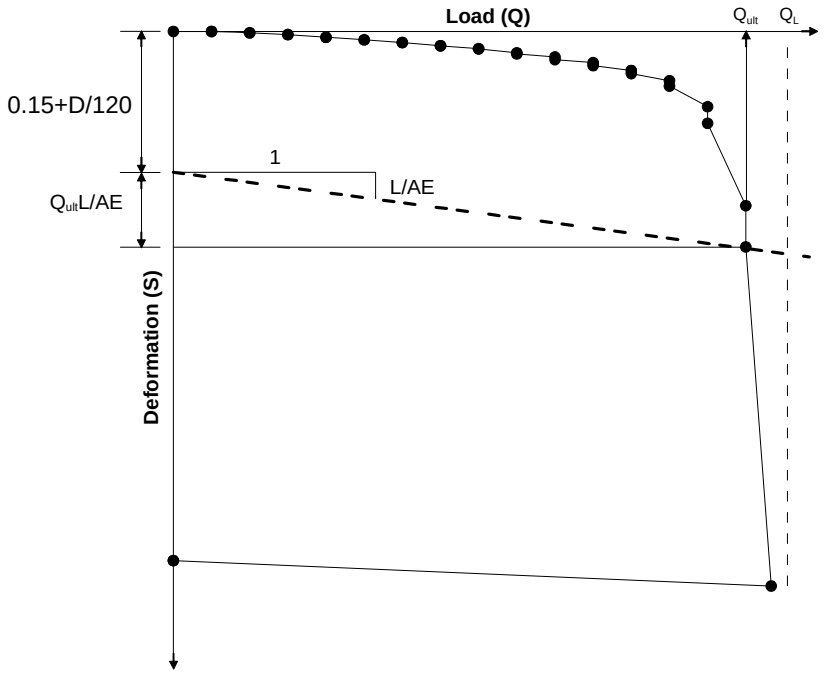


**Figure 8**
**Estimation of ultimate bearing resistance using Davisson *[39]* method after Salgado *[41]***

## Soil Identification and Classification

In addition to the soil classification determined based on soil borings and results of laboratory testing, the probabilistic region estimation CPT method was also used for soil classification and identification of site stratigraphy *[24]*. This method is similar to the classic soil classification methods since it is based on soil composition. It identifies three soil types:

clayey, silty, and sandy soils. The probabilistic region classification method provides a profile of the probability or the chance of having each soil type (clay, silt, and sand) with depth. In this study, the probability of soil types for each soil layer was used in connection with CPT pile prediction methods to calculate the appropriate correlation factors needed to estimate $q_b$ and $f$ from CPT data. A typical soil profile obtained by the probabilistic region estimation is shown in Figure 9.

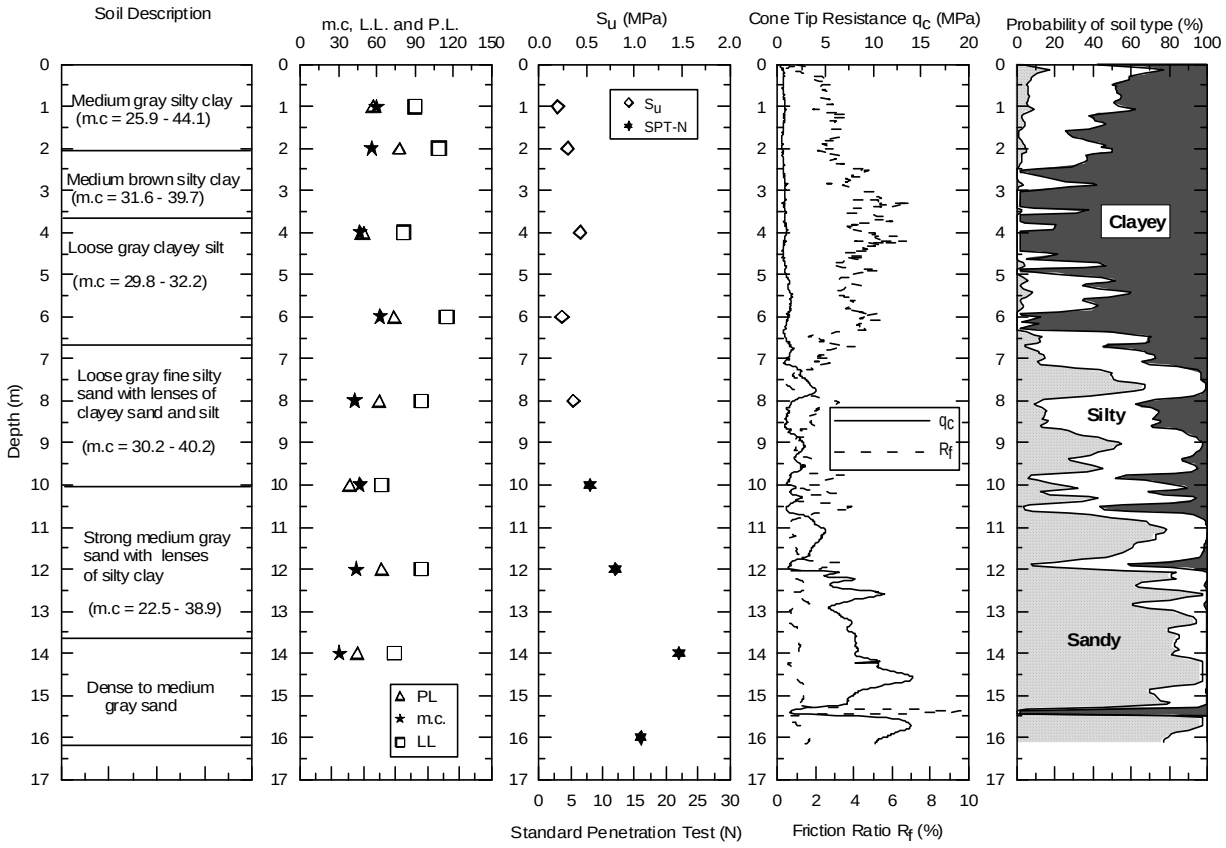


**Figure 9**
**Typical summary of geotechnical data for a tested pile**

# DISCUSSION OF RESULTS

## Predicted versus Measured Ultimate Pile Resistances

Based on the analysis of 53 driven piles, a statistical analysis was performed on the collected database to evaluate the accuracy and performance of the different pile capacity estimation methods. Table 4 presents the summary of the analysis performed on the investigated piles. The table shows the pile size, type, length, location of the pile, measured ultimate load resistance, and predicted load capacities of different methods. The mean and standard deviation of the predicted to measured pile capacity ratios ($R_p/R_m$), which are the inverses of the bias factor ($\lambda$), were calculated for the previously mentioned methods and are summarized in Table 5. Figures 10 through 16 present the comparison between the estimated pile capacities and the measured pile capacity using the Davisson method and modified Davisson method for the different pile design methods. Linear regression analysis was conducted on all methods to obtain the best fit line of the predicted/measured pile capacities ($R_p/R_m$) assuming zero intercept. The relationship $R_p/R_m$ and the corresponding coefficient of determination ($R^2$) determined for all estimation methods are presented in Figures 10 through 16 and also summarized in Table 5.

The comparison of static calculated pile capacities versus the measured load tests compiled from all soil types are presented in Figure 10. The results indicated the ratio $R_{fit}/R_m$ for the static calculation method is 1.0 with an $R^2$ of 0.84. The coefficient (slope) of 1.0 from the regression analysis implies that the relative bias of the pile capacity prediction based on the static calculation method does not vary with the measured capacities because the adhesion factor $\alpha$ already included the adjustment of biases inherent in the soil strengths. The mean and standard deviation of the $R_p/R_m$ ratio for static method are 1.12 and 0.32, respectively, indicating an average of 12 percent overestimation using the static calculation method which includes Tomlinson's $\alpha$–method in clay and Nordlund's method in sand.

Figures 11 through 14 depict the comparison between the CPT estimation methods and measured pile capacities using the Davisson interpretation method. It should be noted that the correlations resulted in $R_{fit}/R_m$ ratios ranging from 0.94 to 1.20. The De Ruiter Beringen method had the lowest ratio of 0.94. All other methods had $R_{fit}/R_m$ ratios higher than 1 indicating an increasing bias in pile capacity estimation with the increase in actual capacity. In other work, the CPT methods tend to overestimate the capacity for high capacity piles. The average ratios of $R_p/R_m$ of the CPT methods range from 0.90 to 1.20. The De Ruiter-Beringen method has the smallest ratio implying an average of 10 percent underestimation of

pile capacity while the other CPT methods overestimate the capacity by 5 to 20 percent. On average, the LCPC method overestimates the ultimate pile capacity by 5 percent and the Schmertmann method overestimates the pile capacity by 20 percent. The comparison between the average of CPT methods (CPT-average method) and measured pile capacities are presented in Figure 14. The $R_{fit}/R_m$ for the average of CPT methods is 1.08 with $R^2$ = 0.82. This is not surprising due to the fact that the CPT methods generally overestimate pile capacities for high capacity piles as discussed earlier. The mean and standard deviation of the ratio $R_p/R_m$ for CPT-average method are 1.05 and 0.33, respectively. The use of the average CPT methods overestimates the pile capacity by 5 percent in average.

Figures 15 and 16 present the results of signal matching using CAPWAP, which show the average end of driving (EOD) resistance is about 35 percent of the average load test value indicating a setup factor of about 2.9. The 14-day beginning of restrike (BOR) data show the CAPWAP estimation of pile resistance still underestimated the measured value by 17 percent.

**Table 4**
**Results of the analysis conducted on square precast prestressed concrete piles driven into Louisiana soils**

| | State Project Identification | 003-07-0019 | 005-01-0056 | 005-01-0056 | 005-01-0056 |
|---|---|---|---|---|---|
| | | BNSS Overpass - Jennings | Southern pacfic railroad overpass | Southern pacfic railroad overpass | Southern pacfic railroad overpass |
| Pile and Soil Identification | Pile ID | TP1, 24" Square PPC | TP1, 24" Square PPC | TP2, 14" Square PPC | TP3, 24" Square PPC |
| | Pile Length (ft.) | 60 | 90 | 74 | 92 |
| | Embedded Length (ft.) | 54.2 | 85 | 63.7 | 87 |
| | Pile Classification | Friction | Skin | Skin | Skin |
| | Predominant Soil* | Cohesive | Cohesive | Cohesive | Cohesive |
| Methods of Predicting Pile Capacity by Cone Penetration Test | Predicted Ultimate Load (ton) | $Q_u$ | $Q_u$ | $Q_u$ | $Q_u$ |
| | Schmertmann | — | 246.0 | 94.6 | 324.5 |
| | de Ruiter & Beringen | — | 174.9 | 75.4 | 293.8 |
| | LCPC | — | 196.5 | 92.7 | 340.7 |
| | Average | — | 205.8 | 87.6 | 319.6 |
| Static Analysis | α-method and Nordlund method | 217.3 | 271 | — | 363.7 |
| Dynamic measurement | CAPWAP (EOD) | 75.0 | — | — | — |
| | CAPWAP (14 days-BOR) | 238.8 | — | — | — |
| Load Test Interpretation Method | Davisson method | 272 | 225 | 132 | 320 |

* Cohesive (mainly clayey and silty clay soils) and Cohesionless (mainly sandy soils); $Q_u$: Total ultimate capacity

**Table 4**
**Results of the analysis conducted on square precast prestressed concrete piles driven into Louisiana soils (continued)**

| | State Project Identification | 005-05-0065 | 008-01-0042 | 065-90-0024 | 065-90-0024 |
|---|---|---|---|---|---|
| | | St. Louis Canal Bridge | La 415 - La 983 | Houma I.C.W.W. Bridges | Houma I.C.W.W. Bridges |
| Pile and Soil Identification | Pile ID | TP1, 16" Square PPC | TP1, 16" Square PPC | TP1, 14" Square PPC | TP2, 14" Square PPC |
| | Pile Length (ft.) | 92 | 81.3 | 85 | 73.5 |
| | Embedded Length (ft.) | 79.2 | 50.7 | 80 | 70 |
| | Pile Classification | Skin | Skin | Skin | Skin |
| | Predominant Soil* | — | — | Cohesive | Cohesive |
| Methods of Predicting Pile Capacity by Cone Penetration Test | Predicted Ultimate Load (ton) | $Q_u$ | $Q_u$ | $Q_u$ | $Q_u$ |
| | Schmertmann | — | — | 174.4 | 90.0 |
| | de Ruiter & Beringen | — | — | 110.6 | 82.1 |
| | LCPC | — | — | 152.6 | 79.7 |
| | Average | — | — | 145.9 | 83.9 |
| Static Analysis | α-method and Nordlund method | — | — | 162.4 | 115.5 |
| Dynamic measurement | CAPWAP (EOD) | 20 | 10.6 | — | — |
| | CAPWAP (14 days-BOR) | 70 | — | — | — |
| Load Test Interpretation Method | Davisson method | 109 | 86 | 115 | 55 |

* Cohesive (mainly clayey and silty clay soils) and Cohesionless (mainly sandy soils); $Q_u$: Total ultimate capacity

**Table 4**
**Results of the analysis conducted on square precast prestressed concrete piles driven into Louisiana soils (continued)**

| | State Project Identification | 065-90-0024 | 260-05-0020 | 260-05-0020 | 260-05-0020 |
|---|---|---|---|---|---|
| | | Houma I.C.W.W. Bridges | Tichfaw River Bridge and Approaches | Tichfaw River Bridge and Approaches | Tichfaw River Bridge and Approaches |
| Pile and Soil Identification | Pile ID | TP3, 14" Square PPC | TP1, 30" Square PPC | TP2, 30" Square PPC | TP3, 30" Square PPC |
| | Pile Length (ft.) | 94.5 | 73 | 118 | 81 |
| | Embedded Length (ft.) | 80 | 59.3 | 61.2 | 73.9 |
| | Pile Classification | Skin | Skin | Skin | Skin |
| | Predominant Soil* | Cohesive | Cohesive | Cohesionless | Cohesive |
| Methods of Predicting Pile Capacity by Cone Penetration Test | Predicted Ultimate Load (ton) | $Q_u$ | $Q_u$ | $Q_u$ | $Q_u$ |
| | Schmertmann | 184.3 | 361.5 | — | 344.5 |
| | de Ruiter & Beringen | 72.2 | 325.6 | — | 288.7 |
| | LCPC | 94.7 | 301.9 | — | 325.5 |
| | Average | 117.1 | 329.7 | — | 319.6 |
| Static Analysis | α-method and Nordlund method | 139.9 | 441.9 | 578.9 | 396.9 |
| Dynamic measurement | CAPWAP (EOD) | — | 136.3 | — | 182.3 |
| | CAPWAP (14 days-BOR) | — | 517.1 | — | 379.6 |
| Load Test Interpretation Method | Davisson method | 120 | 478 | 542.5 | 464 |

* Cohesive (mainly clayey and silty clay soils) and Cohesionless (mainly sandy soils); $Q_u$: Total ultimate capacity

**Table 4**
**Results of the analysis conducted on square precast prestressed concrete piles driven into Louisiana soils (continued)**

| | State Project Identification | 262-06-0009 & 262-07-0012 | 424-05-0078 | 424-05-0078 | 424-04-0027 |
|---|---|---|---|---|---|
| | | Bridge #1 Tickfaw River | Bayou Boeuf Bridge Main Span | Bayou Boeuf Bridge Main Span | US 90 Interchange at John Darnell Rd. |
| Pile and Soil Identification | Pile ID | TP1, 24" Square PPC | TP1, 14" Square PPC | TP2, 14" Square PPC | TP2, 14" Square PPC |
| | Pile Length (ft.) | 85 | 80 | 80 | 60 |
| | Embedded Length (ft.) | 84.9 | 77 | 75 | 38 |
| | Pile Classification | Skin | Skin | Skin | Skin |
| | Predominant Soil* | Cohesionless | Cohesionless | Cohesionless | Cohesive |
| Methods of Predicting Pile Capacity by Cone Penetration Test | Predicted Ultimate Load (ton) | $Q_u$ | $Q_u$ | $Q_u$ | $Q_u$ |
| | Schmertmann | 443.3 | — | 123.9 | — |
| | de Ruiter & Beringen | 371.8 | — | 118.8 | — |
| | LCPC | 536.0 | — | 149.1 | — |
| | Average | 450.3 | — | 130.6 | — |
| Static Analysis | α-method and Nordlund method | — | 185.6 | 147.3 | 104.1 |
| Dynamic measurement | CAPWAP (EOD) | — | — | — | 39 |
| | CAPWAP (14 days-BOR) | — | — | — | — |
| Load Test Interpretation Method | Davisson method | 240 | 165 | 112.5 | 135 |

* Cohesive (mainly clayey and silty clay soils) and Cohesionless (mainly sandy soils); $Q_u$: Total ultimate capacity

**Table 4**
**Results of the analysis conducted on square precast prestressed concrete piles driven into Louisiana soils (continued)**

| | State Project Identification | 424-05-0078 | 424-05-0081 | 424-05-0081 | 424-06-0005 |
|---|---|---|---|---|---|
| | | Bayou Boeuf Bridge Main Span | Bayou Boeuf Bridge (West Approach) | Bayou Boeuf Bridge (West Approach) | Bayou Boeuf Bridge |
| Pile and Soil Identification | Pile ID | TP5, 14" Square PPC | TP1, 14" Square PPC | TP4, 16" Square PPC | TP1, 14" Square PPC |
| | Pile Length (ft.) | 85 | 96 | 80 | 75 |
| | Embedded Length (ft.) | 80.5 | 89.5 | 69.9 | 67 |
| | Pile Classification | Skin | Skin | Skin | Skin |
| | Predominant Soil* | Cohesive | Cohesive | Cohesive | Cohesive |
| Methods of Predicting Pile Capacity by Cone Penetration Test | Predicted Ultimate Load (ton) | $Q_u$ | $Q_u$ | $Q_u$ | $Q_u$ |
| | Schmertmann | 71 | 134.9 | 130.4 | 85.9 |
| | de Ruiter & Beringen | 88.2 | 86.9 | 84.8 | 66.7 |
| | LCPC | 75.4 | 110.1 | 96.4 | 66.4 |
| | Average | 78.2 | 110.6 | 103.8 | 73.0 |
| Static Analysis | α-method and Nordlund method | 118.0 | 124.9 | 100.7 | 122.9 |
| Dynamic measurement | CAPWAP (EOD) | — | — | — | — |
| | CAPWAP (14 days-BOR) | — | 113.4 | 96 | — |
| Load Test Interpretation Method | Davisson method | 124 | 115 | 100 | 98 |

* Cohesive (mainly clayey and silty clay soils) and Cohesionless (mainly sandy soils); $Q_u$: Total ultimate capacity

**Table 4**
**Results of the analysis conducted on square precast prestressed concrete piles driven into Louisiana soils (continued)**

| | State Project Identification | 424-06-0005 | 424-07-0021 | 450-15-0085 | 424-05-0087 |
|---|---|---|---|---|---|
| | | Bayou Boeuf Bridge | Bayou L'ourse | I-10 Williams Boulevard Interchange | Morgan City - Gibson Highway |
| Pile and Soil Identification | Pile ID | TP2, 14" Square PPC | TP1, 30" Square PPC | TP3A, 14" Square PPC | TP1, 16" Square PPC |
| | Pile Length (ft.) | 85 | 124 | 87 | 85 |
| | Embedded Length (ft.) | 71 | 117 | 75.5 | 69.5 |
| | Pile Classification | Skin | Skin | Skin | Skin |
| | Predominant Soil* | Cohesive | Cohesive | Cohesive | Cohesive |
| Methods of Predicting Pile Capacity by Cone Penetration Test | Predicted Ultimate Load (ton) | $Q_u$ | $Q_u$ | $Q_u$ | $Q_u$ |
| | Schmertmann | 94.9 | 369.9 | — | 115.9 |
| | de Ruiter & Beringen | 75.7 | 296.7 | — | 81.9 |
| | LCPC | 75.1 | 294.3 | — | 97.9 |
| | Average | 81.9 | 320.3 | — | 98.6 |
| Static Analysis | α-method and Nordlund method | 111.5 | 411.9 | 140.2 | — |
| Dynamic measurement | CAPWAP (EOD) | — | 123.3 | — | — |
| | CAPWAP (14 days-BOR) | — | 374.6 | 150.1 | — |
| Load Test Interpretation Method | Davisson method | 98 | 380 | 172 | 105 |

* Cohesive (mainly clayey and silty clay soils) and Cohesionless (mainly sandy soils); $Q_u$: Total ultimate capacity

**Table 4**
**Results of the analysis conducted on square precast prestressed concrete piles driven into Louisiana soils (continued)**

| | State Project Identification | 424-05-0087 | 424-05-0087 | 424-05-0087 | 424-05-0081 |
|---|---|---|---|---|---|
| | | Morgan City - Gibson Highway | Morgan City - Gibson Highway | Morgan City - Gibson Highway | Bayou Boeuf Bridge (West Approach) |
| Pile and Soil Identification | Pile ID | TP3, 30" Square PPC | TP5, 30" Square PPC | TP7, 16" Square PPC | TP3, 14" Square PPC |
| | Pile Length (ft.) | 115 | 115 | 85 | 74 |
| | Embedded Length (ft.) | 104.1 | 113 | 77 | 64.5 |
| | Pile Classification | Skin | Skin | Skin | Skin |
| | Predominant Soil* | Cohesionless | Cohesive | Cohesive | Cohesive |
| Methods of Predicting Pile Capacity by Cone Penetration Test | Predicted Ultimate Load (ton) | $Q_u$ | $Q_u$ | $Q_u$ | $Q_u$ |
| | Schmertmann | 603.1 | 794.5 | 131.5 | 135.0 |
| | de Ruiter & Beringen | 532.2 | 603.8 | 95.6 | 108.1 |
| | LCPC | 612.1 | 776.2 | 111.5 | 131.6 |
| | Average | 582.5 | 724.8 | 112.9 | 124.9 |
| Static Analysis | α-method and Nordlund method | 526.6 | 454.7 | 133.1 | 119.7 |
| Dynamic measurement | CAPWAP (EOD) | — | — | — | — |
| | CAPWAP (14 days - BOR) | — | — | — | 66.5 |
| Load Test Interpretation Method | Davisson method | 482 | 565 | 111 | 165 |

* Cohesive (mainly clayey and silty clay soils) and Cohesionless (mainly sandy soils); $Q_u$: Total ultimate capacity

**Table 4**
**Results of the analysis conducted on square precast prestressed concrete piles driven into Louisiana soils (continued)**

| | State Project Identification | 424-06-0005 | 424-06-0005 | 014-02-0018 | 047-02-0022 |
|---|---|---|---|---|---|
| | | Bayou Boeuf Bridge | Bayou Boeuf Bridge | Union Pacific Railroad Overpass | Bogue Chitto Bridge |
| Pile and Soil Identification | Pile ID | TP3, 14" Square PPC | TP5, 14" Square PPC | TP1, 30" Square PPC | TP2, 30" Square PPC |
| | Pile Length (ft.) | 78 | 85 | 107 | 92 |
| | Embedded Length (ft.) | 77.5 | 79 | 45.5 | 58 |
| | Pile Classification | Skin | Skin | Skin | Skin |
| | Predominant Soil* | Cohesive | Cohesive | Cohesive | Cohesionless |
| Methods of Predicting Pile Capacity by Cone Penetration Test | Predicted Ultimate Load (ton) | $Q_u$ | $Q_u$ | $Q_u$ | $Q_u$ |
| | Schmertmann | 99.8 | 94.4 | — | 468.5 |
| | de Ruiter & Beringen | 71.5 | 57.4 | — | 418.4 |
| | LCPC | 82.8 | 67.6 | — | 503.3 |
| | Average | 84.7 | 73.1 | — | 463.4 |
| Static Analysis | α-method and Nordlund method | 98.8 | 100.6 | 289.1 | 475.8 |
| Dynamic measurement | CAPWAP (EOD) | — | — | 162.5 | 120 |
| | CAPWAP (14 days-BOR) | — | — | — | — |
| Load Test Interpretation Method | Davisson method | 100 | 90 | 455 | 390 |

* Cohesive (mainly clayey and silty clay soils) and Cohesionless (mainly sandy soils); $Q_u$: Total ultimate capacity

**Table 4**
**Results of the analysis conducted on square precast prestressed concrete piles driven into Louisiana soils (continued)**

| | State Project Identification | 424-05-0087 | 064-06-0036 | 090-01-0015 | 090-01-0015 |
|---|---|---|---|---|---|
| | | Morgan City - Gibson Highway | Bayou Lafourche Bridge and Approaches | Lake Bistineau Spillway Bridge | Lake Bistineau Spillway Bridge |
| Pile and Soil Identification | Pile ID | TP4, 30" Square PPC | TP1, 24" Square PPC | TP1, 24" Square PPC | TP2, 24" Square PPC |
| | Pile Length (ft.) | 115 | 59.1 | 56.5 | 65 |
| | Embedded Length (ft.) | 99.3 | 39 | 39.5 | 47 |
| | Pile Classification | Skin | Skin | Skin | Skin |
| | Predominant Soil* | Cohesionless | Cohesionless | Cohesive | Cohesionless |
| Methods of Predicting Pile Capacity by Cone Penetration Test | Predicted Ultimate Load (ton) | $Q_u$ | $Q_u$ | $Q_u$ | $Q_u$ |
| | Schmertmann | 664.6 | 74.4 | 263.4 | 686.9 |
| | de Ruiter & Beringen | 534.4 | 39.3 | 222.8 | 609.0 |
| | LCPC | 619.8 | 52.5 | 272.4 | 529.8 |
| | Average | 606.3 | 55.4 | 252.9 | 608.6 |
| Static Analysis | α-method and Nordlund method | 590.9 | 72.8 | 172.5 | 262.6 |
| Dynamic measurement | CAPWAP (EOD) | — | 17.5 | 149.9 | 60 |
| | CAPWAP (14 days-BOR) | — | — | — | — |
| Load Test Interpretation Method | Davisson method | 570 | 77 | 149 | 120 |

* Cohesive (mainly clayey and silty clay soils) and Cohesionless (mainly sandy soils); $Q_u$: Total ultimate capacity

**Table 4**
**Results of the analysis conducted on square precast prestressed concrete piles driven into Louisiana soils (continued)**

| | State Project Identification | 424-05-0087 | 713-48-0083 | 713-48-0083 | 455-05-0036 |
|---|---|---|---|---|---|
| | | Morgan City - Gibson Highway | Bayou Milhomme Bridge & Approaches | Bayou Milhomme Bridge & Approaches | Sugarhouse Road |
| Pile and Soil Identification | Pile ID | TP2, 30" Square PPC | TP1, 24" Square PPC | TP2, 24" Square PPC | TP1, 14" Square PPC |
| | Pile Length (ft.) | 115 | 72 | 96 | 75 |
| | Embedded Length (ft.) | 89.2 | 55 | 85 | 70 |
| | Pile Classification | Skin | Skin | Skin | Skin |
| | Predominant Soil* | Cohesionless | Cohesive | Cohesive | Cohesive |
| Methods of Predicting Pile Capacity by Cone Penetration Test | Predicted Ultimate Load (ton) | $Q_u$ | $Q_u$ | $Q_u$ | $Q_u$ |
| | Schmertmann | 546.3 | — | — | 130.9 |
| | de Ruiter & Beringen | 433.7 | — | — | 90.3 |
| | LCPC | 574.8 | — | — | 98.9 |
| | Average | 518.3 | — | — | 106.7 |
| Static Analysis | α-method and Nordlund method | 415.1 | 78.4 | 201.5 | — |
| Dynamic measurement | CAPWAP (EOD) | — | — | — | — |
| | CAPWAP (14 days-BOR) | — | — | — | — |
| Load Test Interpretation Method | Davisson method | 518 | 83.2 | 153 | 96 |

* Cohesive (mainly clayey and silty clay soils) and Cohesionless (mainly sandy soils); $Q_u$: Total ultimate capacity

**Table 4**
**Results of the analysis conducted on square precast prestressed concrete piles driven into Louisiana soils (continued)**

| | State Project Identification | 455-05-0036 | 455-05-0036 | 434-01-0002 | 239-01-0080 |
|---|---|---|---|---|---|
| | | Sugarhouse Road | Sugarhouse Road | Mississippi River Bridge at Gramercy (West Approaches) | ICWW Bridge Approaches (Louisa) |
| Pile and Soil Identification | Pile ID | TP2, 14" Square PPC | TP3, 14" Square PPC | TP3, 14" Square PPC | TP3, 14" Square PPC |
| | Pile Length (ft.) | 75 | 65 | 105 | 60 |
| | Embedded Length (ft.) | 70 | 59 | 64 | 55 |
| | Pile Classification | Skin | Skin | Skin | Skin |
| | Predominant Soil* | Cohesive | Cohesive | Cohesionless | Cohesive |
| Methods of Predicting Pile Capacity by Cone Penetration Test | Predicted Ultimate Load (ton) | $Q_u$ | $Q_u$ | $Q_u$ | $Q_u$ |
| | Schmertmann | 111.6 | 121 | 201.8 | 130.5 |
| | de Ruiter & Beringen | 95.4 | 69 | 175.8 | 107.6 |
| | LCPC | 105 | 80.5 | 182.8 | 108.1 |
| | Average | 104 | 90.2 | 186.8 | 115.4 |
| Static Analysis | α-method and Nordlund method | — | — | — | — |
| Dynamic measurement | CAPWAP (EOD) | — | — | — | — |
| | CAPWAP (14 days-BOR) | — | — | — | — |
| Load Test Interpretation Method | Davisson method | 96.5 | 69 | 230 | 115.5 |

* Cohesive (mainly clayey and silty clay soils) and Cohesionless (mainly sandy soils); $Q_u$: Total ultimate capacity

**Table 4**
**Results of the analysis conducted on square precast prestressed concrete piles driven into Louisiana soils (continued)**

| | State Project Identification | 239-01-0080 | 855-14-0003 | Alexandria | 424-06-0005 |
|---|---|---|---|---|---|
| | | ICWW Bridge Approaches (Louisa) | Intercoastal Waterway Bridge (Prospect Ave.) | Pinville-Tioga Highway Railroad Overpass | Bayou Boeuf Bridge |
| Pile and Soil Identification | Pile ID | TP4, 30" Square PPC | TP1, 18" Square PPC | TP1, 14" Square PPC | TP4, 14" Square PPC |
| | Pile Length (ft.) | 91.9 | | | 85 |
| | Embedded Length (ft.) | 84.3 | 95 | 31 | 79 |
| | Pile Classification | Skin | Skin | Skin | Skin |
| | Predominant Soil* | Cohesive | Cohesive | Cohesive | Cohesive |
| Methods of Predicting Pile Capacity by Cone Penetration Test | Predicted Ultimate Load (ton) | $Q_u$ | $Q_u$ | $Q_u$ | $Q_u$ |
| | Schmertmann | 411.2 | 107.8 | 132.2 | 124.3 |
| | de Ruiter & Beringen | 321.8 | 116.7 | 80.5 | 79.5 |
| | LCPC | 310 | 112.2 | 110.1 | 97.4 |
| | Average | 347.7 | 112.2 | 107.6 | 100.4 |
| Static Analysis | α-method and Nordlund method | — | — | — | — |
| Dynamic measurement | CAPWAP (EOD) | — | — | — | — |
| | CAPWAP (14 days-BOR) | — | — | — | — |
| Load Test Interpretation Method | Davisson method | 360.8 | 216 | 90 | 120 |

* Cohesive (mainly clayey and silty clay soils) and Cohesionless (mainly sandy soils); $Q_u$: Total ultimate capacity

**Table 4**
**Results of the analysis conducted on square precast prestressed concrete piles driven into Louisiana soils (continued)**

| | State Project Identification | 424-07-0009 | 424-07-0009 | 450-36-0002 | 283-03-0052 (New Orleans) |
|---|---|---|---|---|---|
| | | Gibson-raceland highway | Gibson-raceland highway | Luling Bridge - US61 | West Bank Expressway |
| Pile and Soil Identification | Pile ID | TP4A, 30" Square PPC | TP4, 30" Square PPC | TP8, 30" Square PPC | TP1, 18" Square PPC |
| | Pile Length (ft.) | 125 | 125 | 120 | |
| | Embedded Length (ft.) | 124 | 120 | 112 | 120 |
| | Pile Classification | — | Skin | End Bearing | Skin |
| | Predominant Soil* | — | Cohesive | Cohesive | Cohesive |
| Methods of Predicting Pile Capacity by Cone Penetration Test | Predicted Ultimate Load (ton) | $Q_u$ | $Q_u$ | $Q_u$ | $Q_u$ |
| | Schmertmann | 739.2 | 740.2 | 794.7 | 128.6 |
| | de Ruiter & Beringen | 506 | 507 | 656.4 | 179.2 |
| | LCPC | 606.3 | 607.3 | 796.6 | 169.1 |
| | Average | 617.2 | 618.2 | 749.2 | 159 |
| Static Analysis | α-method and Nordlund method | — | — | — | — |
| Dynamic measurement | CAPWAP (EOD) | — | — | — | — |
| | CAPWAP (14 days-BOR) | — | — | — | — |
| Load Test Interpretation Method | Davisson method | 633 | 320 | 482 | 372 |

* Cohesive (mainly clayey and silty clay soils) and Cohesionless (mainly sandy soils); $Q_u$: Total ultimate capacity

**Table 4**
**Results of the analysis conducted on square precast prestressed concrete piles driven into Louisiana soils (continued)**

| | | |
|---|---|---|
| | State Project Identification | 090-01-0015 |
| | | Lake Bistineau Spillway Bridge & Approaches |
| Pile and Soil Identification | Pile ID | TP6, 24" Square PPC |
| | Pile Length (ft) | — |
| | Embedded Length (ft) | 60 |
| | Pile Classification | End Bearing |
| | Predominant Soil* | Cohesive |
| Methods of Predicting Pile Capacity by Cone Penetration Test | Predicted Ultimate Load (ton) | $Q_u$ |
| | Schmertmann | 347.7 |
| | de Ruiter & Beringen | 241.5 |
| | LCPC | 258.3 |
| | Average | 282.5 |
| Static Analysis | α-method and Nordlund method | — |
| Dynamic measurement | CAPWAP (EOD) | — |
| | CAPWAP (14 days - BOR) | — |
| Load Test Interpretation Method | Davisson method | 270.5 |

* Cohesive (mainly clayey and silty clay soils) and Cohesionless (mainly sandy soils); $Q_u$: Total ultimate capacity

**Table 5**
**Evaluation summary of the different prediction methods**

| Pile Capacity Prediction Method | $R_p/R_m$* | | Best fit calculations | |
|---|---|---|---|---|
| | Mean | σ | $R_{fit}/R_m$* | $R^2$ |
| Static α-method | 1.12 | 0.32 | 1.00 | 0.84 |
| Schmertmann method | 1.20 | 0.37 | 1.20 | 0.81 |
| LCPC method | 1.05 | 0.38 | 1.11 | 0.78 |
| de-Ruiter & Beringen method | 0.90 | 0.28 | 0.94 | 0.84 |
| Average of CPT methods | 1.05 | 0.33 | 1.08 | 0.82 |
| CAPWAP–EOD method | 0.35 | 0.23 | 0.32 | 0.69 |
| CAPWAP–14 days BOR method | 0.83 | 0.22 | 0.92 | 0.91 |

* Davisson method and modified Davisson method

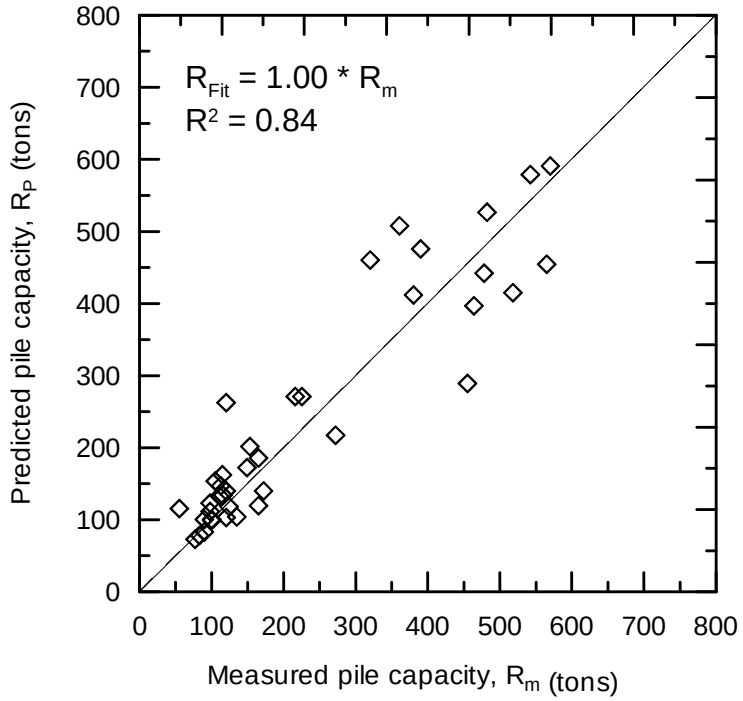


**Figure 10**
**$R_m$ versus $R_p$ (Static method)**

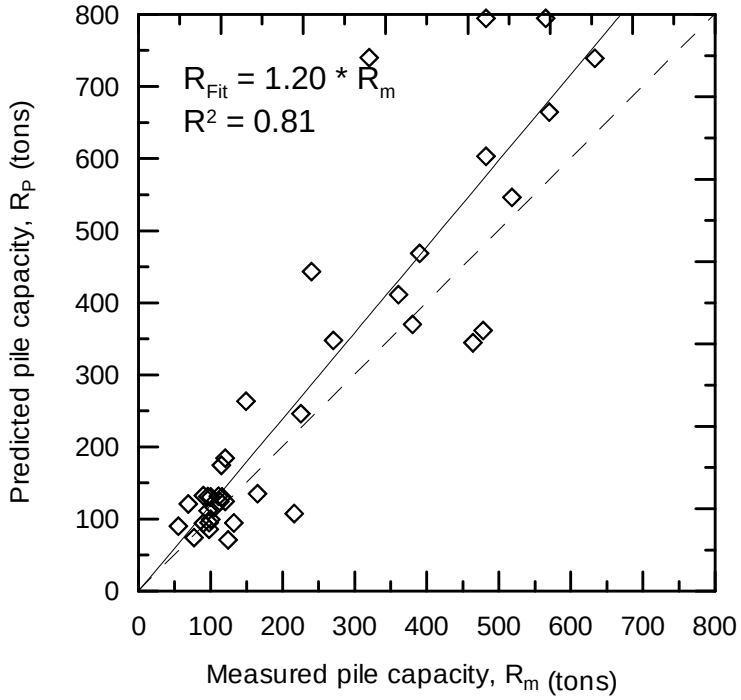


**Figure 11**
**$R_m$ versus $R_p$ (Schmertmann method)**

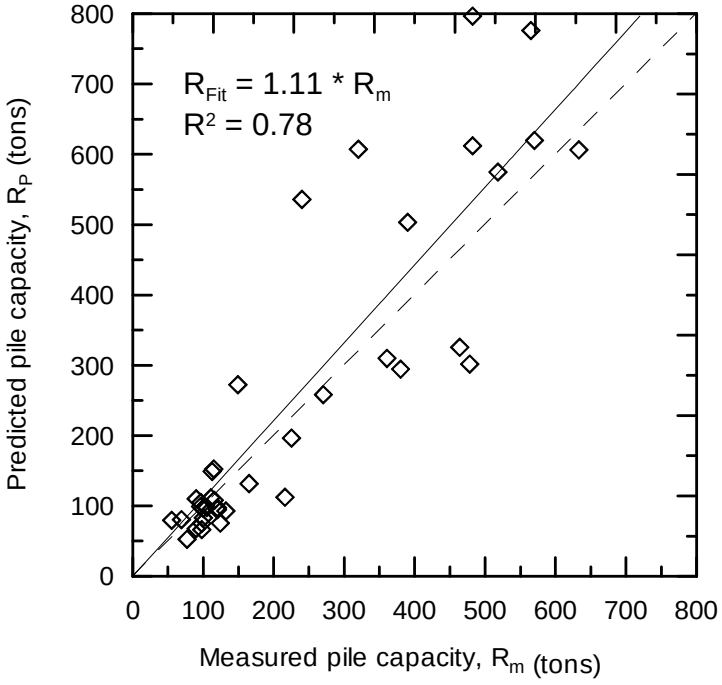


**Figure 12**
**$R_m$ versus $R_p$ (LCPC method)**

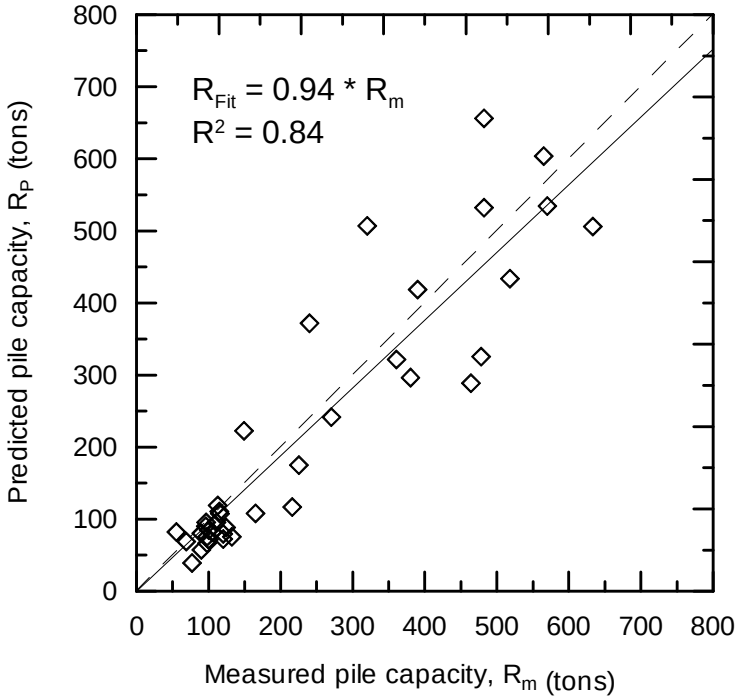


**Figure 13**
**$R_m$ versus $R_p$ (De Ruiter method)**

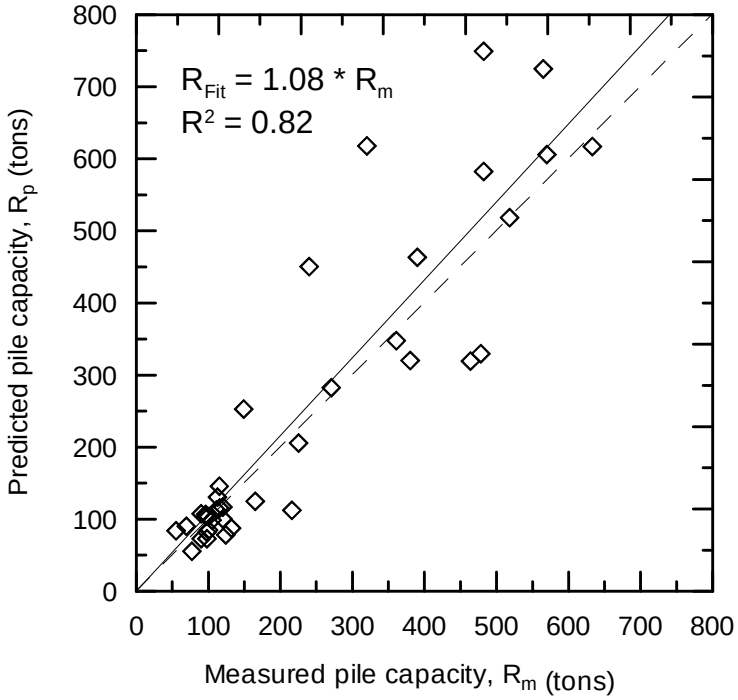


**Figure 14**
**$R_m$ versus $R_p$ (CPT - Average method)**

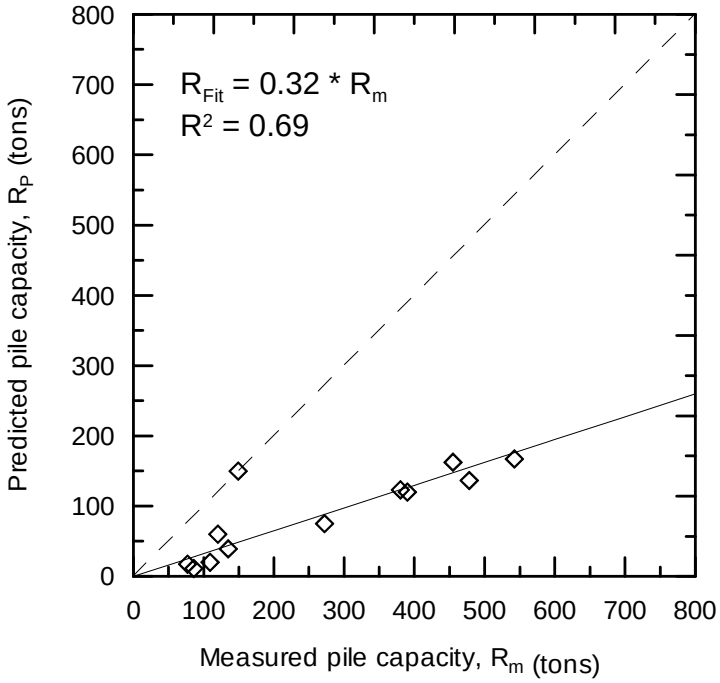


**Figure 15**
**$R_m$ versus $R_p$ (CAPWAP-EOD)**

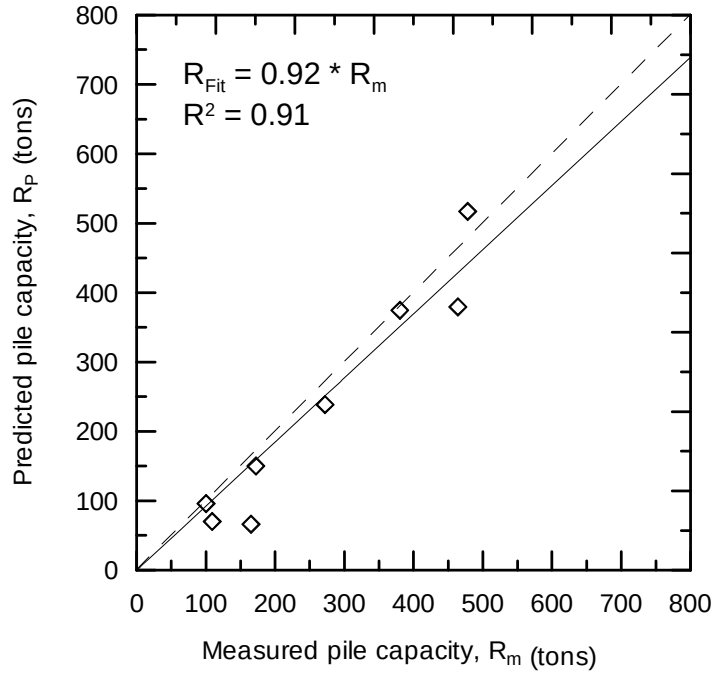


**Figure 16**
**$R_m$ versus $R_p$ (CAPWAP-14 days BOR)**

## LRFD Calibration

Figures 17 to 23 present the histogram and the normal and log-normal distribution of the measured to predicted pile resistance ($R_m/R_p$) of the static method, three CPT methods, the average of three CPT methods, and dynamic measurement with signal matching analysis (CAPWAP), respectively. Also Figures 24 to 30 illustrate the cumulative distribution function (CDF) of the bias values for each design method. As shown in the figures, generally the log-normal distribution matches the histogram and CDF better than the normal distribution. In addition, the resistance bias factor ($\lambda_R = R_m/R_p$) can range theoretically from 0 to infinity with an optimum value of one; therefore, the distribution of the resistance bias can be assumed to follow a log-normal distribution *[42]*. In this study, the log-normal distribution was used to evaluate the different methods based on prediction accuracy and to calibrate the resistance factors.

Reliability analyses were conducted and the resistance factors for all pile design methods were calibrated at $Q_D/Q_L = 3$. This ratio was selected since the reliability index (β) converges for $Q_D/Q_L$ exceeding 3 *[23]*. Figures 31 through 37 present the resistance factors determined for various reliability indexes (β) for the different pile design methods. As shown in the figures, the resistance factors (ϕ) determined by the advanced methods (FORM and Monte Carlo simulation method) are relatively close and generally higher than the resistance factors (ϕ) obtained from FOSM.

A review of the literature indicates that the required target reliability indexes are between 2.33 and 3 for geotechnical applications. The resistance factors (ϕ) determined by FOSM, FORM, and the Monte Carlo simulation method for different pile design methods corresponding to reliability index of 2.33 are tabulated in Table 6. The resistance factors for the static method determined in this study are 0.56 (FOSM) and 0.63 (FORM and Monte Carlo simulation method), which is higher than the ϕ value recommended by AASHTO (e.g., ϕ = 0.34-0.45 for static method, and ϕ = 0.50 for Schmertmann method) *[11]*. It should be noted that this value is only valid for subsurface conditions similar to Louisiana soils that consist mainly of soft cohesive soils with some cohesionless inter-layering soils. For this condition, the driven pile resistance was determined using the α-Tomlinson method dominantly and the Nordlund method was employed for cohesionless inter-layering soils. Among the three direct CPT methods, the De Ruiter and Beringen method shows the highest resistance factor [ϕ = 0.66 (FOSM), 0.74 (FORM), and 0.73 (Monte Carlo simulation method)], while the Schmertmann method shows the lowest resistance factor [ϕ = 0.44 (FOSM), 0.48 (FORM), and 0.49 (Monte Carlo simulation)], which is lower than the

AASHTO value of 0.5. For the dynamic measurement with signal matching analysis, the resistance factors obtained for the CAPWAP (EOD) is 1.31 (FOSM) and 1.41 (FORM), which is higher than those of CAPWAP (14 days BOR) of 0.55 (FOSM), 0.61 (FORM) and 0.62 (Monte Carlo simulation method). This is mainly due to the pile setup effect. Although the CAPWAP (EOD) has a high resistance factor, it is not an economical and reliable approach because it significantly underestimates the resistance and has low efficiency factors of 0.36 (FOSM) and 0.39 (FORM). The dynamic measurement is mainly used for pile drivability rather than for design.

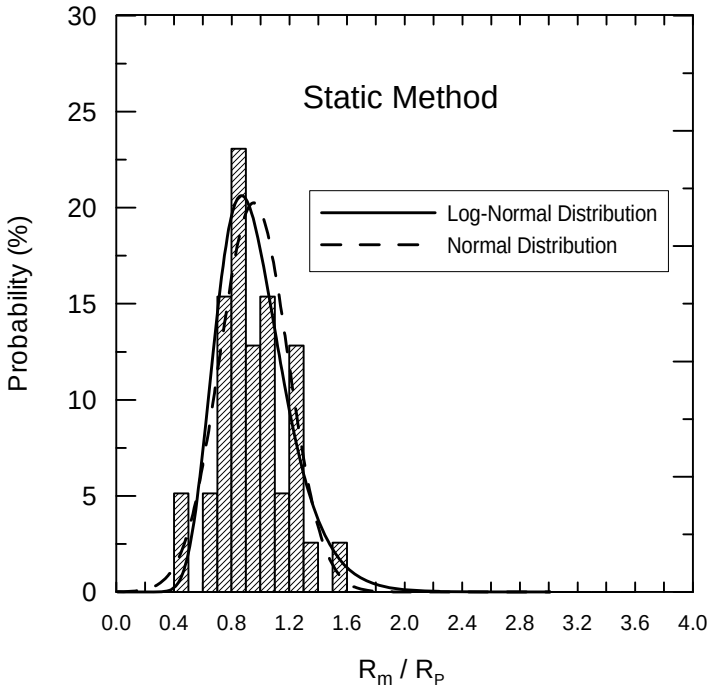


**Figure 17**
**Histogram and PDF of resistance bias factors (Static method)**

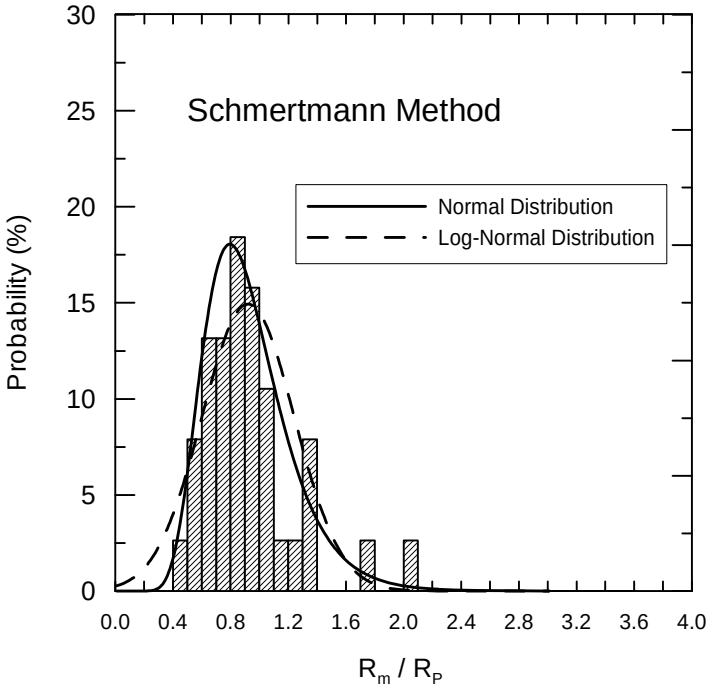


**Figure 18**
**Histogram and PDF of resistance bias factors (Schmertmann method)**

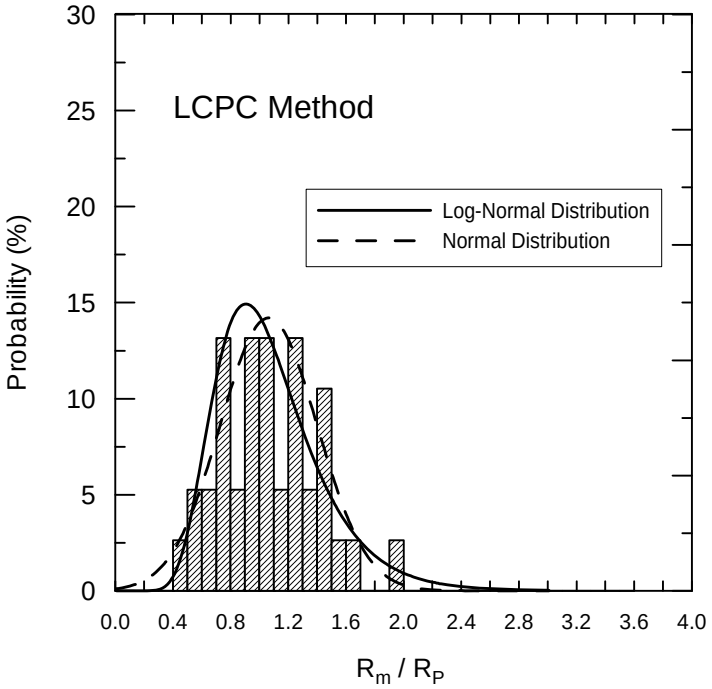


**Figure 19**
**Histogram and PDF of resistance bias factors (LCPC method)**

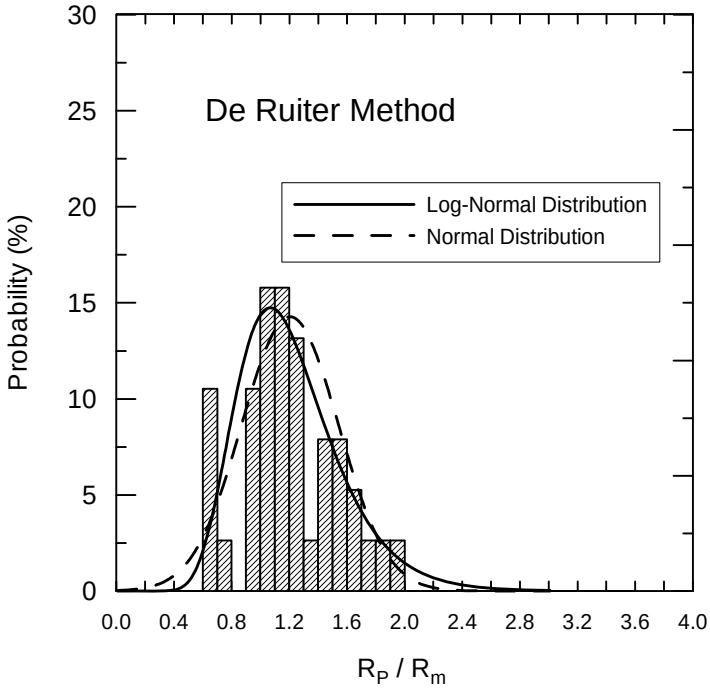


**Figure 20**
**Histogram and PDF of resistance bias factors (De Ruiter method)**

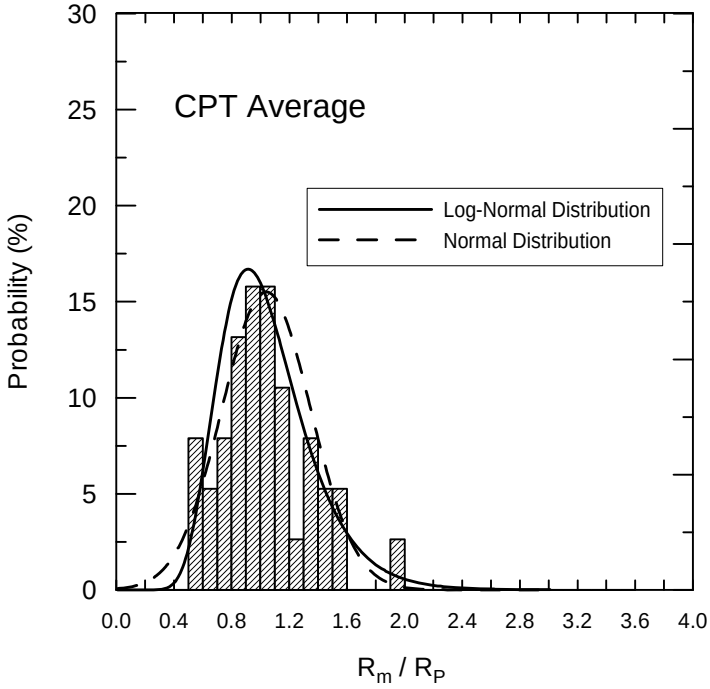


**Figure 21**
**Histogram and PDF of resistance bias factors (CPT - Average method)**

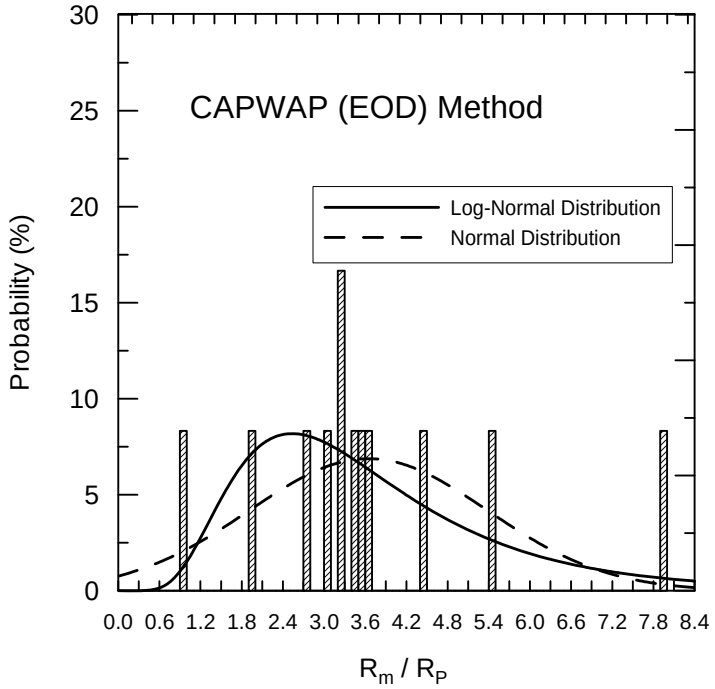


**Figure 22**
**Histogram and PDF of resistance bias factors (CAPWAP-EOD)**

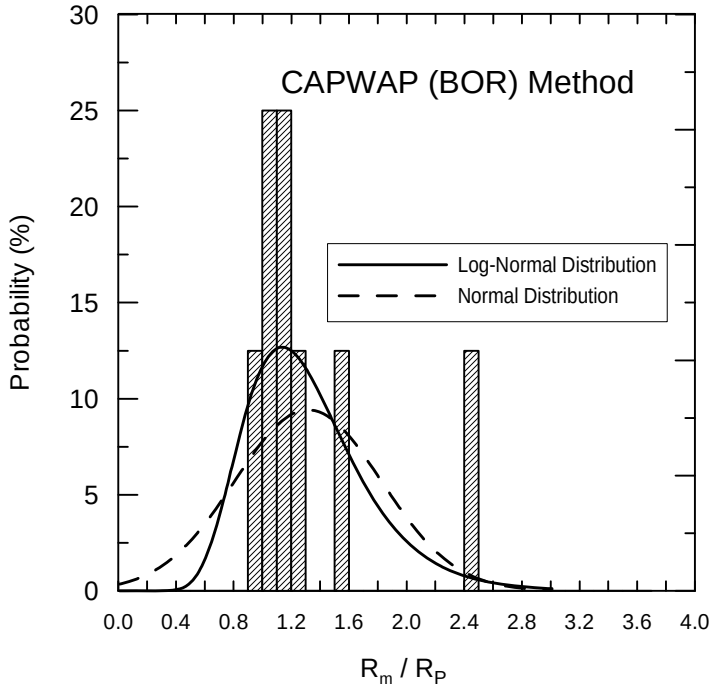


**Figure 23**
**Histogram and PDF of resistance bias factors (CAPWAP-14 days BOR)**

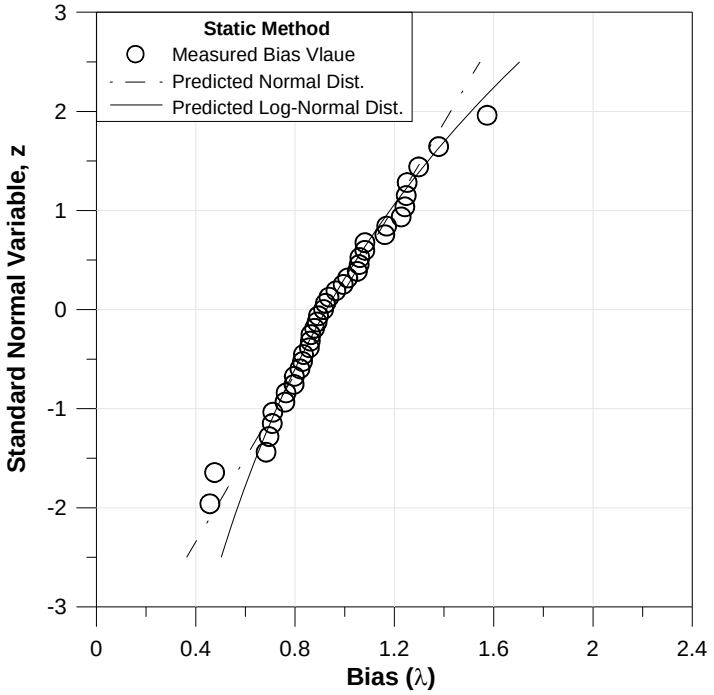


**Figure 24**
**Cumulative distribution function (CDF) of bias values (Static method)**

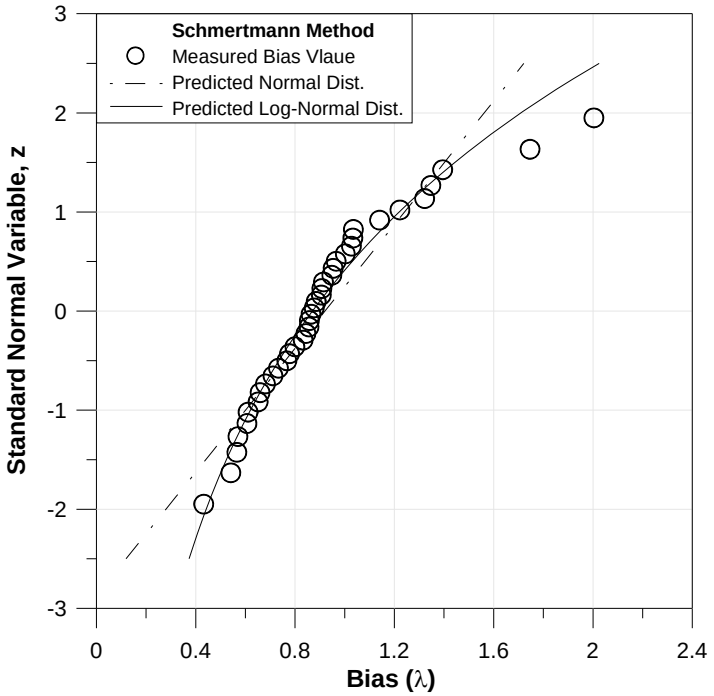


**Figure 25**
**Cumulative distribution function (CDF) of bias values (Schmertmann method)**

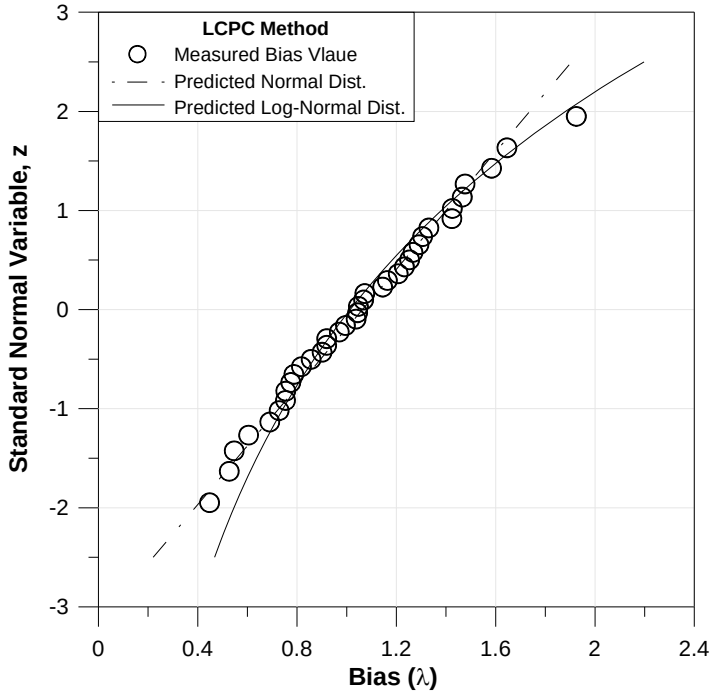


**Figure 26**
**Cumulative distribution function (CDF) of bias values (LCPC method)**

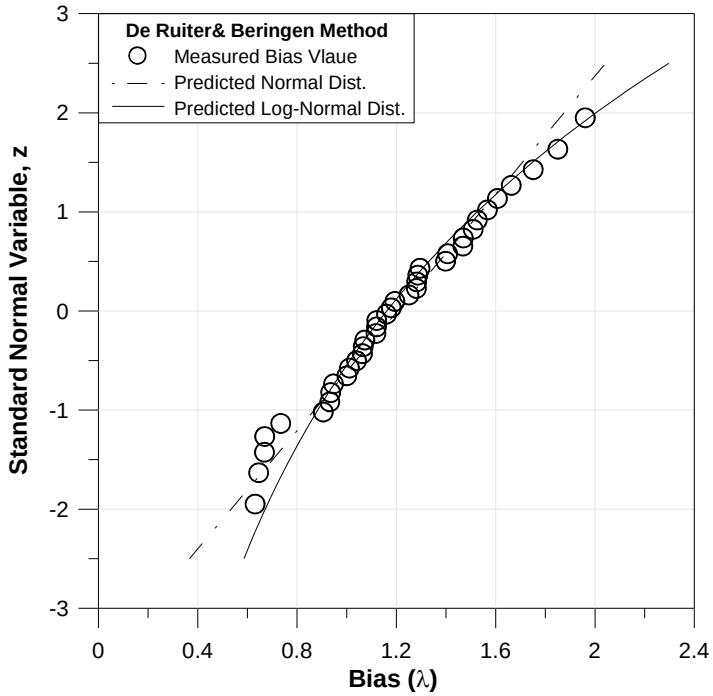


**Figure 27**
**Cumulative distribution function (CDF) of bias values (De Ruiter method)**

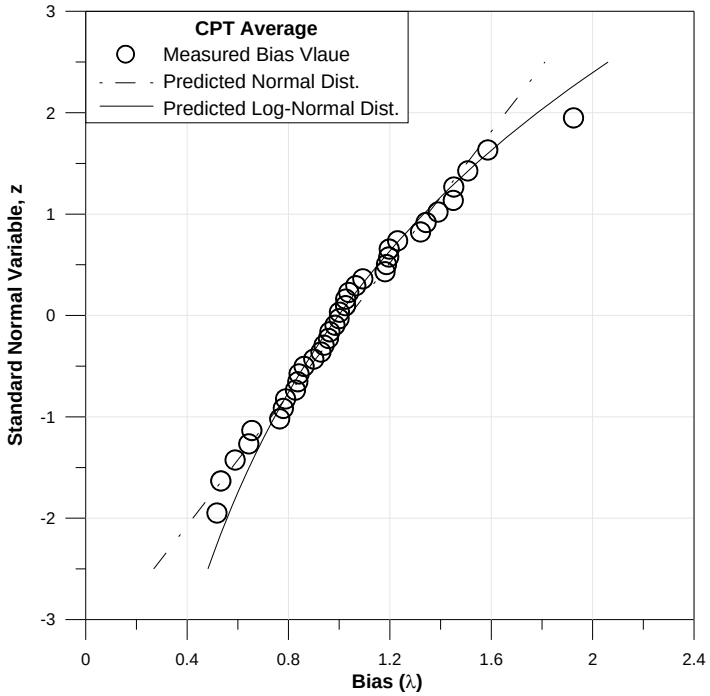


**Figure 28**

**Cumulative distribution function (CDF) of bias values (CPT-Average method)**

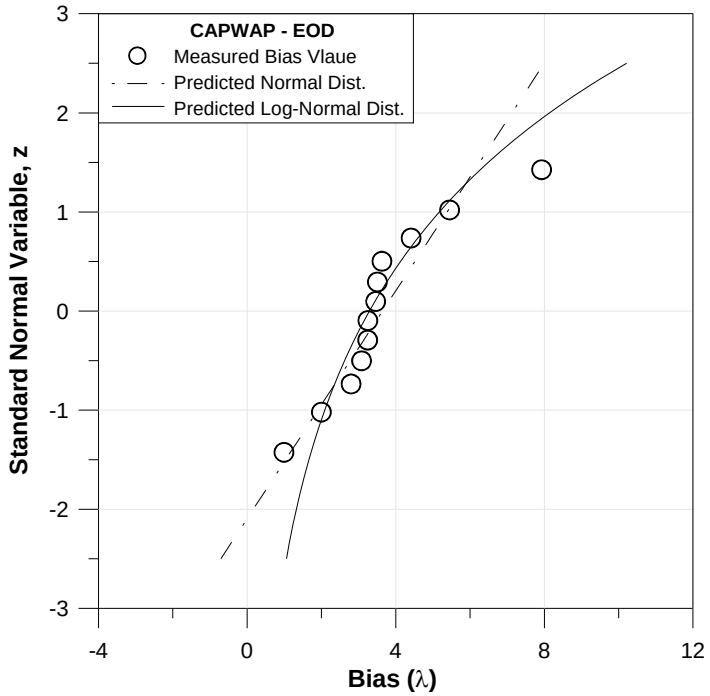


**Figure 29**

**Cumulative distribution function (CDF) of bias values (CAPWAP-EOD)**

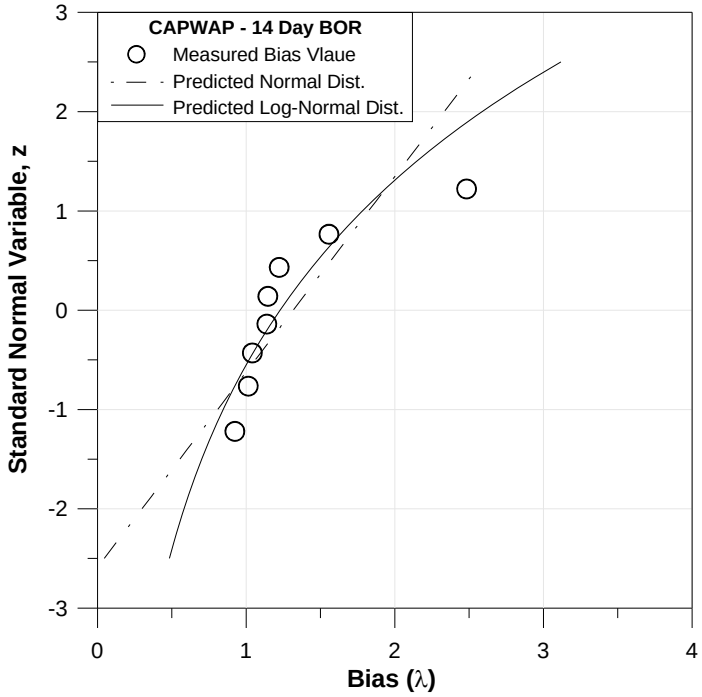


**Figure 30**
**Cumulative distribution function (CDF) of bias values (CAPWAP-14 days BOR)**

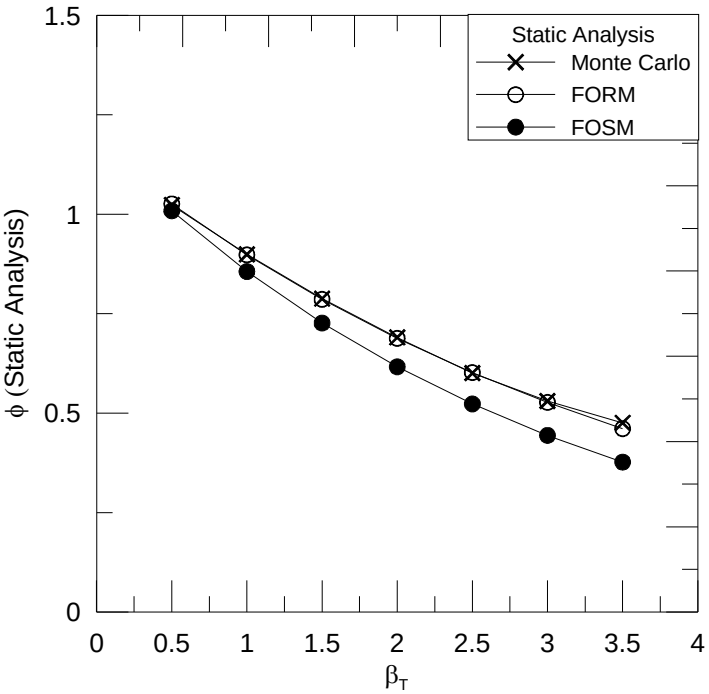


**Figure 31**
**Resistance factors for different reliability indexes (Static method)**

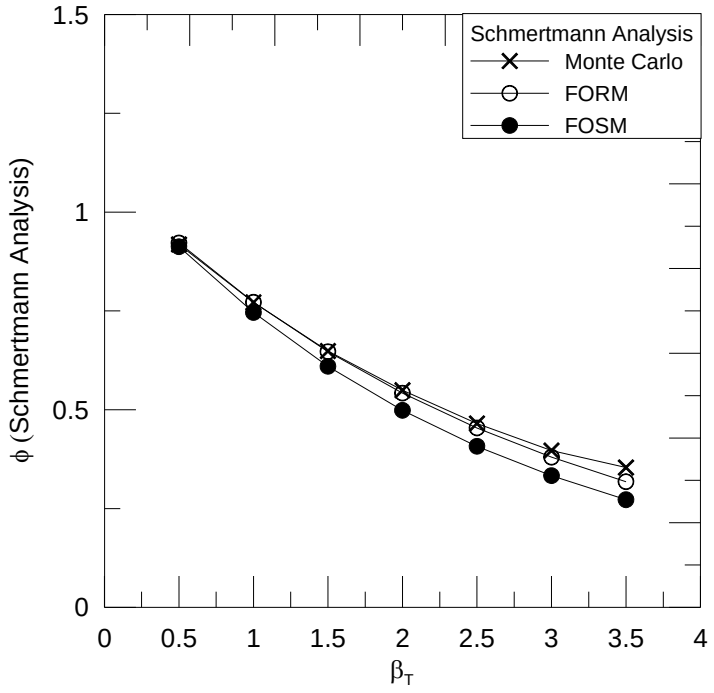


**Figure 32**
**Resistance factors for different reliability indexes (Schmertmann method)**

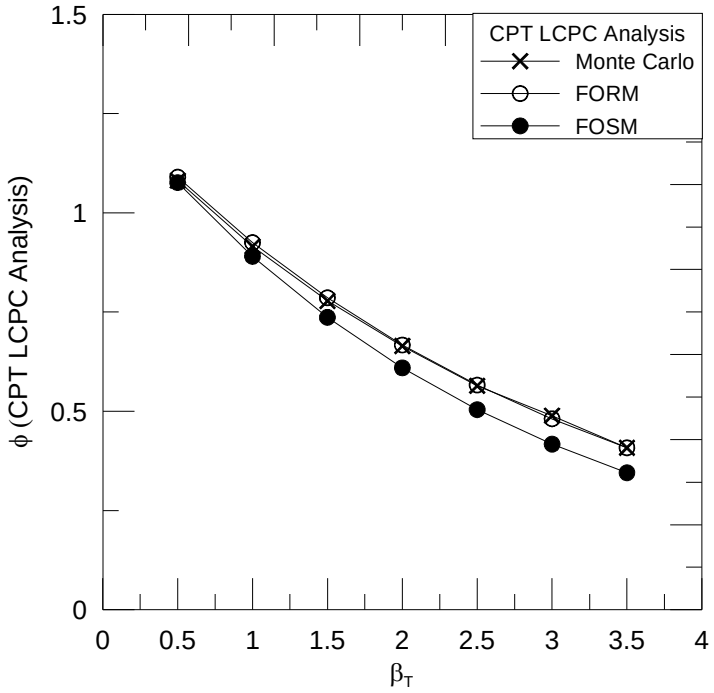


**Figure 33**
**Figure 26 Resistance factors for different reliability indexes (LCPC method)**

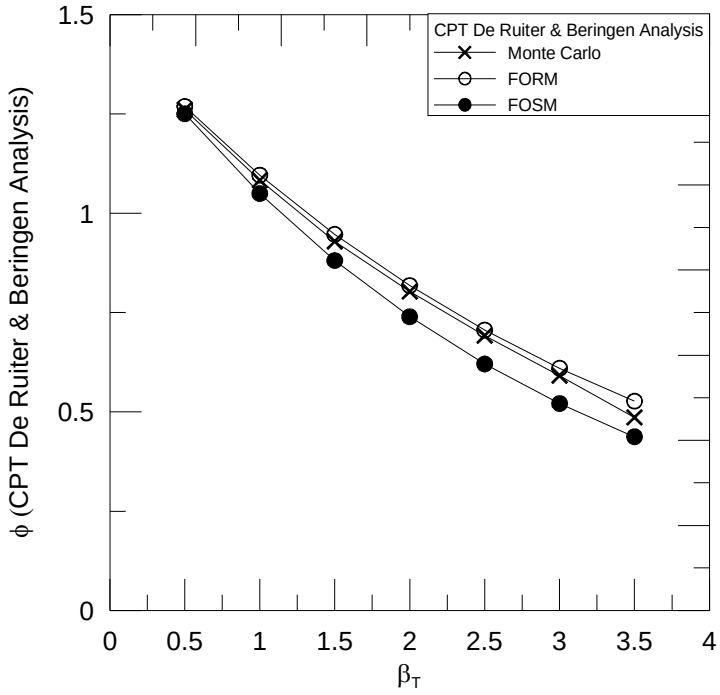


**Figure 34**
**Resistance factors for different reliability indexes (De Ruiter method)**

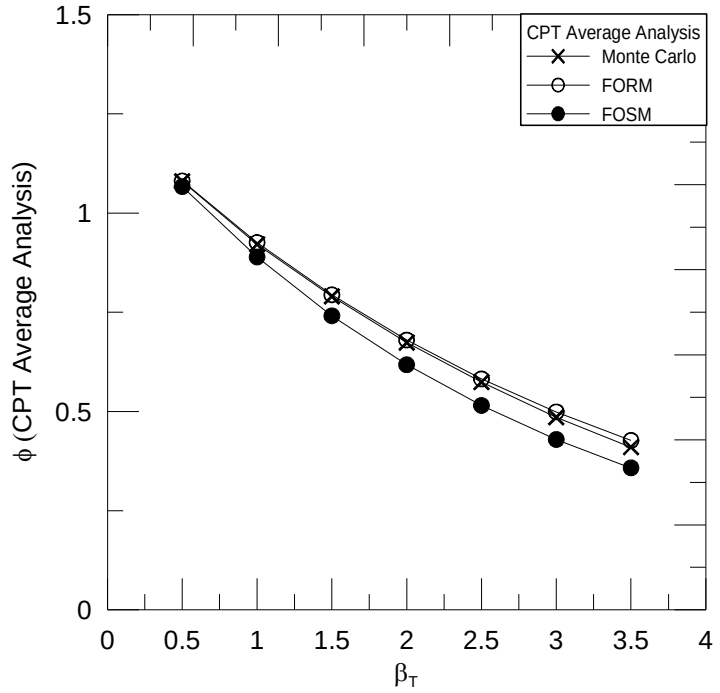


**Figure 35**
**Resistance factors for different reliability indexes (CPT - Average method)**

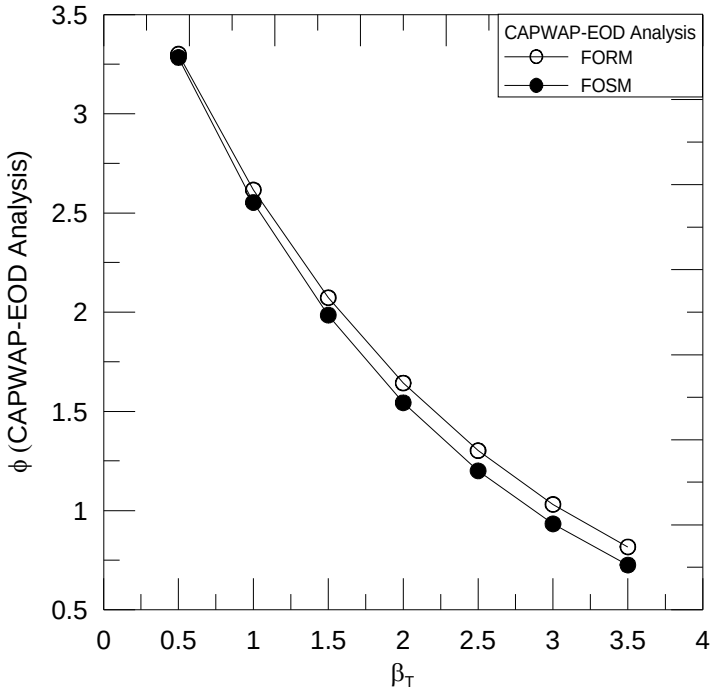


**Figure 36**
**Resistance factors for different reliability indexes (CAPWAP-EOD)**

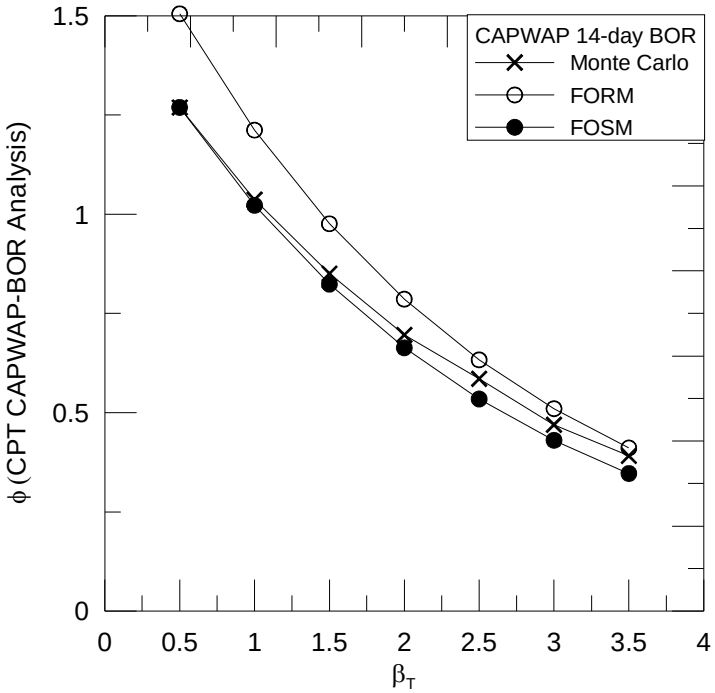


**Figure 37**
**Resistance factors for different reliability indexes (CAPWAP-14 days BOR)**

**Table 6**
**Resistance Factors ($\phi$) for Driven Piles ($\beta_T = 2.33$)**

| Design Method | | Proposed Resistance Factor ($\phi$) and Efficiency Factor ($\phi/\lambda$) for Louisiana Soil | | | | | | Resistance Factor, $\phi$ [AASHTO (11)] |
|---|---|---|---|---|---|---|---|---|
| | | FOSM | | FORM | | Monte Carlo Simulation | | |
| | | $\phi$ | $\phi/\lambda$ | $\phi$ | $\phi/\lambda$ | $\phi$ | $\phi/\lambda$ | |
| Static method | $\alpha$-Tomlinson method and Nordlund method | 0.56 | 0.58 | 0.63 | 0.66 | 0.63 | 0.66 | 0.35-0.45 |
| Direct CPT method | Schmertmann | 0.44 | 0.47 | 0.48 | 0.52 | 0.49 | 0.53 | 0.50 |
| | LCPC/LCP | 0.54 | 0.51 | 0.60 | 0.56 | 0.59 | 0.56 | — |
| | De Ruiter and Beringen | 0.66 | 0.55 | 0.74 | 0.62 | 0.73 | 0.61 | — |
| | CPT average | 0.55 | 0.53 | 0.61 | 0.59 | 0.62 | 0.59 | — |
| Dynamic measurement | CAPWAP (EOD) | 1.31 | 0.36 | 1.41 | 0.39 | — | — | — |
| | CAPWAP (14 days BOR) | 0.55 | 0.44 | 0.61 | 0.52 | 0.62 | 0.47 | 0.65 |

# CONCLUSIONS

This study presents a reliability based evaluation of different design methods for predicting the ultimate axial resistance of piles driven into Louisiana soils. Resistance factors ($\phi$) of single driven piles needed to implement the LRFD design methodology were determined for each design method. A pile load test (a soil database of 53 square PPC piles of different sizes and lengths) that was tested to failure was collected from LADOTD archives and used to calibrate the resistance factors. For each pile load test, the measured ultimate pile resistance was estimated using the Davisson interpretation method and modified Davisson method for piles with a larger size. In addition, the load carrying resistance of each pile was predicted using the static method, three CPT methods (Schmertmann, De Ruiter-Beringen, and LCPC methods), the average of three CPT methods, and the dynamic CAPWAP (EOD and BOR) methods.

Statistical analyses comparing the predicted and measured pile resistances were conducted to evaluate the performance of the different pile design methods. The results of the statistical analyses showed that the static method ($\alpha$-Tomlinson method and Nordlund method) over-predicted the pile resistance by 12 percent. Among the three direct CPT methods, the De Ruiter-Beringen method was the most consistent prediction method with the lowest COV. Both dynamic measurements with signal matching analysis methods (CAPWAP-EOD and 14 days BOR) showed under-predication of pile resistance with a setup factor of 2.9.

Reliability analyses based on FOSM, FORM, and the Monte Carlo simulation method were conducted to calibrate the resistance factors ($\phi$) for the investigated pile design methods. These factors are needed to comply with the FHWA mandate in the LRFD design of single driven piles. The design input parameters were adopted from the AASHTO LRFD design specifications for bridge substructure. The resistance factors ($\phi$) that corresponded to a dead load to live load ratio ($Q_D/Q_L$) of 3 as a function of target reliability index ($\beta_T$) were presented. Based on the results of reliability analyses for $\beta_T = 2.33$, the De Ruiter-Beringen method showed the highest resistance factor [$\phi_{\text{De-Ruiter}} = 0.66$ (FOSM), 0.74 (FORM), and 0.73 (Monte Carlo simulation method)], while the Schmertmann method showed the lowest resistance factor [$\phi_{\text{Schmertmann}} = 0.44$ (FOSM), 0.48 (FORM), and 0.49 (Monte Carlo simulation method)], which is lower than the AASHTO recommended value of 0.5. The resistance factors obtained for the CAPWAP (EOD) were 1.31 (FOSM), 1.41 (FORM), which is higher than CAPWAP (14 day BOR) resistance factors of 0.55 (FOSM), 0.61 (FORM), and 0.62 (Monte Carlo simulation method). This is mainly due to pile setup. Although the CAPWAP (EOD) has a high resistance factor, it is not an economical and

reliable approach because it significantly underestimates the resistance and has a low efficiency factor. However, the dynamic measurement is mainly used for pile drivability rather than for design.

# RECOMMENDATIONS

1. LADOTD engineers need to start implementing the resistance factors ($\phi$) recommended for the different pile design methods based on Louisiana pile load test—a soil database in the LRFD design of driven piles for all future state projects.

2. It is recommended to select a few projects to demonstrate the cost benefit study and comparison between the LRFD design and the traditional ASD design.

3. It is recommended to hold a workshop to train LADOTD engineers in the LRFD design of pile foundations.

4. It is recommended to continue collecting pile load test data from new projects, especially for those cases in which the end bearing and side frictional capacities can be separated for possible future re-calibration of resistance factors of different pile design methods every two years.

5. Since the Co-PI's are from the geotechnical design section at LADOTD, they are already in the process of implementing previously mentioned recommendation items 1, 2, and 3 based on the findings of this research project.

6. It should be noted that performing complete reliability analyses of a pile foundation requires the inclusions of all risk factors. Scour is a critical factor in the selection of pile tip elevations. The risk associated with scouring directly impacts the reliability of pile foundations. This is mainly due to expected changes on the in-situ stress state (overburden and stress history) of the subsurface soil that will affect the laboratory and in-situ test results. However, the scope of this study does not include the evaluation of scour and is recommended to be considered in the future.

# ACRONYMS, ABBREVIATIONS, AND SYMBOLS

| | |
|---|---|
| AASHTO | American Association of Highway and Transportation Officials |
| ASD | Allowable Stress Design |
| BOR | Beginning of Restrike |
| CAPWAP | Case Pile Wave Analysis Program |
| EOD | End of Driving |
| CDF | Cumulative Distribution Function |
| COV | Coefficient of Variation |
| CPT | Cone Penetration Test |
| DOT | Department of Transportation |
| EOD | End of Driving |
| FHWA | Federal Highway Administration |
| FORM | First Order Reliability Method |
| FOSM | Fisrt Order Second Moment |
| FS | Factor of Safety |
| LADOTD | Louisiana Department of Transportation and Development |
| LCPC | Laboratiore Central Des Ponts et Chausses |
| LDP-CPT | Louisiana Pile Design by Cone Penetration Test |
| LRFD | Load and Resistance Factor Design |
| LTRC | Louisiana Transportation Research Center |
| MC | Monte Carlo Method |
| NC | Normally Consolidated |
| OC | Overconsolidated |
| PDF | Probability Density Function |
| PPC | Precast-Prestressed Concrete |
| SLS | Serviceability Limit State |
| SPT | Standard Penetration Test |
| ULS | Ultimate Limit State or Strength Limit State |

# REFERENCES


1. AASHTO. "LRFD Highway Bridge Design Specifications," 1st Edition, American Association of State Highway and Transportation Officials, Washington, D.C., USA, 1994.
2. AASHTO. "LRFD Bridge Design Specifications," 2nd Edition, American Association of State Highway and Transportation Officials, Washington, D.C., USA, 1998.
3. Paikowsky, S. G. "Load and Resistance Factor Design (LRFD) for Deep Foundations," NCHRP Report 507, *Transportation Research Board*, Washington, DC., 2004.
4. Allen, Tony M. "Development of the WSDOT Pile Driving Formula and Its Calibration and Resistance Factor Design (LRFD)," FHWA Report, WA-RD 610.1, Washington State Department of Transportation, 2005.
5. McVay, M.; Birgisson, B.; Zhang, L.; Perez, A; and Putcha, S. "Load and Resistance Factor Design (LRFD) for Driven Piles Using Dynamic Methods—A Florida Perspective." *Geotechnical Testing Journal*, Vol. 23, No. 1, 2000, pp. 55-66.
6. McVay, M;, Birgisson, B.; Nguyen, T.; and Kuo, C. "Uncertainty in LRFD phi, $\phi$, Factors for Driven Prestressed Concrete Piles," In *Transportation Research Record: Journal of the Transportation Research Board, No. 1808*, TRB, National Research Council, Washington, DC., 2002, pp. 99-107.
7. Allen, T. "Development of a New Pile Driving Formula and Its Calibration for Load and Resistance Factor Design," Proceedings for the 86th TRB Annual meeting. Washington, DC, TRB, 2006.
8. Yang, L, and Liang, R. "Incorporating Setup into Load and Resistance Factor Design of Driven Piles in Sand," Proceedings for the 86th TRB Annual meeting. Washington, DC, TRB, 2006.
9. Nowak, A. S., "Calibration of LRFD Bridge Design Code," NCHRP Report 368, Transportation Research Board, Washington, DC., 1999.
10. Allen, T.; Nowak, A.; and Bathurst, R. "Calibration to Determine Load and Resistance Factors for Geotechnical and Structural Design." TRB Circular E-C079, Transportation Research Board, Washington, D.C., 2005.
11. AASHTO. "LRFD Bridge Design Specifications," 4th Edition, American Association of State Highway and Transportation Officials, Washington, D.C., USA, 2007.
12. DiMaggio, J.; Saad, T.; Allen, T.; Passe, P.; Goble, G.; Christopher, B.; DiMillio, A.; Person, G.; and Shike, T. "FHWA Summary Report of the Geotechnical Engineering Study Tour (GEST)." FHWA International Technology Scanning Program, December, FHWA, 1998.

13. Paikowsky, S.; Regan, J.; and McDonnell, J. "A Simplified Field Method for Capacity Evaluation of Driven Piles." FHWA RD- 94-042, FHWA, 1994.
14. Schmertmann, J. H. "Guidelines for Cone Penetration Test, Performance, and Design." Report No. FHWA-TS-79-209, U.S. Department of Transportation, Federal Highway Administration, Washington, D.C., 1978.
15. De Ruiter, J., and Beringen F. L. "Pile Foundations for Large North Sea Structures." *Marine Geotechnology*, Vol. 3, No. 3, 1979, pp. 267-314.
16. Bustamante, M., and Gianeselli L. "Pile Bearing Capacity Prediction by Means of Static Penetrometer CPT." Proc. 2nd European Symposium Penetration Testing, Vol. 2, Balkema, Amsterdam, 1982, pp. 493-500.
17. Eslami, A., and Fellenius, B. H. "Pile Capacity by Direct CPT and CPTU Methods Applied to 102 Case Histories," *Canadian Geotech. Journal*, Vol. 34, 1997, pp. 886-904.
18. Tomlinson, M.J. *Foundation Design and Construction*, 4th Edition, Pitman Advanced Publishing Program, 1980.
19. Hannigan, P.; Goble, G.; Thendean, G; Likins, G; and Rausche, F. "Design and Construction of Driven Pile Foundations, Volume 1." FHWA-HI-97-013, Federal Highway Administration. 1998.
20. Thurman, A.G. "Discussion of Bearing Capacity of Piles in Cohesionless Soils." American Society of Civil Engineers, ASCE, *Journal of the Soil Mechanics and Foundations Division*, SM1, 1964, pp. 127-129.
21. Nordlund, R.L. "Bearing Capacity of Piles in Cohesionless Soils." American Society of Civil Engineers, ASCE, *Journal of the Soil Mechanics and Foundations Division*, SM3, 1963, pp. 1-35.
22. Nordlund, R.L. "Point Bearing and Shaft Friction of Piles in Sand." Missouri-Rolla 5th Annual Short Course on the Fundamentals of Deep Foundation Design, 1979.
23. Abu-Farsakh M. Y., and Titi H., "Probabilistic CPT Method for Estimating the Ultimate Capacity of Friction Piles," *Geotechnical Testing Journal*, Vol. 30, Issue 5 (September 2007), ASTM, 2007.
24. Zhang, Z., and Tumay, M.T. "Statistical to Fuzzy Approach Toward CPT Soil Classification." *Journal of Geotechnical and Geoenvironmental Engineering,* ASCE, Vol. 125, No. 3, 1999, pp. 179-186.
25. Paikowsky, S., and Whitman, R. "The Effect of Plugging on Pile Performance and Design." *Canadian Geotechnical Journal*, Vol. 27, No. 4, 1990, pp. 429-440.
26. Goble, G.; Linkins, G.; and Rausche, F. "Dyanmic Studies on the Bearing Capacity of Piles-Phase III." Report No. 48. Division of Solid Mechanics, Structures, and

Mechanical Design. Case Western Reserve University, 1970.
27. Paikowsky, S.G., Baecher, G.B., and Christian, J.T., "Statistical Issues of LRFD Calibration for Deep Foundations." *Proceedings of Soil and Rock America (SARA), 12th Pan-American Conference on Soil Mechanics and Geotechnical Engineering and the 39th U.S. Rock Mechanics Symposium.* MIT, Cambridge, MA, June 22-26, 2003, Vol. 2, pp. 2839-2844.
28. Withiam, J. L.; Voytko, E. P.; Barker, R. M.; Duncan, J. M.; Kelly, B. C.; Musser, S. C.; and Elias, V. *Load and Resistance Factor Design (LRFD) for Highway Bridge Substructures*, FHWA HI-98-032, Federal Highway Administration, Washington, D.C. 1998.
29. O'Neill, M. "LRFD Factors for Deep Foundations through Direct Experimentation." *In Proceedings of US/Taiwan Geotechnical Engineering Collaboration Workshop.* Sponsored by the National Science Foundation (USA) and the National Science Council (Taiwan, ROC), Taipei, 1995. pp. 100-114.
30. Becker, D. E. "Eighteenth Canadian Geotechnical Colloquium: Limit States Design for Foundations. Parts I and II. An Overview of the Foundation Design Process," *Canadian Geotechnical Journal*, Vol. 33, 1996, pp. 956-1007.
31. Zhang, L.; Tang, W. H.; and Ng, C. W. W. "Reliability of Axially Loaded Driven pile Groups," *Journal of Geotechnical and Geoenvironmental Engineering*, ASCE, Vol. 127, No. 12, 2001, pp. 1051-1060.
32. Kim, J.; Gao, X.; and Srivatsan, T.S. "Modeling of Void Growth in Ductile Solids: Effects of Stress Triaxiality and Initial Porosity." *Engineering Fracture Mechanics*, Volume 71, No. 3, 2004. pp. 379-400.
33. McVay, M.C. "Load and Resistance Factor Design, Cost, and Risk: Designing a Drilled Shaft Load Test in Florida Limestone," *Soil Mechanics*, 2003, pp. 98-106.
34. Hansell, W. C., and Viest I. M. "Load Factor Design for Steel Highway Bridges," *AISC Engineering Journal*, Vol. 8, No. 4, 1971, pp. 113-123.
35. Barker, R. M.; Duncan, J. M.; Rojiani, K. B.; Ooi, P. S. K.; Tan, C. K.; and Kim, S. G. "Manuals for the Design of Bridge Foundations: Shallow Foundations, Driven Piles, Retaining Walls and Abutments, Drilled Shafts, Estimating Tolerable Movements, and Load Factor Design Specifications and Commentary," NCHRP Report 343, TRB, National Research Council, Washington, D.C., 1991.
36. Hasofer, A. M., and Lind, N. C. "An Exact and Invariant First-Order Reliability Format." *Journal of Engineering Mechanics*, Vol. 100. No. EM1, 1974. pp. 111-121.
37. Nowak, S., A., Collins, K., R., *Reliability of structures*, McGraw Hill, International edition, 2000.

38. Rackwitz, R., and Fiessler, B. “Structural Reliablity under combined Random Loads.” *Computers and Structures*, Vol. 9, 1978.
39. Davisson, M. T. Pile Load Capacity. Proc. ASCE Conf. “Design Construction and Performance of Deep Foundations,” ASCE, University of California, Berkeley, 1975.
40. Kyfor, Z.G., Schnore, A.S., Carlo, T.A. and Bailey, P.F. “Static Testing of Deep Foundations.” Report No. FHWA-SA-91-042, U.S. Department of Transportation, FHWA, Washington, D.C., 1992.
41. Salgado, R. *Engineering of Foundations*, 1st Edition, McGraw Hill, 2007.
42. Briaud, J-L and Tucker, L.M., “Measured and Predicted Axial Response of 98 Piles,” *Journal of Geotechnical Engineering*, ASCE, Vol. 114, No. 8, 1988, pp. 984-1001.

# APPENDIX

## Summary of Geotechnical Data for the State Projects Investigated

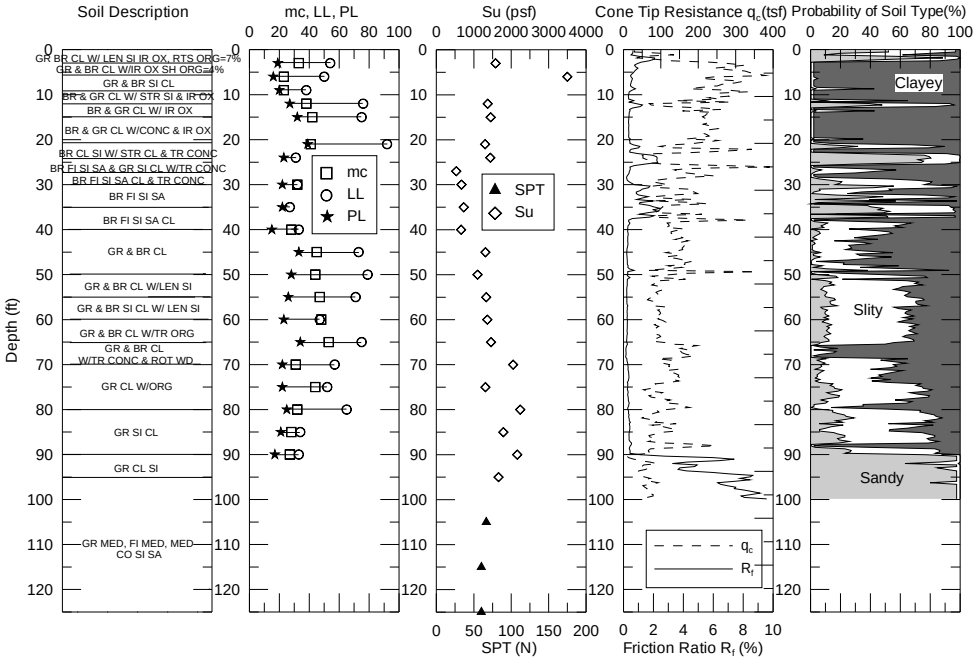


**Figure 38**
**003-07-0019 TP#1**

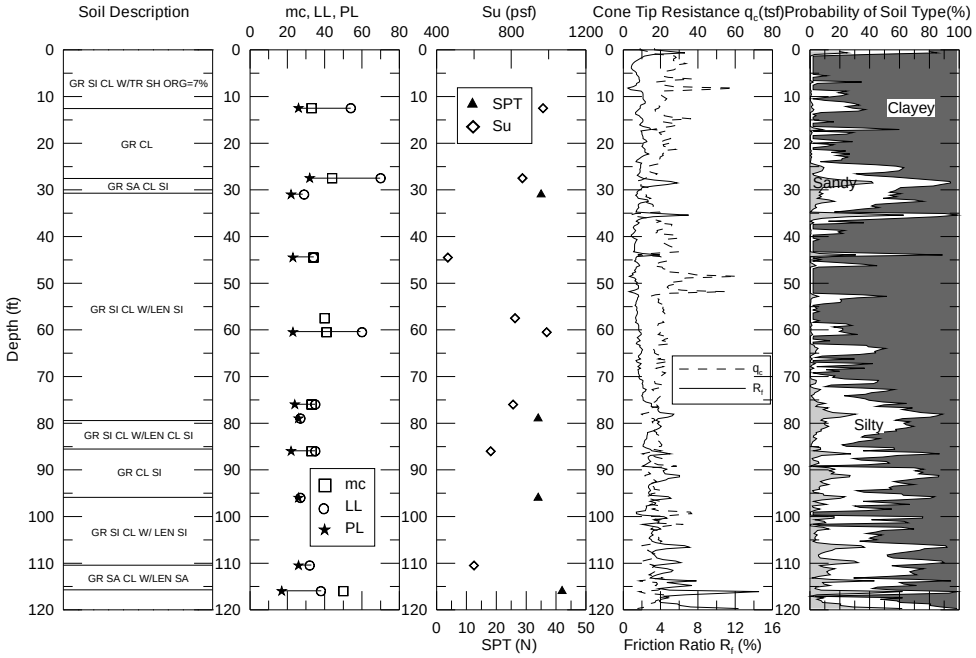


**Figure 39**
**005-01-0056 TP#1**

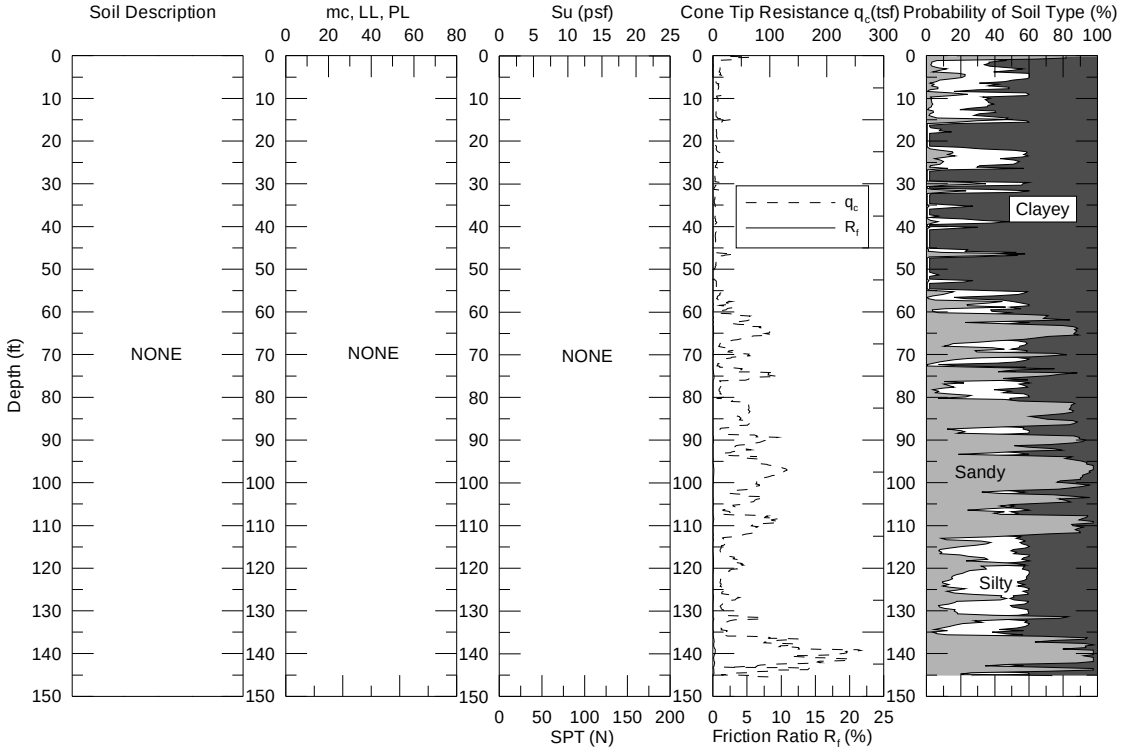


**Figure 40**
**005-01-0056 TP#2**

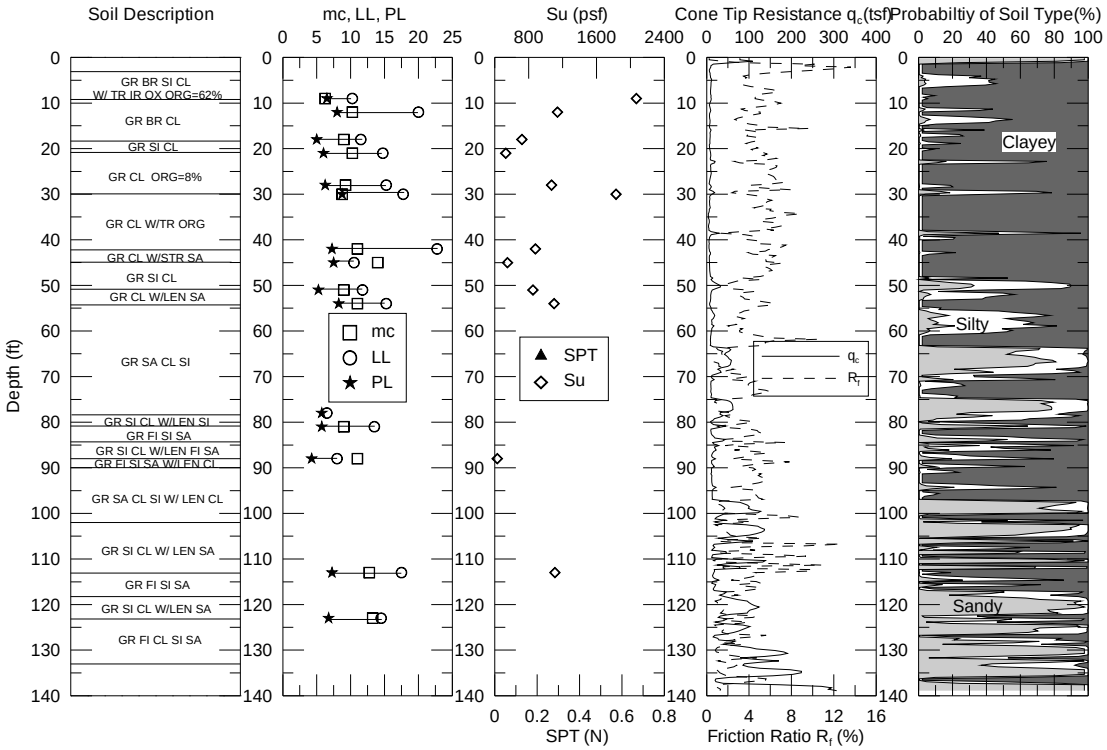


**Figure 41**
**005-01-0056 TP#3**

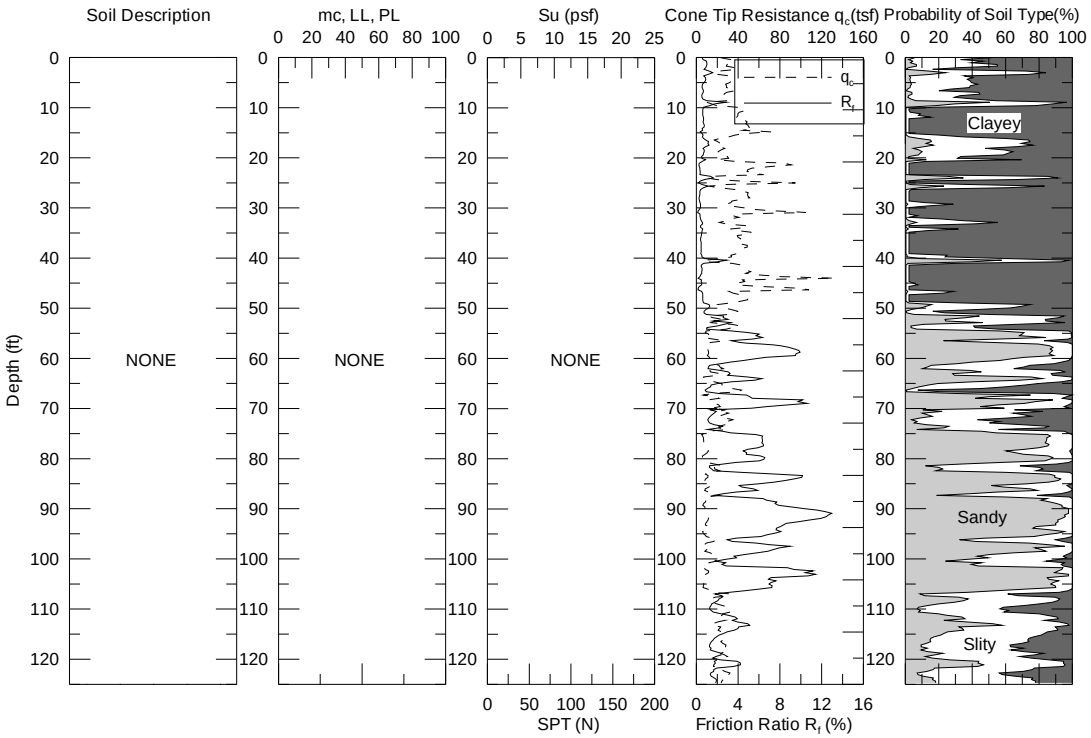


**Figure 42**
**005-05-0065 TP#1**

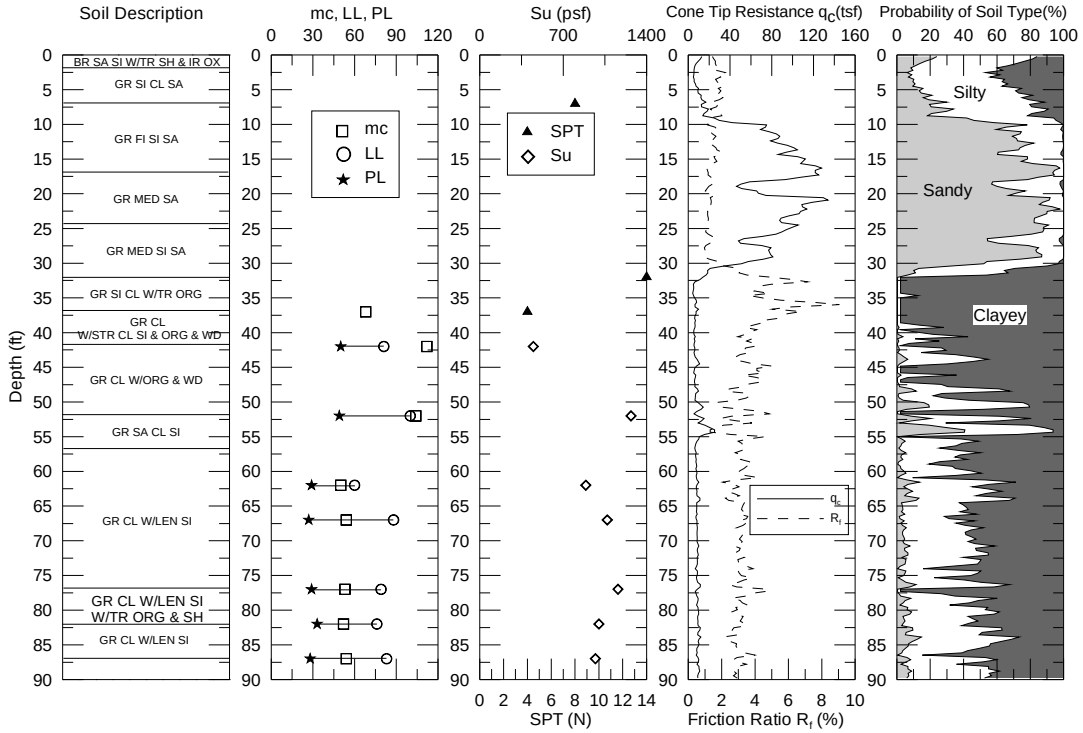


**Figure 43**
**065-90-0024 TP#1**

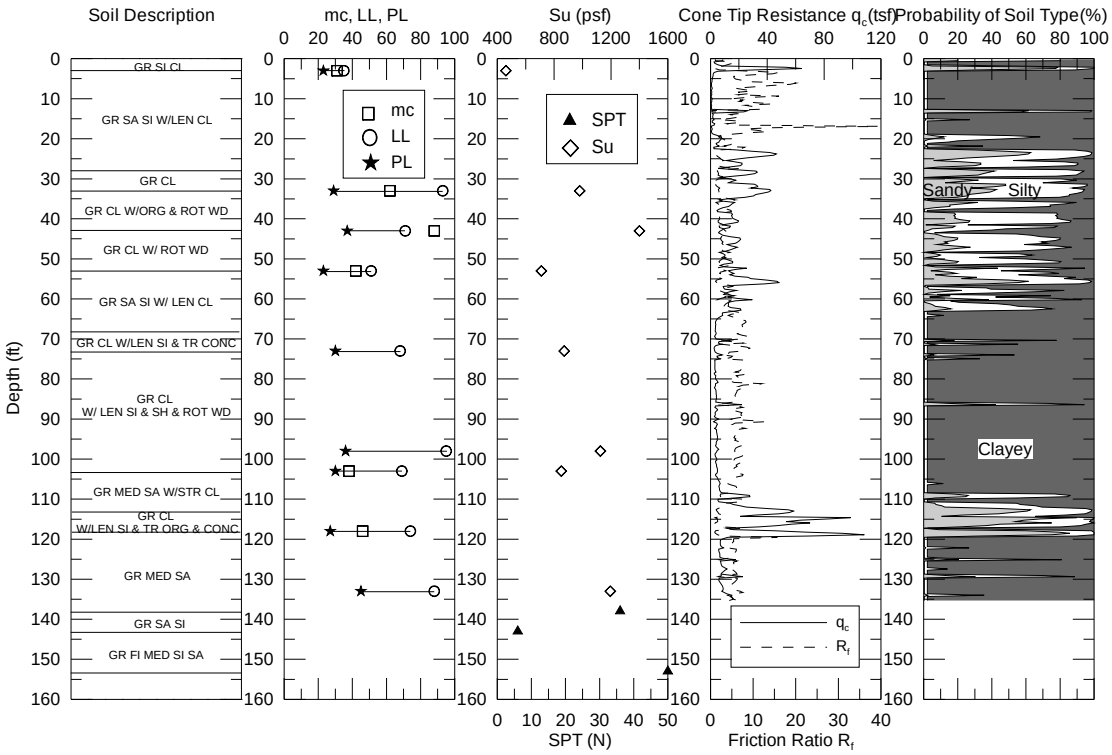


**Figure 44**
**065-90-0024 TP#2**

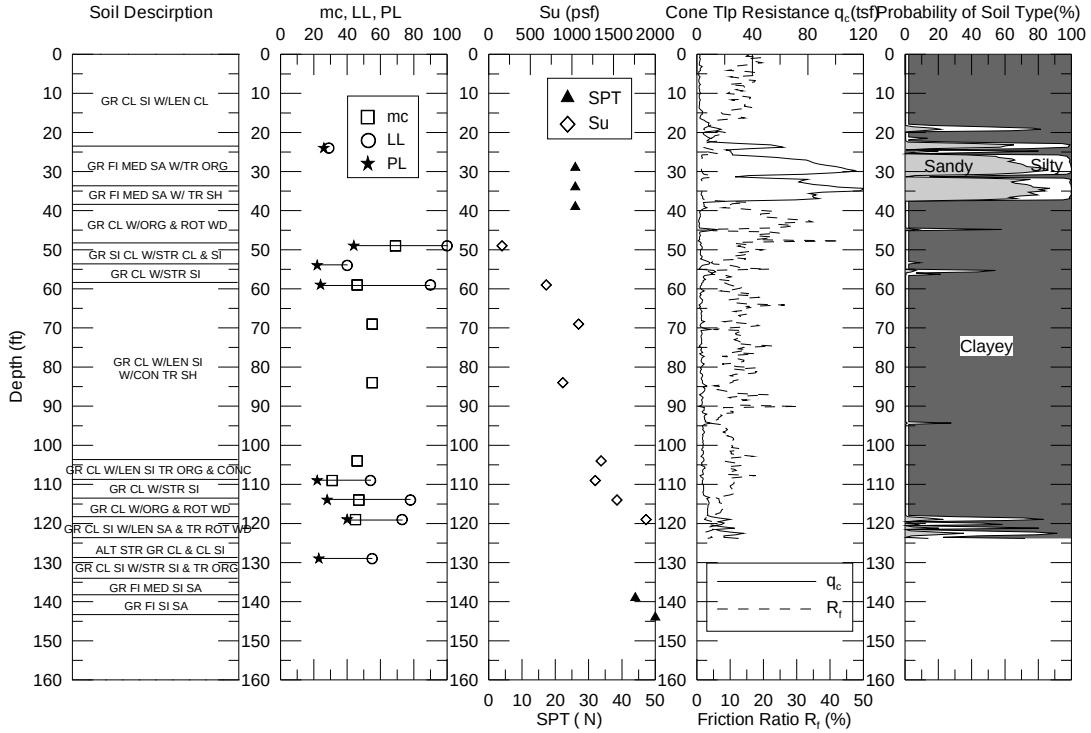


**Figure 45**
**065-90-0024 TP#3**

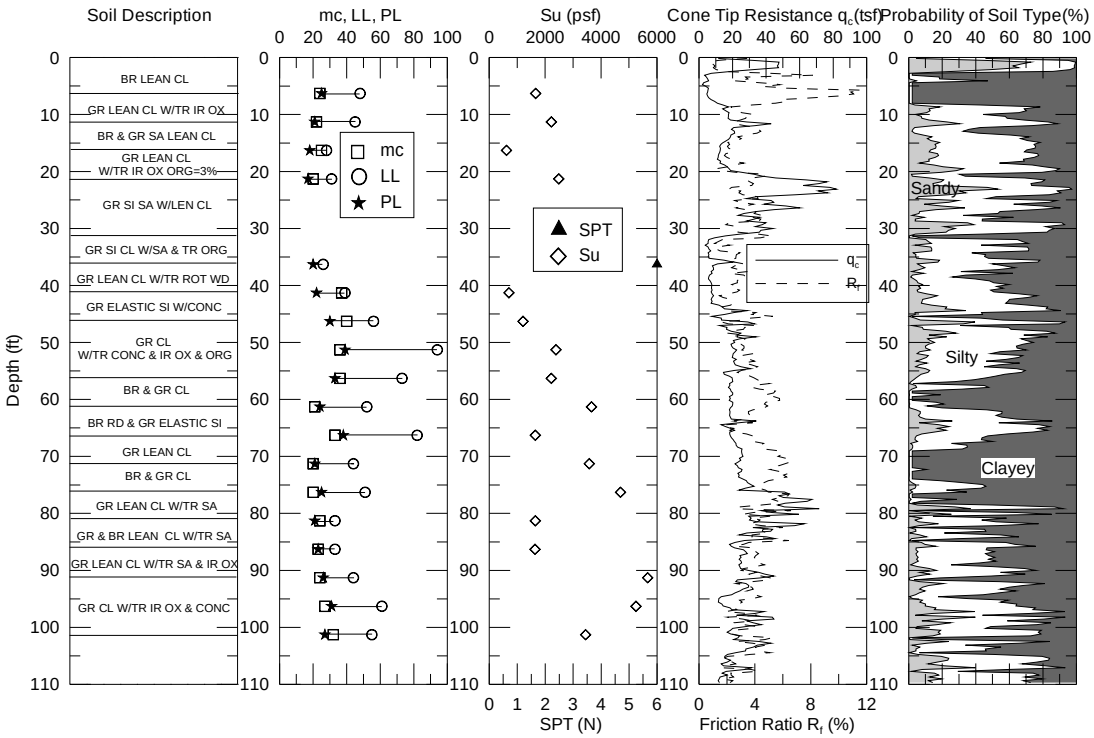


**Figure 46**
**260-05-0020 TP#1**

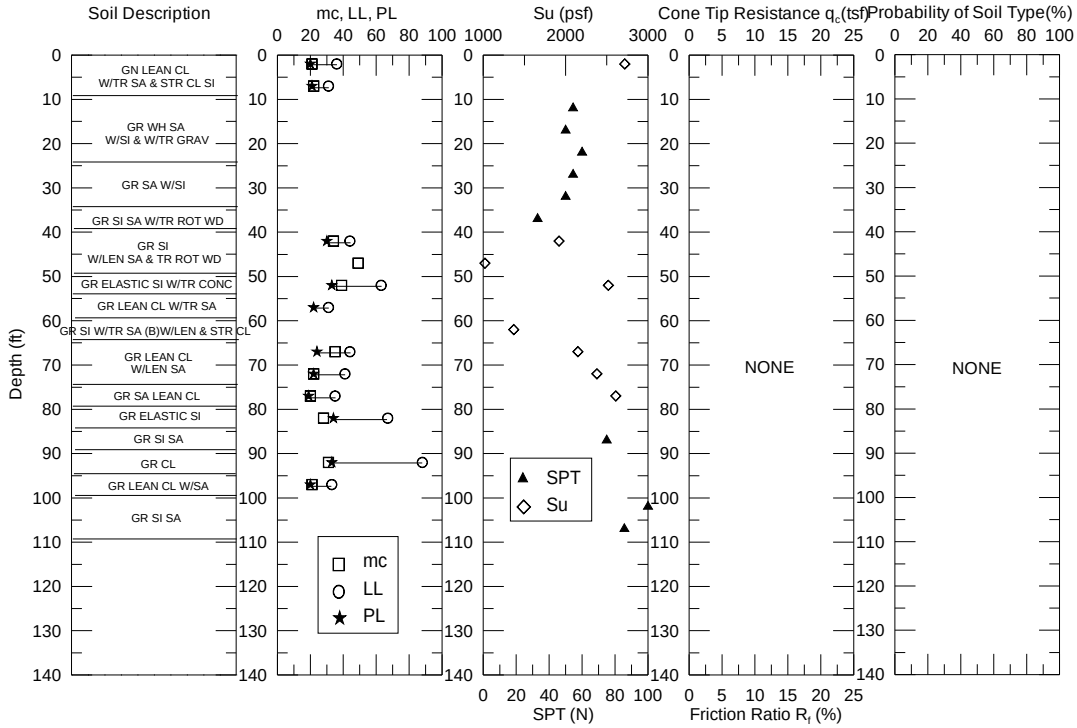


**Figure 47**
**260-05-0020 TP#2**

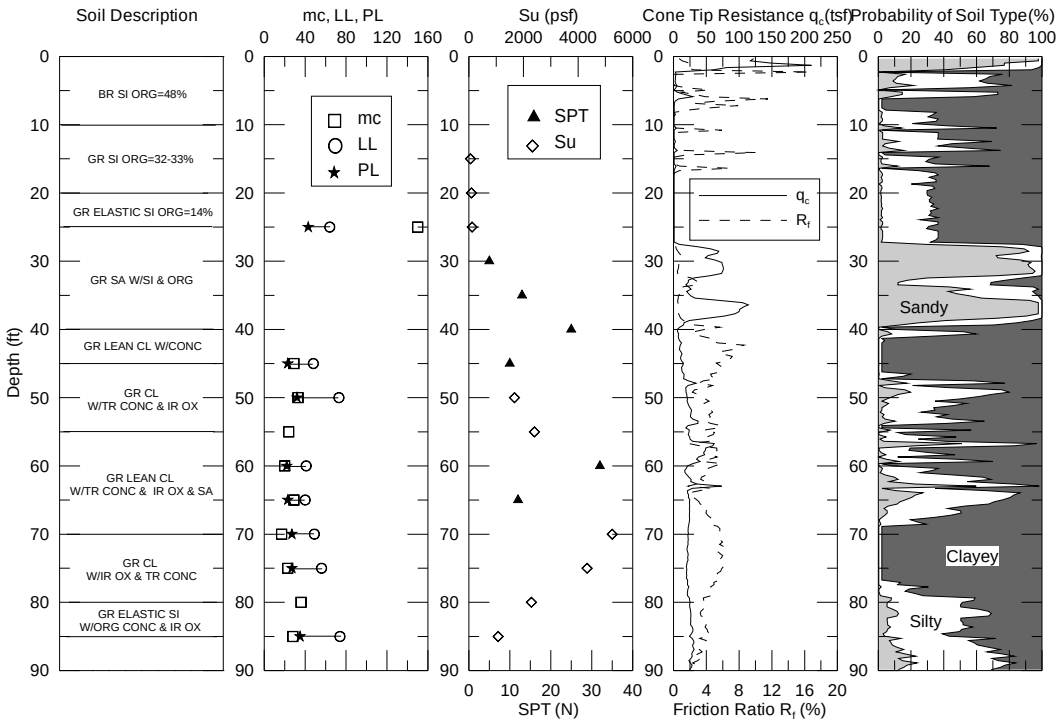


**Figure 48**
**260-05-0020 TP#3**

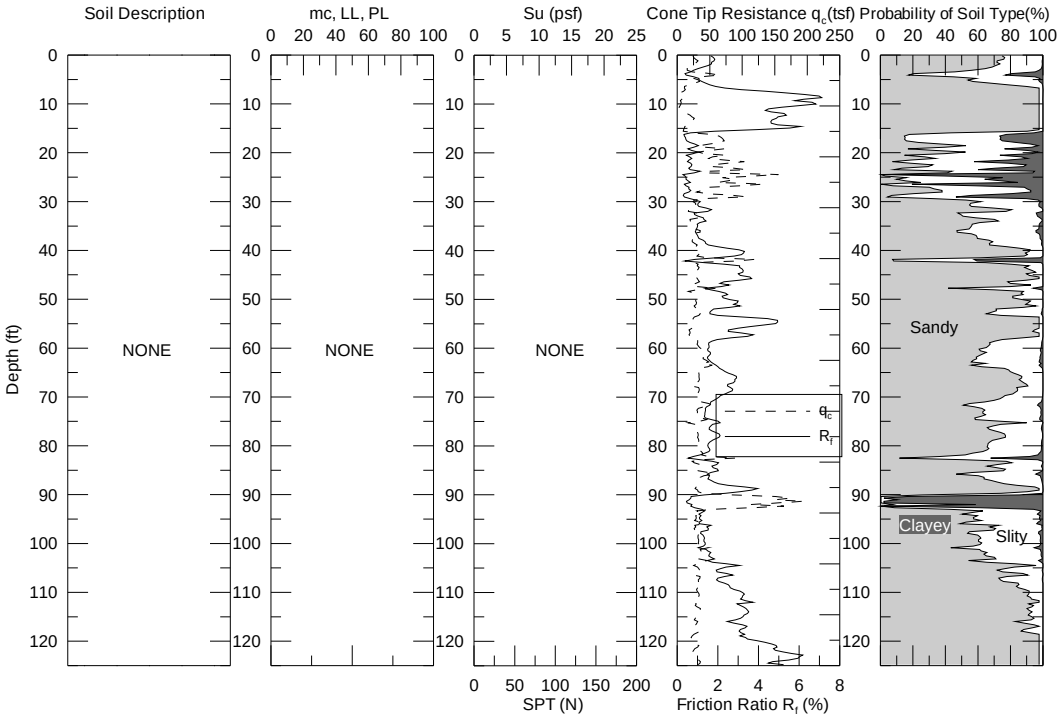


**Figure 49**
**262-06-0009 & 262-07-0012 TP#1**

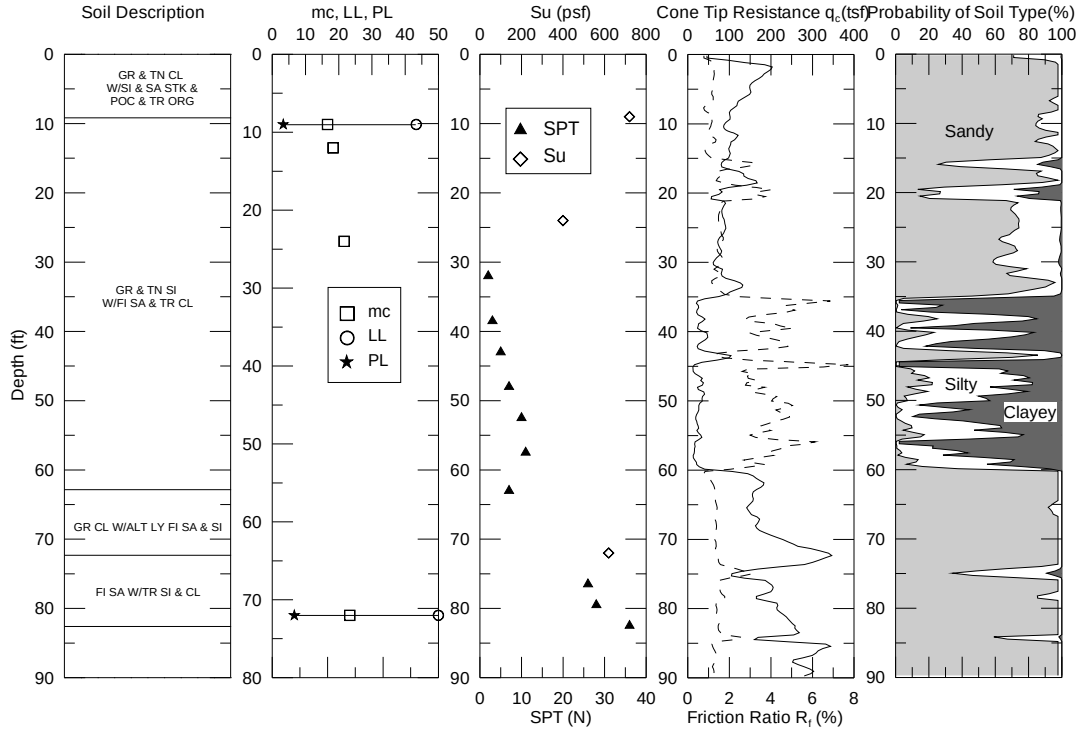


**Figure 50**
**424-05-0078 TP#1**

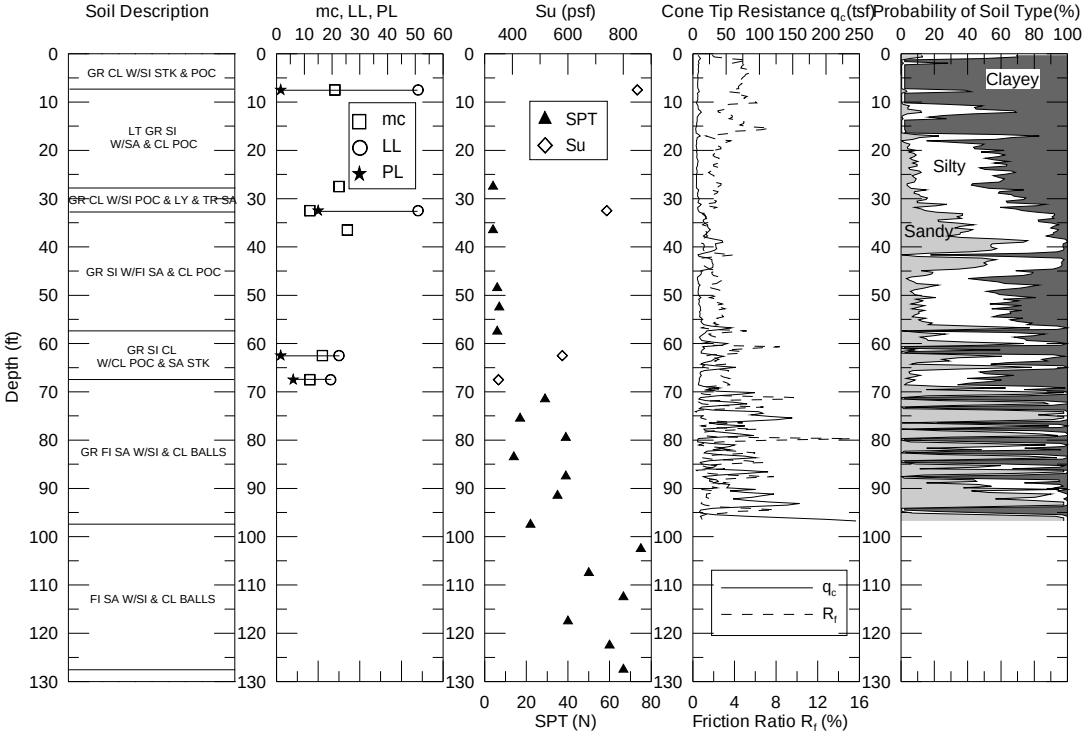


**Figure 51**
**424-05-0078 TP#2**

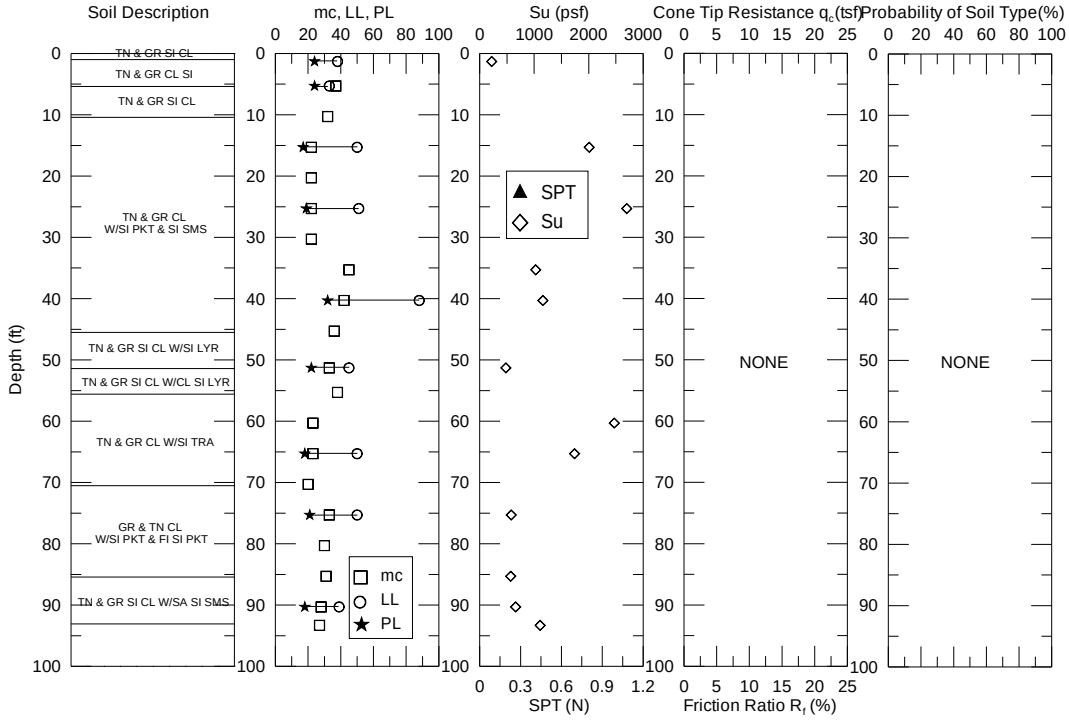


**Figure 52**
**424-04-0027 TP#2**

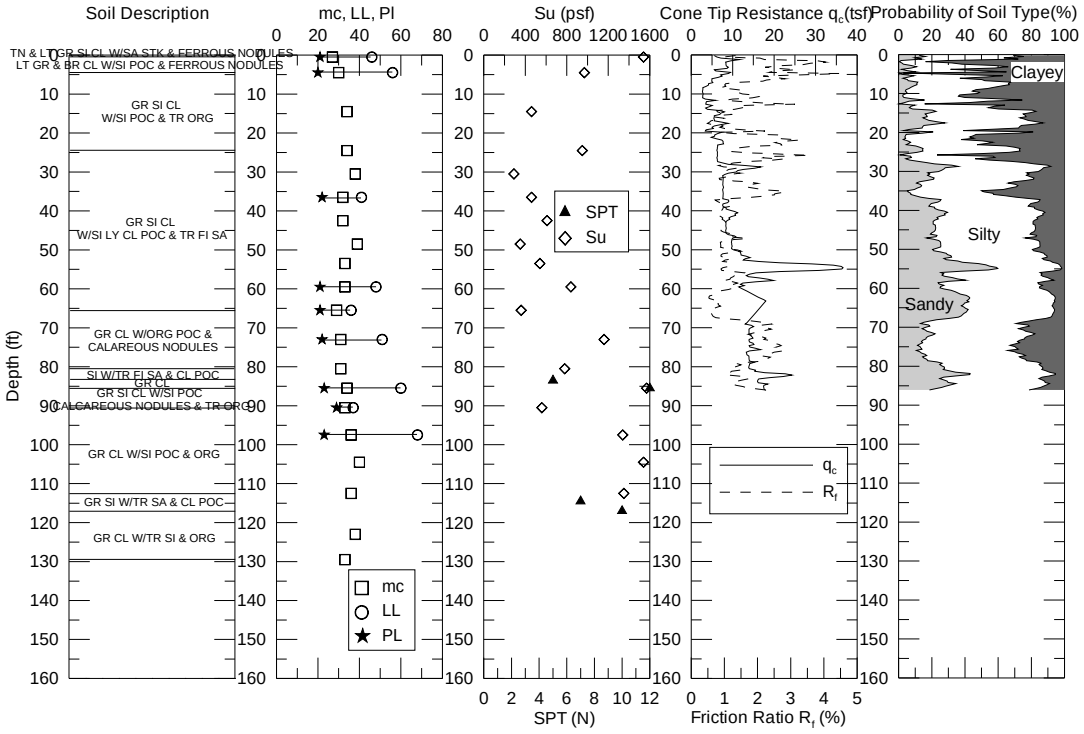


**Figure 53**
**424-05-0078 TP#5**

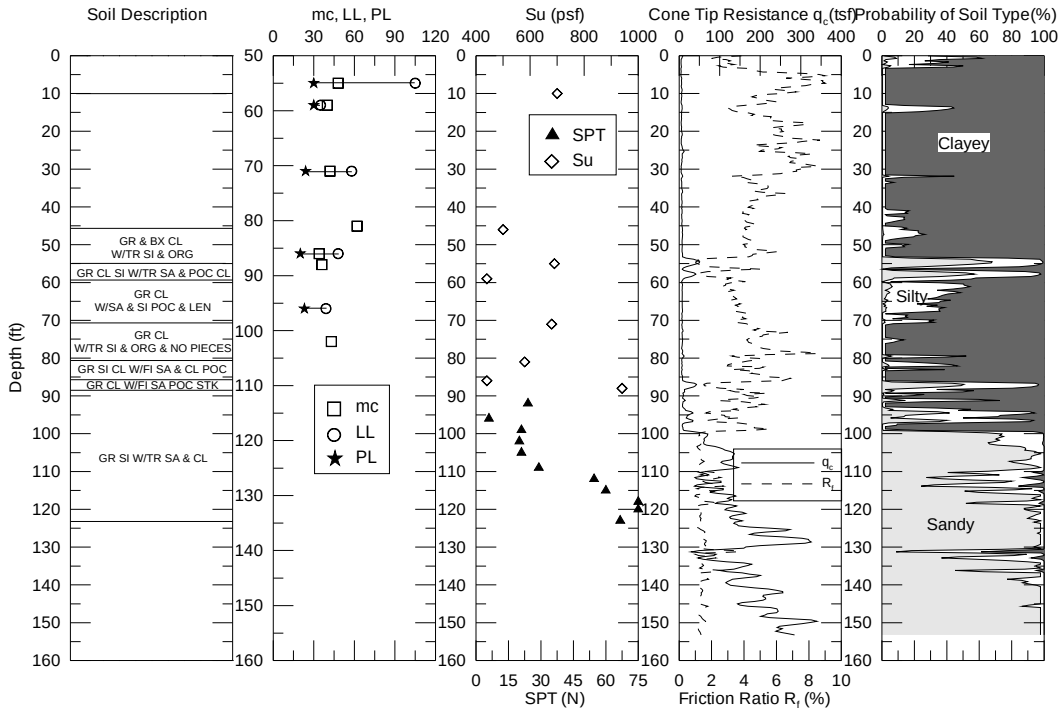


**Figure 54**
**424-05-0081 TP#1**

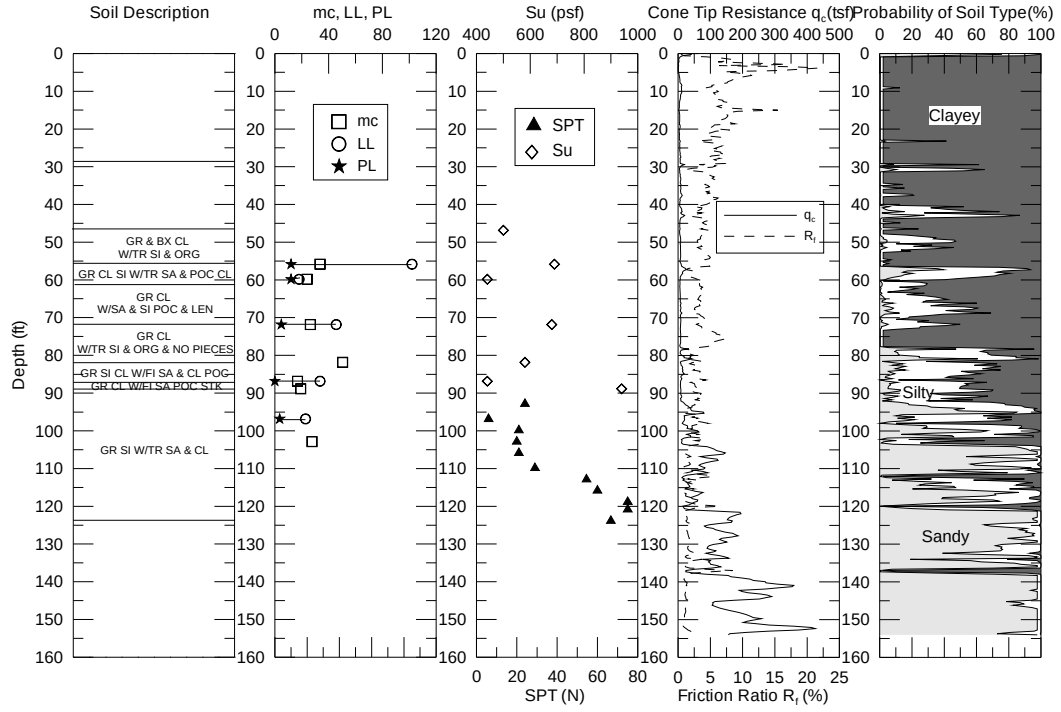


**Figure 55**
**424-05-0081 TP#4**

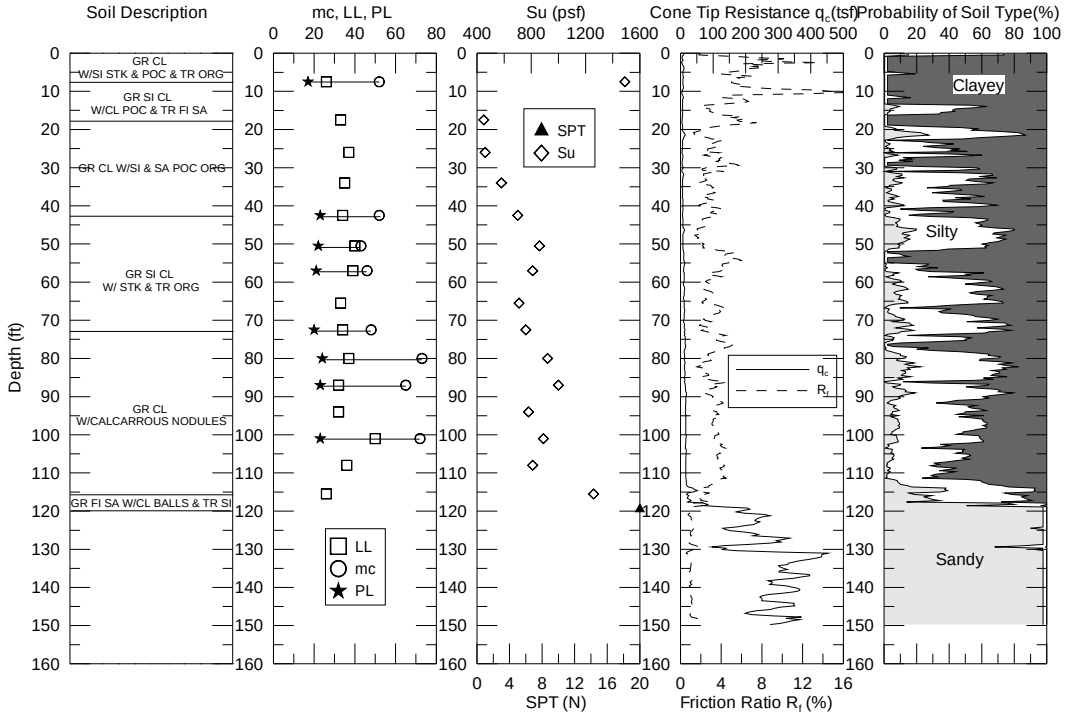


**Figure 56**
**424-06-0005 TP#1**

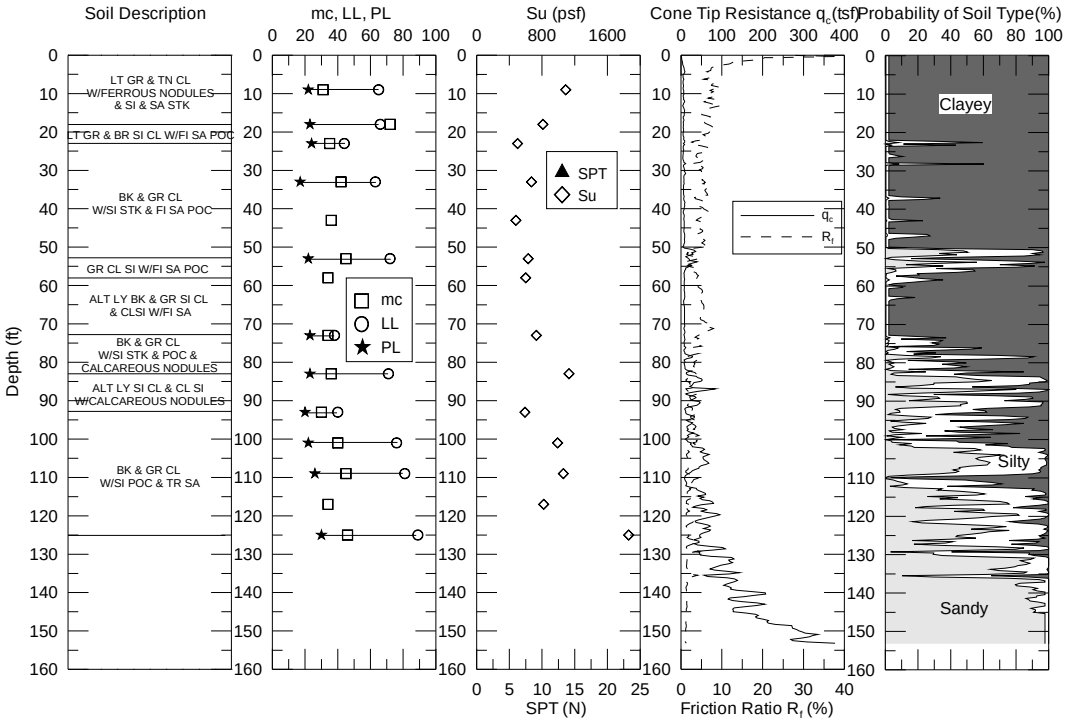


**Figure 57**
**424-06-0005 TP#2**

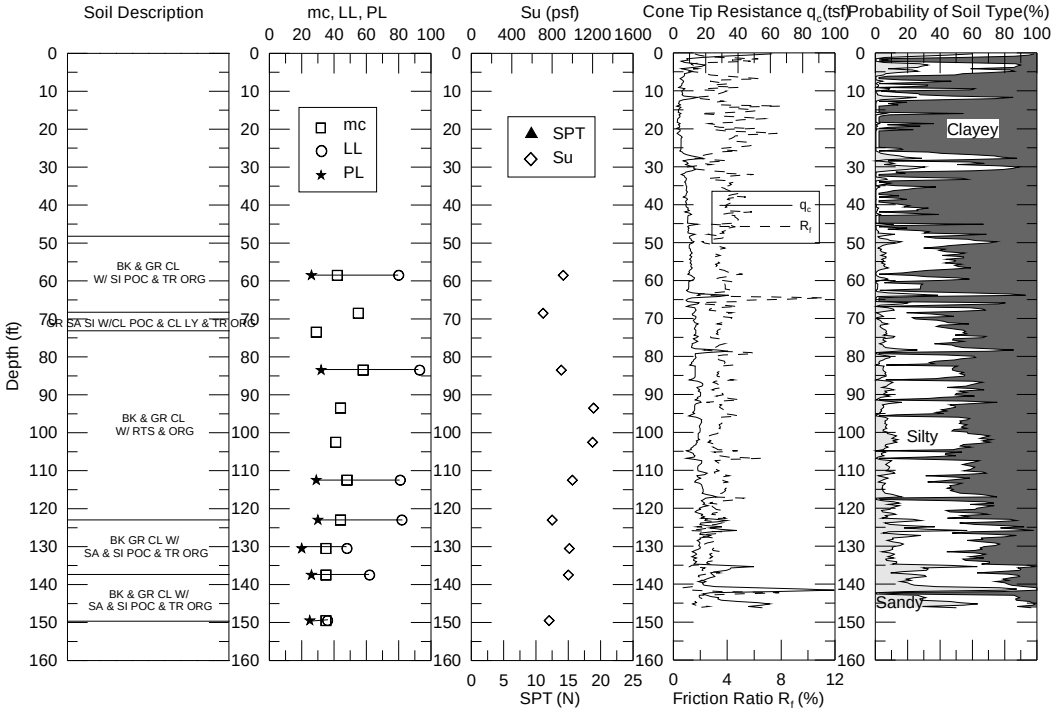


**Figure 58**
**424-07-0021 TP#1**

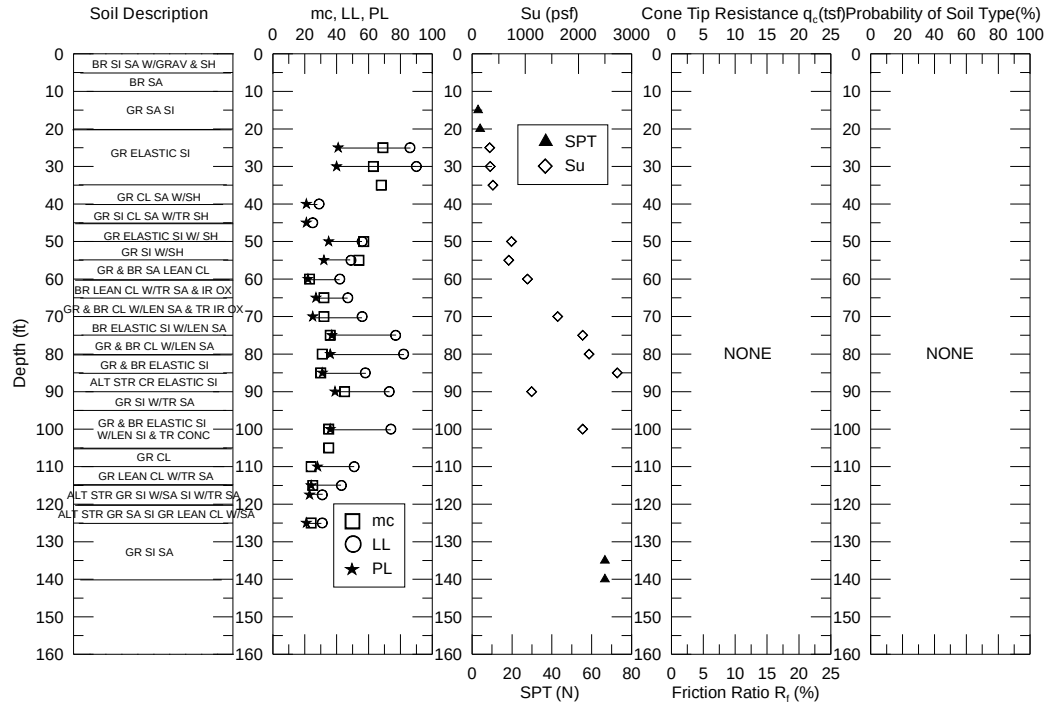


**Figure 59**
**450-15-0085 TP#3A**

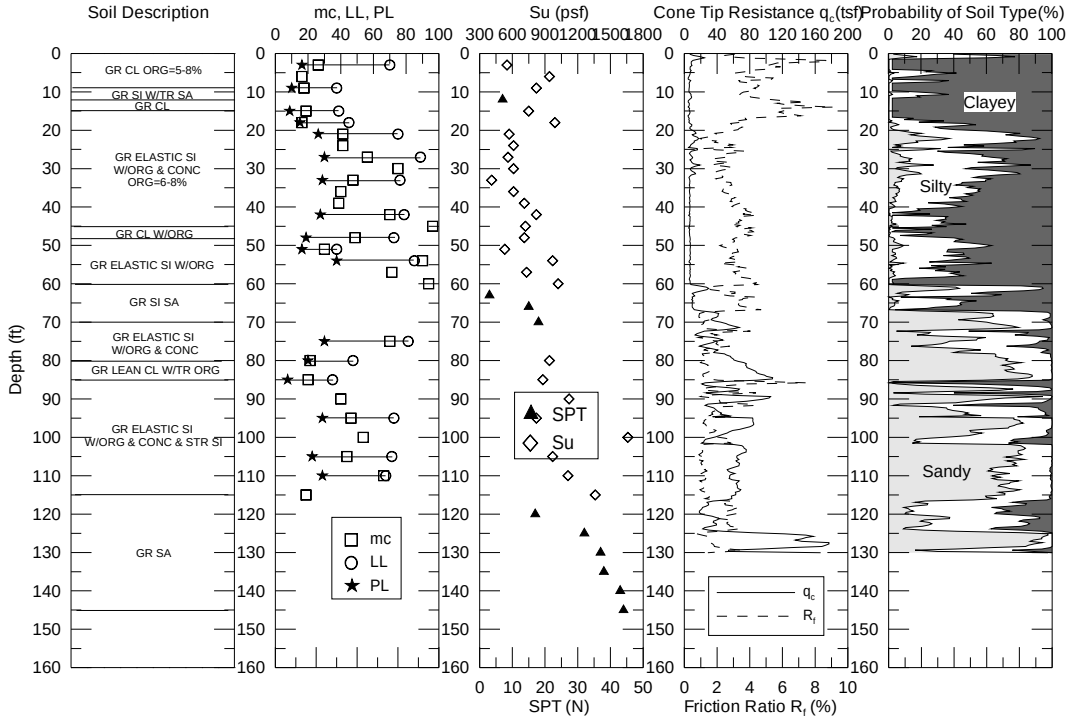


**Figure 60**
**424-05-0087 TP#1**

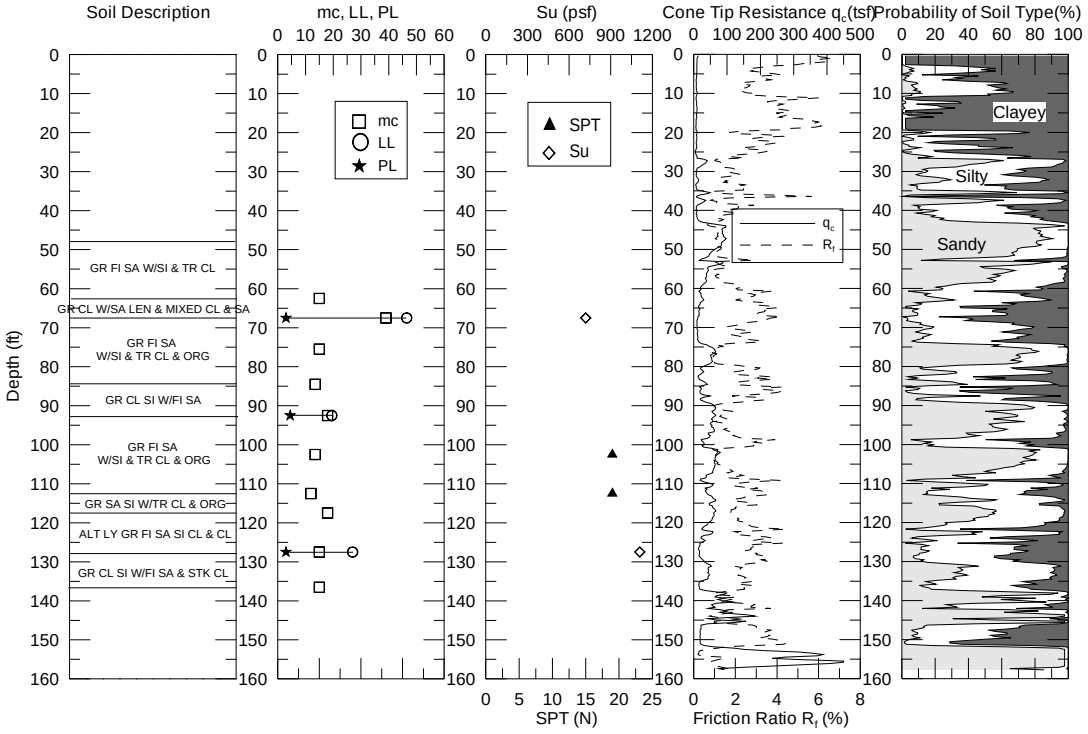


**Figure 61**
**424-05-0087 TP#3**

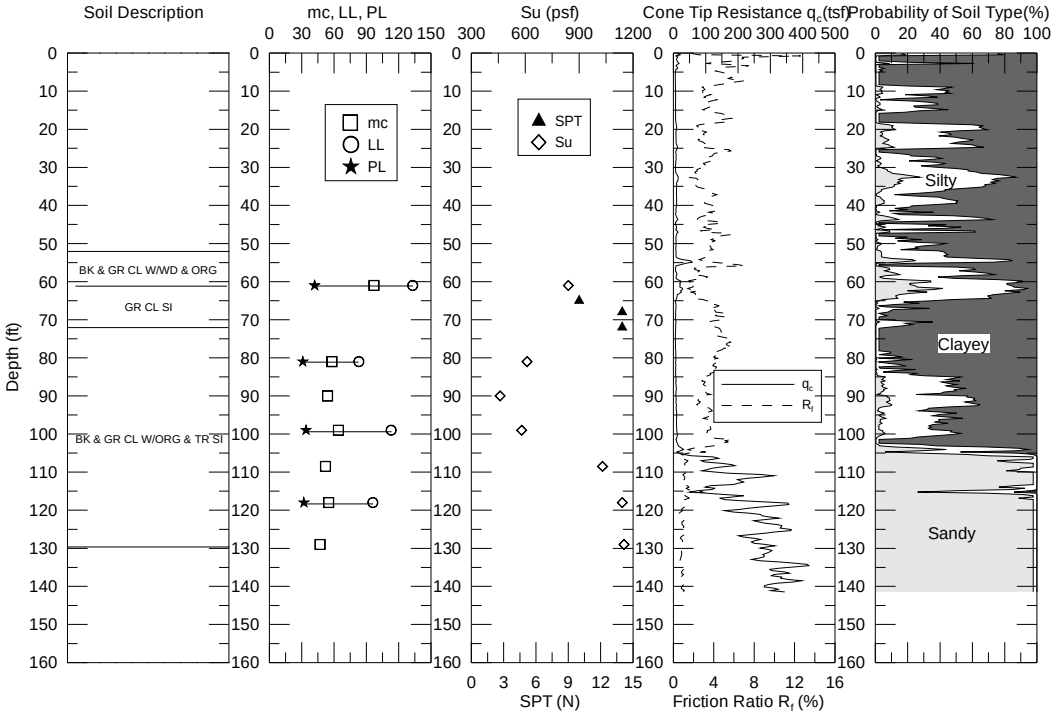


**Figure 62**
**424-05-0087 TP#5**

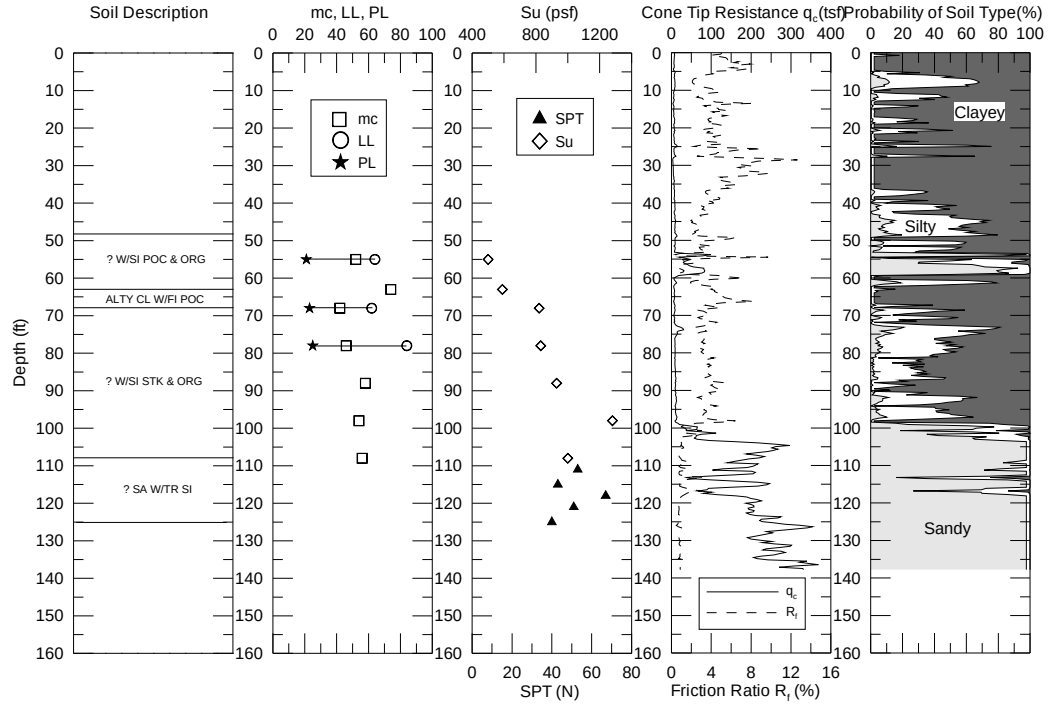


**Figure 63**
**424-05-0087 TP#7**

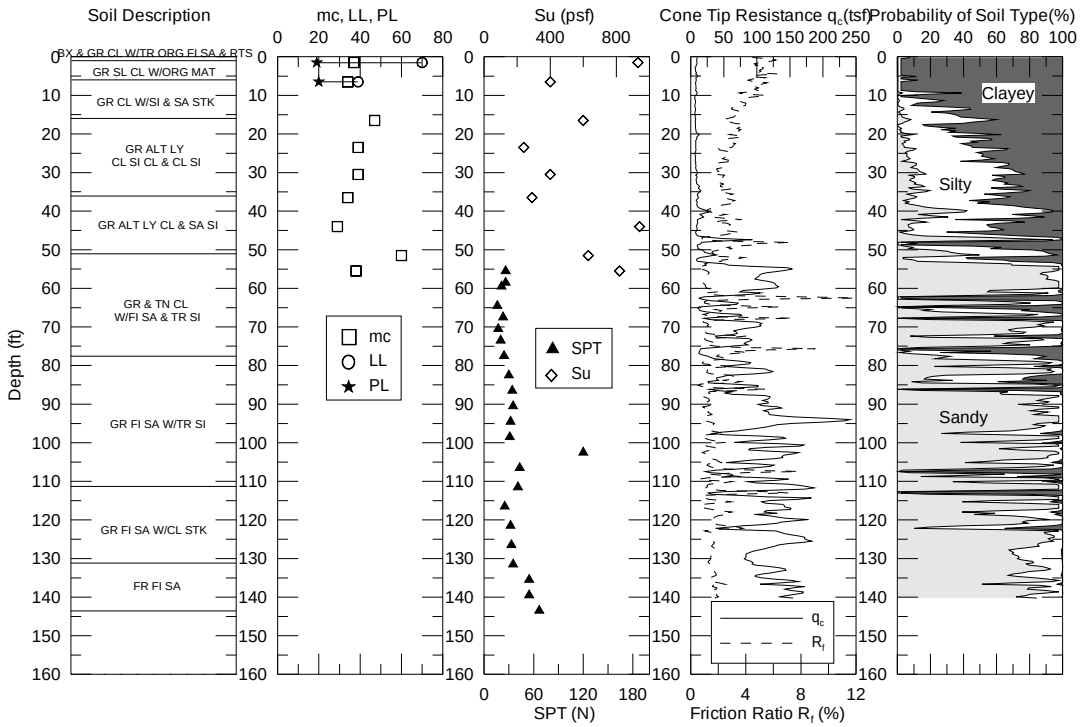


**Figure 64**
**424-05-0081 TP#3**

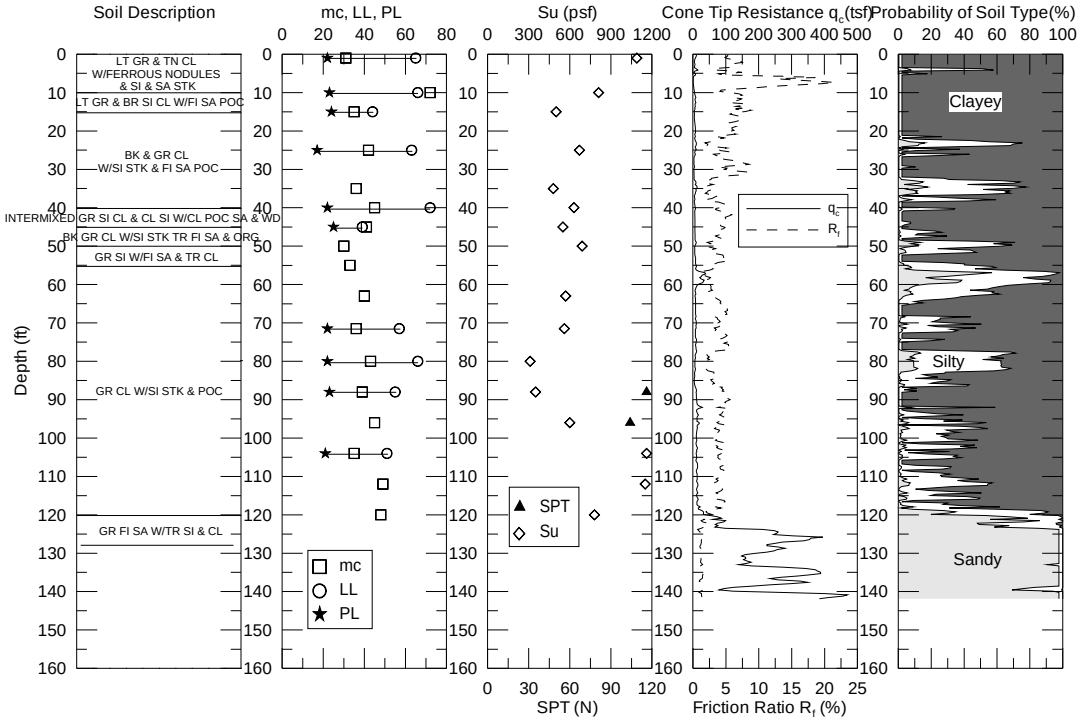


**Figure 65**
**424-06-0005 TP#3**

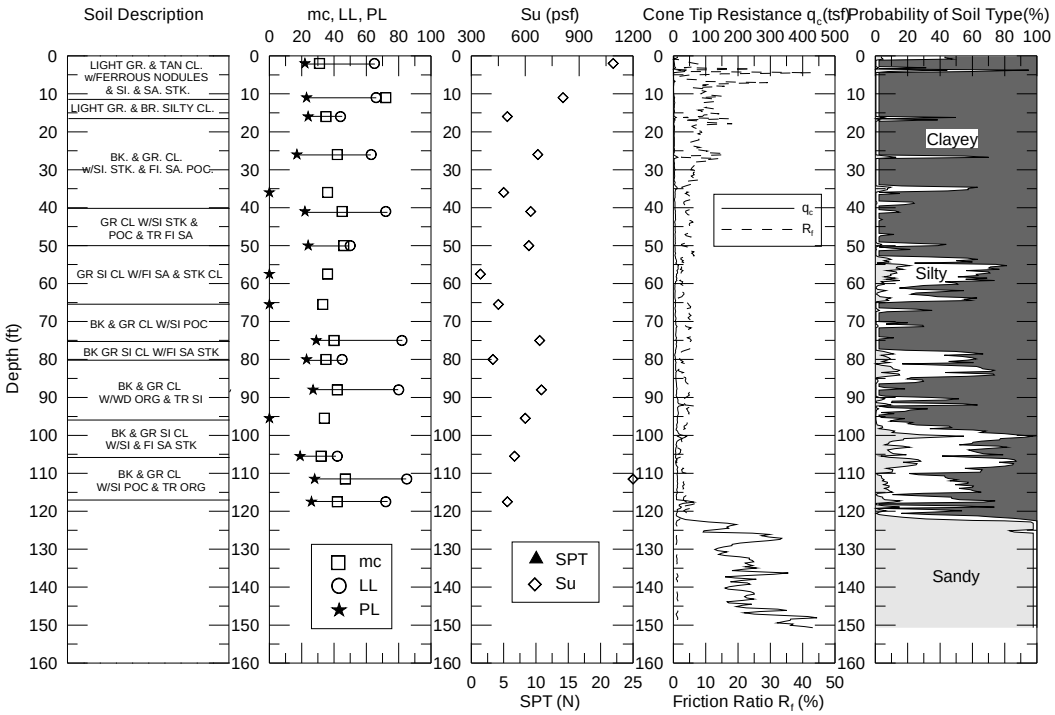


**Figure 66**
**424-06-0005 TP#5**

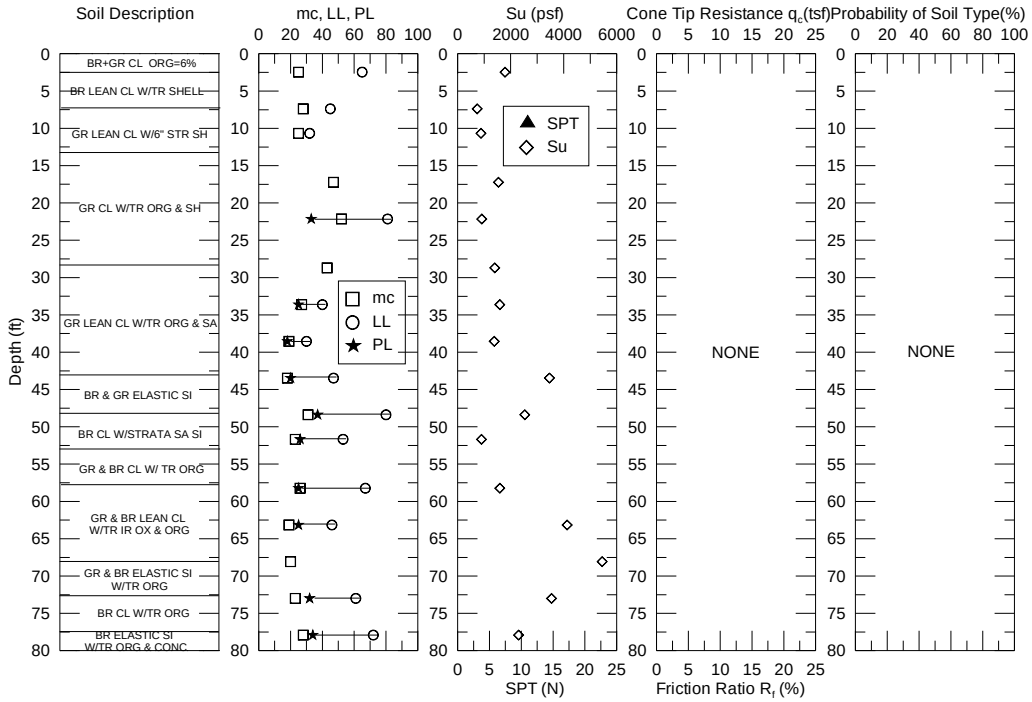


**Figure 67**
**014-02-0018 TP#1**

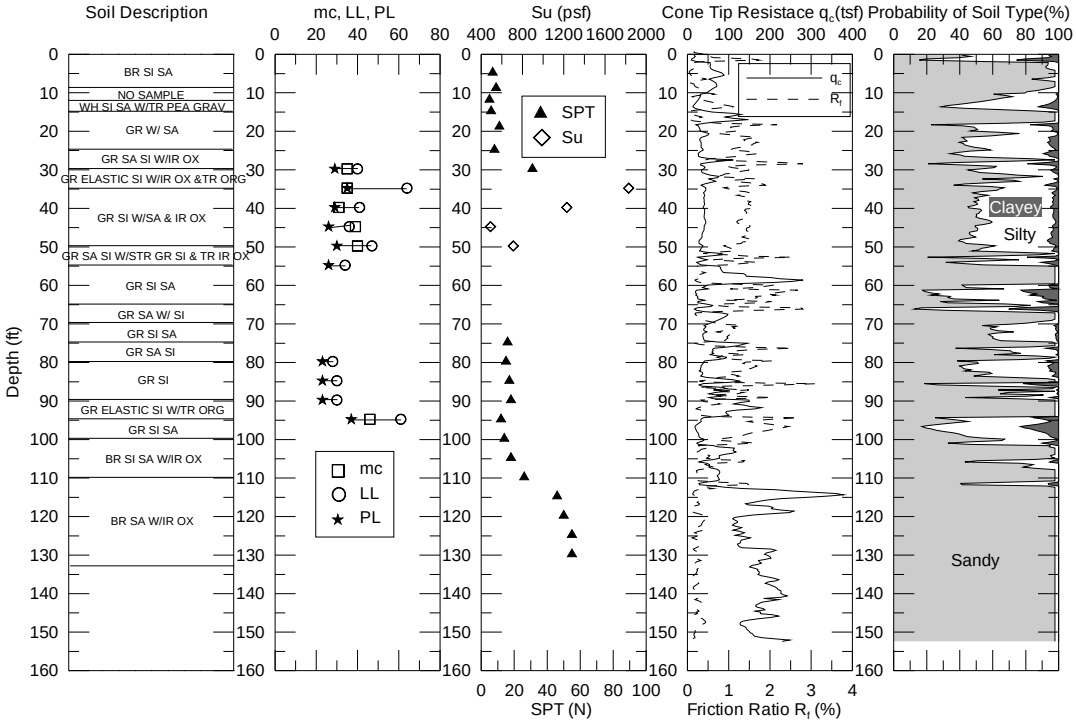


**Figure 68**
**047-02-0022 TP#2**

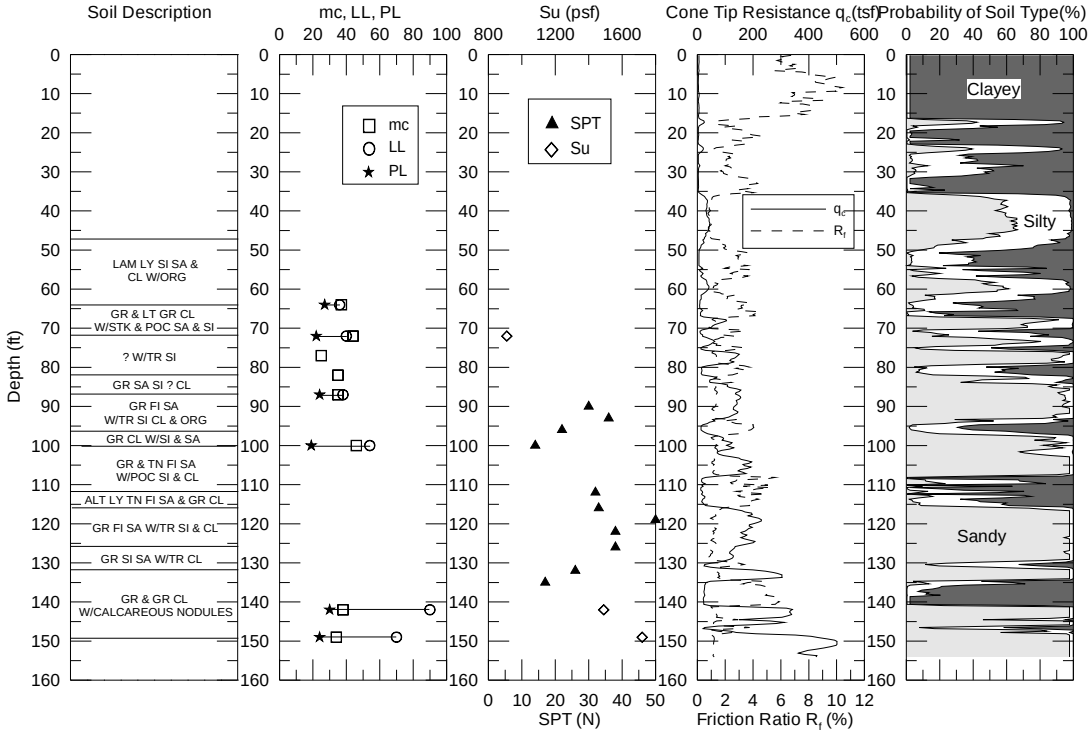


**Figure 69**
**424-05-0087 TP#4**

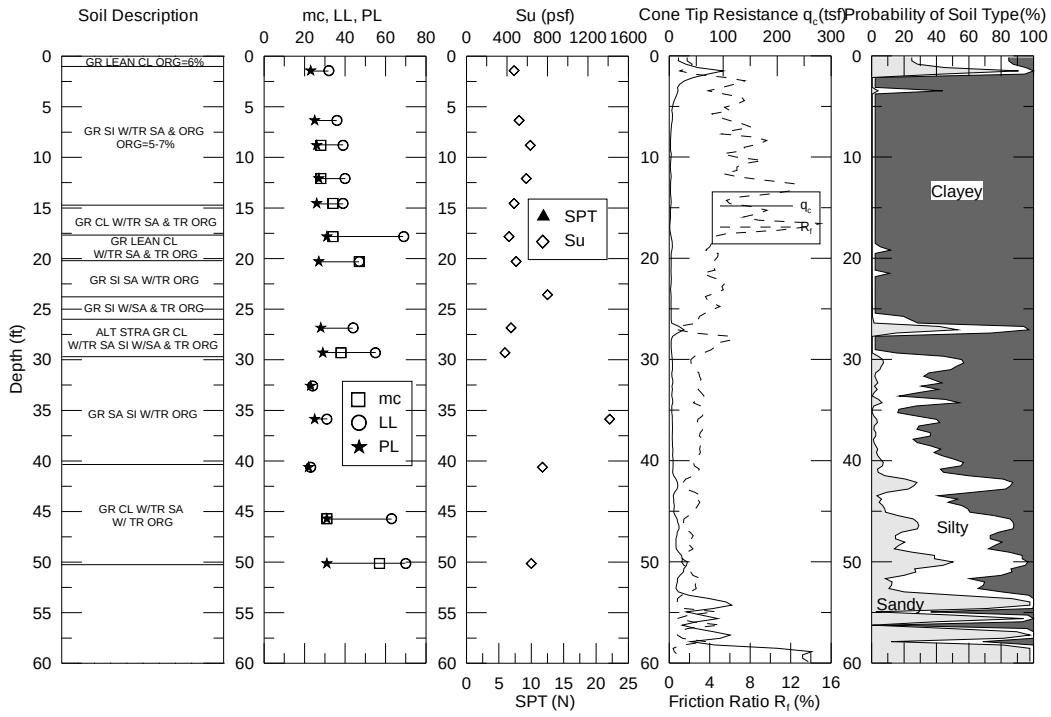


**Figure 70**
**064-06-0036 TP#1**

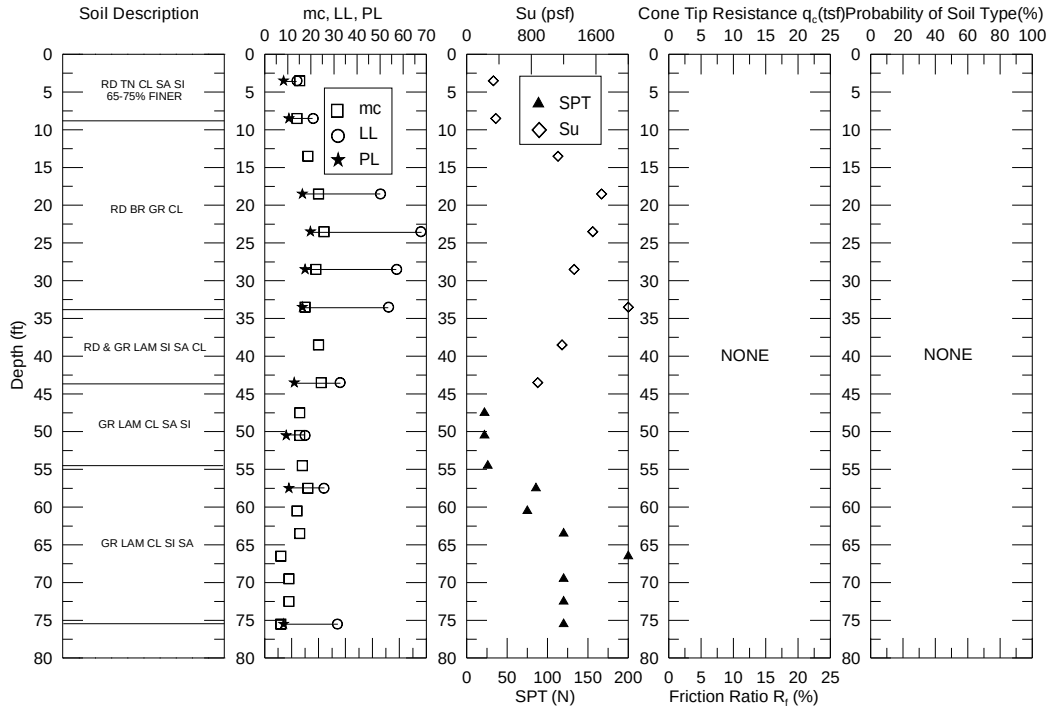


**Figure 71**
**090-01-0015 TP#1**

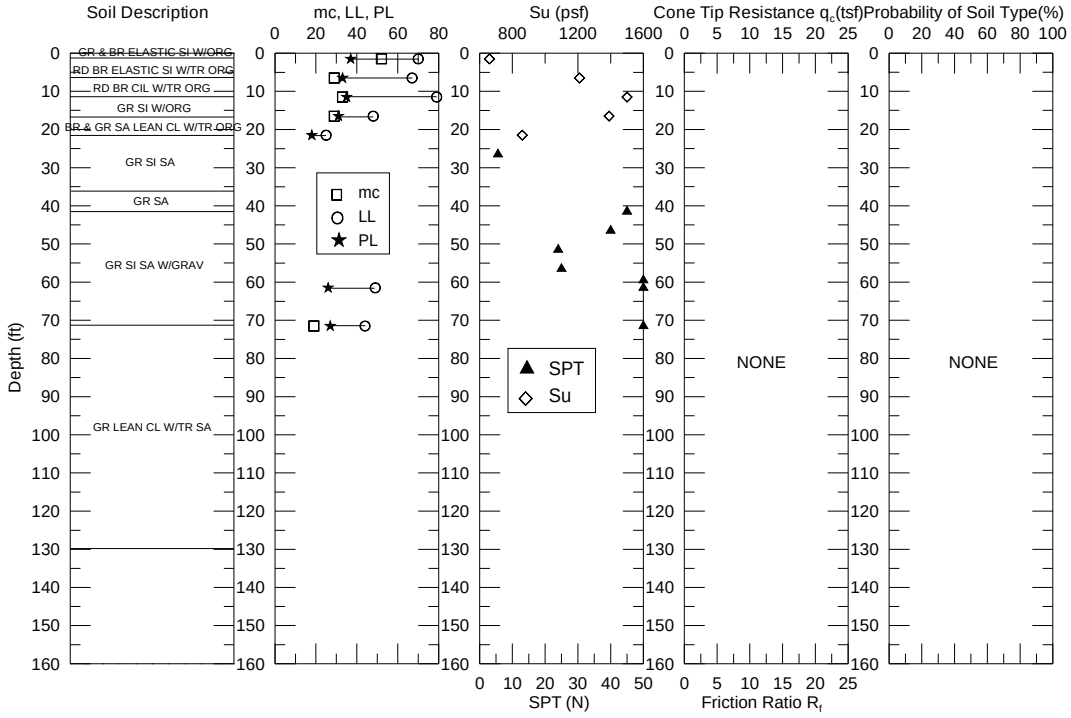


**Figure 72**
**090-01-0015 TP#2**

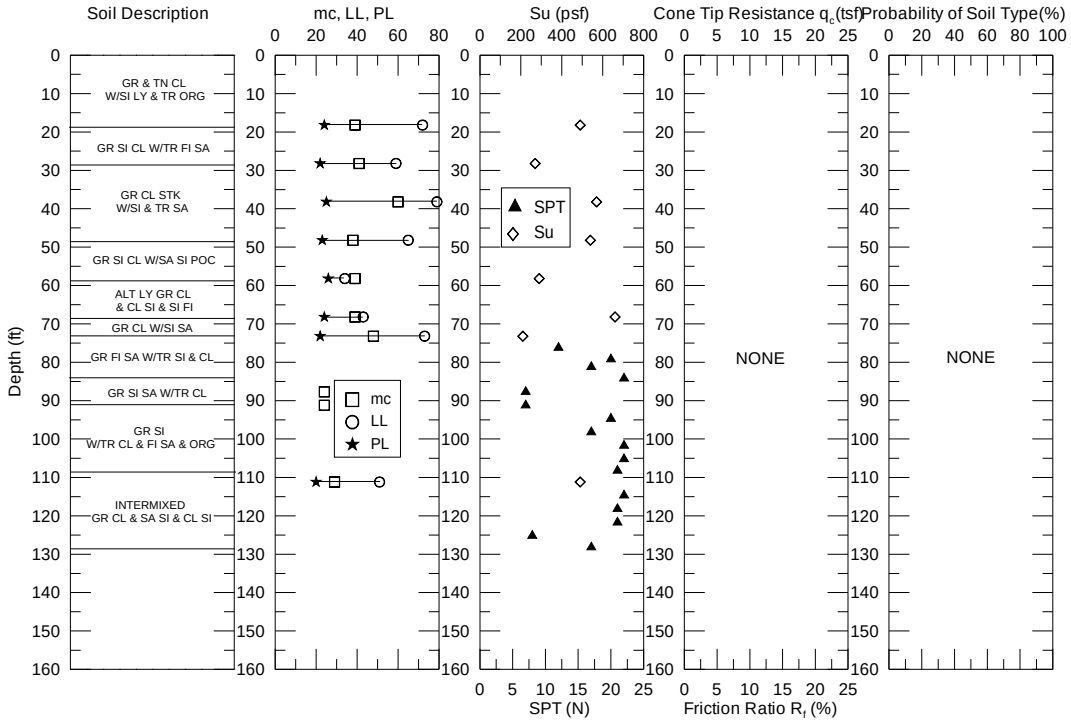


**Figure 73**
**424-05-0087 TP#2**

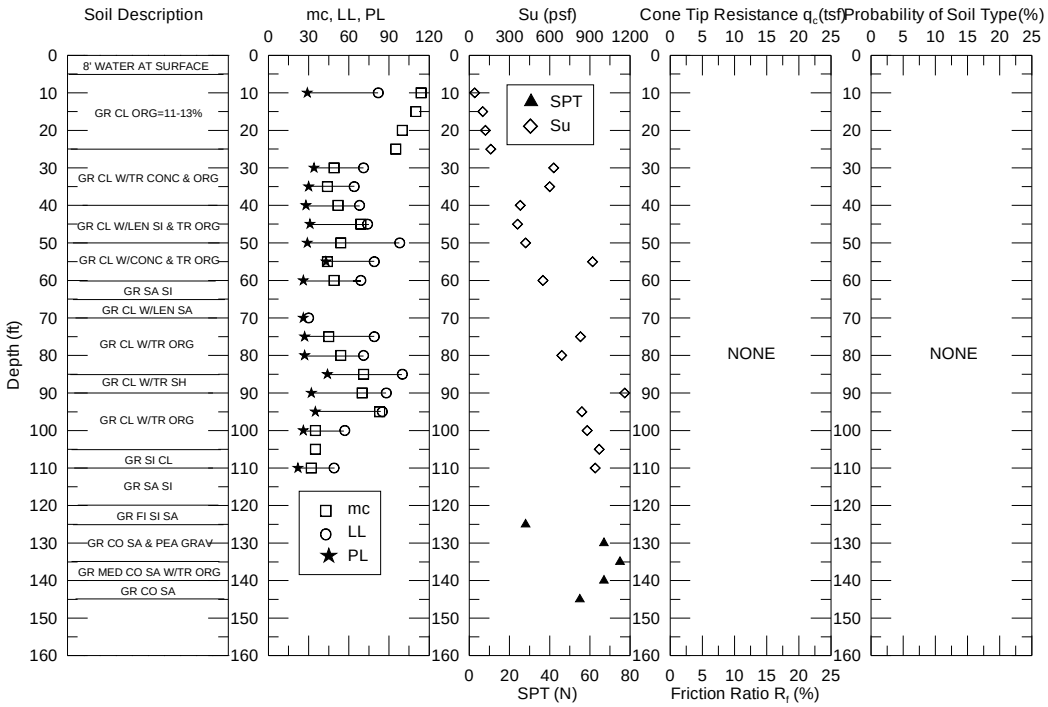


**Figure 74**
**713-48-0083 TP#1**

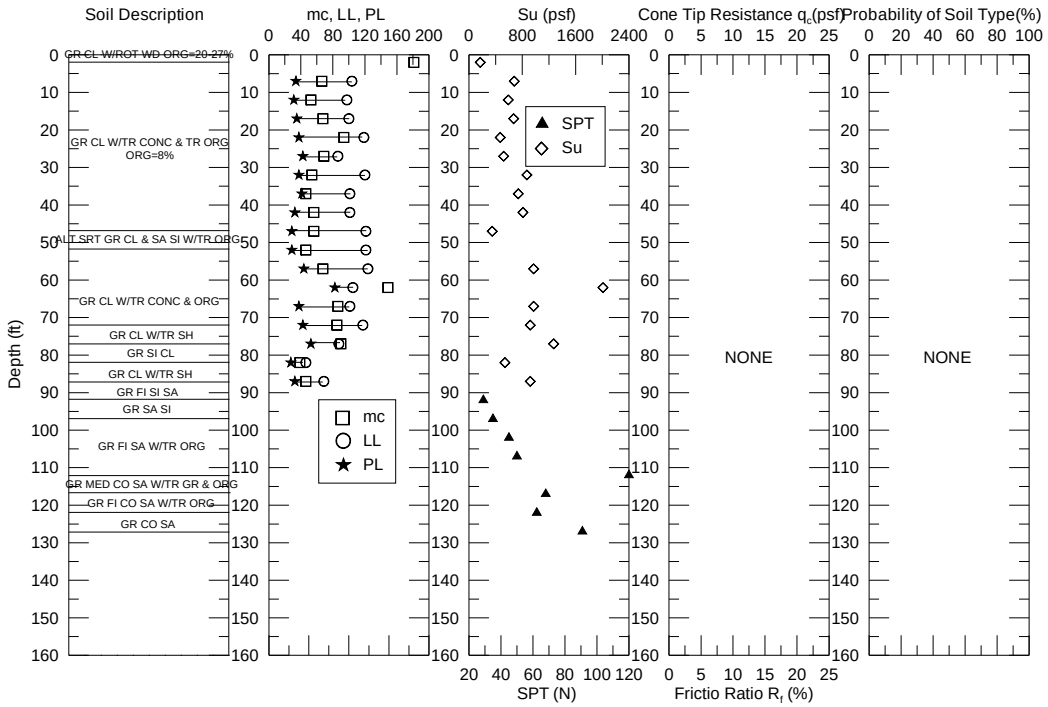


**Figure 75**
**713-48-0083 TP#2**

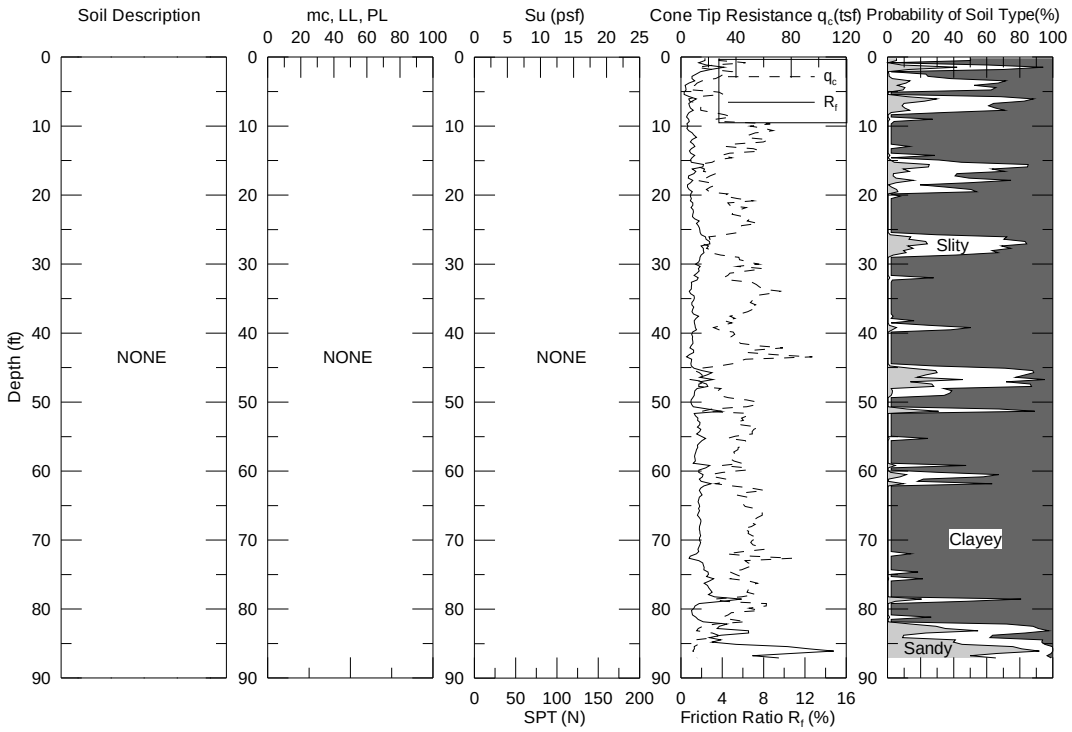


**Figure 76**
**455-05-0036 TP#1**

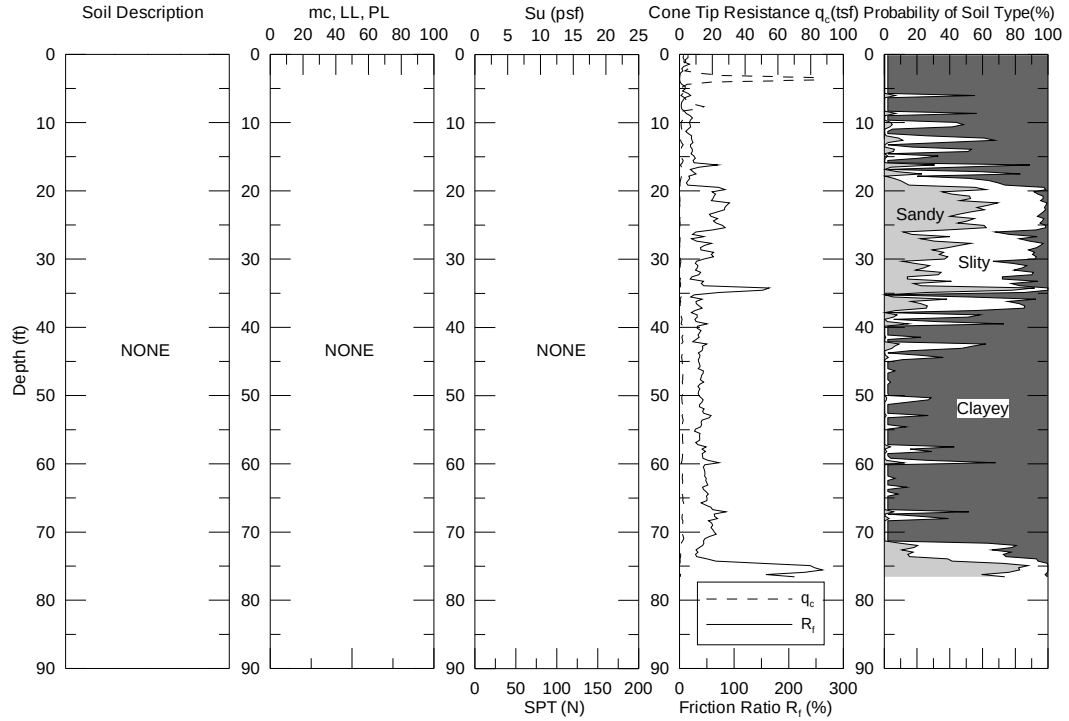


**Figure 77**
**455-05-0036 TP#2**

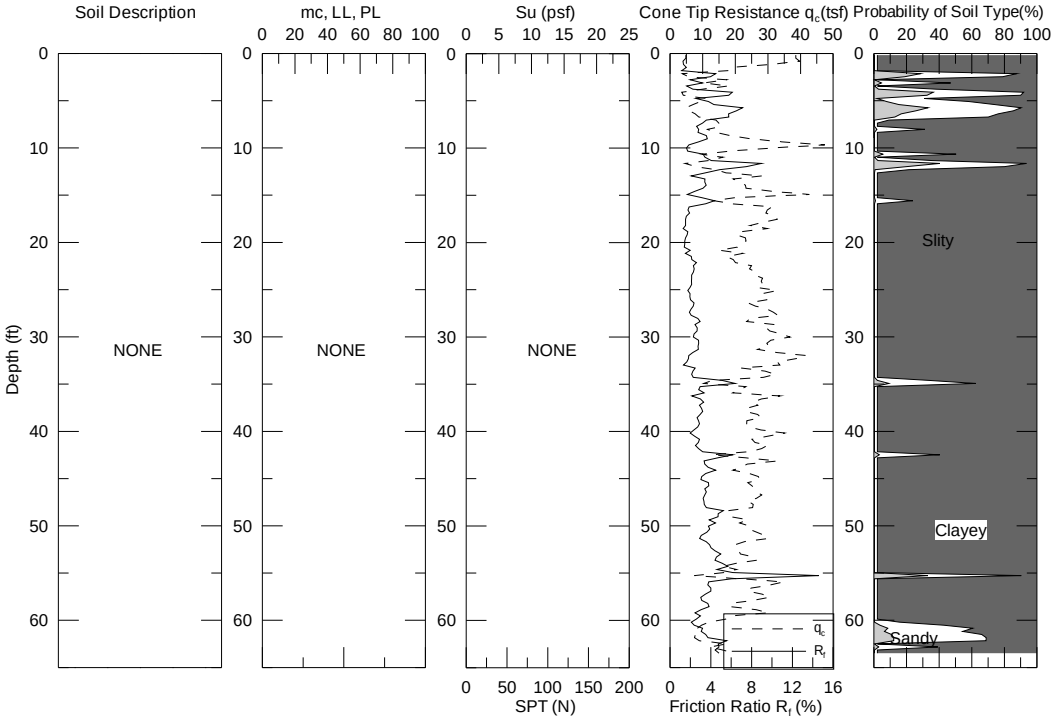


**Figure 78**
**455-05-0036 TP#3**

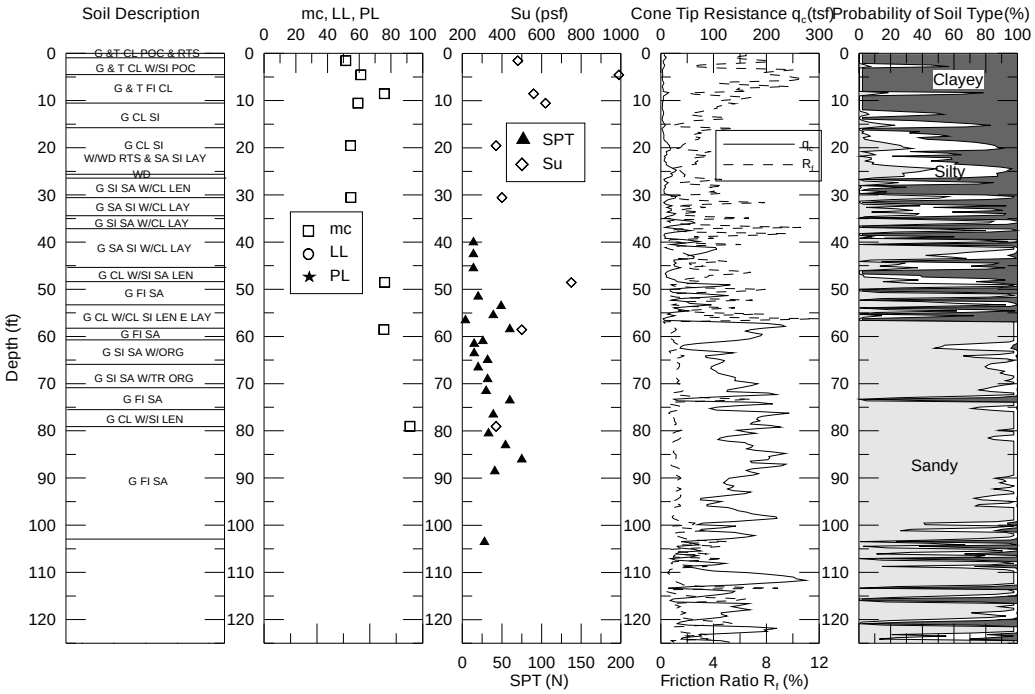


**Figure 79**
**434-01-0002 TP#3**

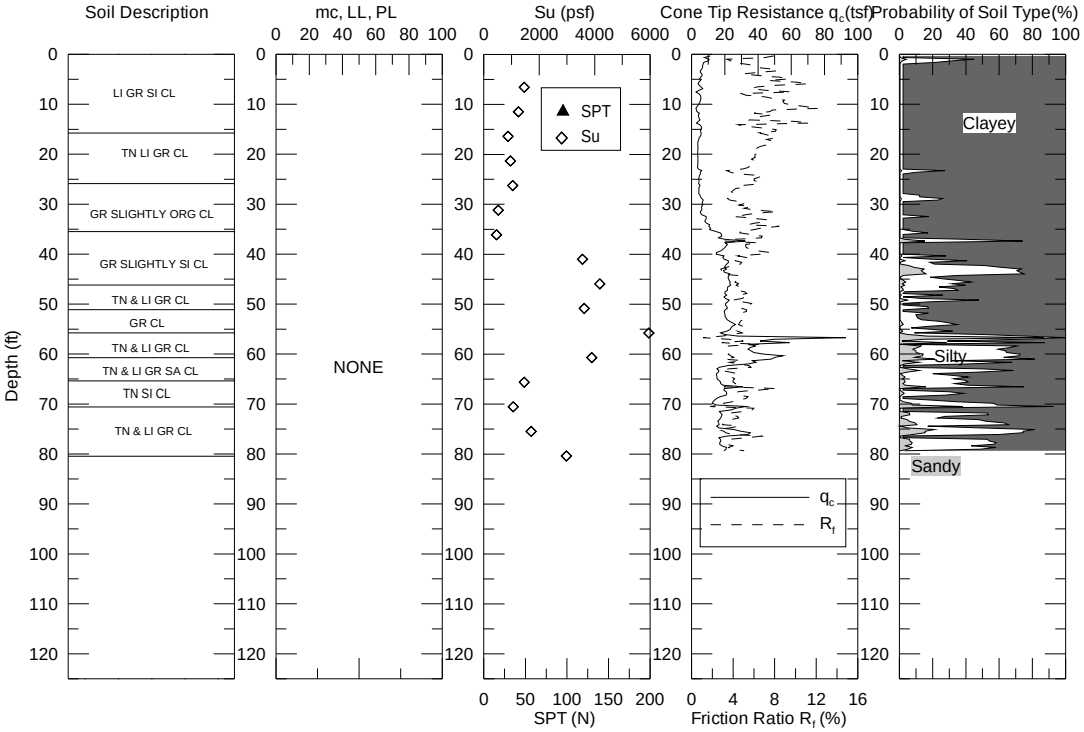


**Figure 80**
**239-01-0080 TP#3**

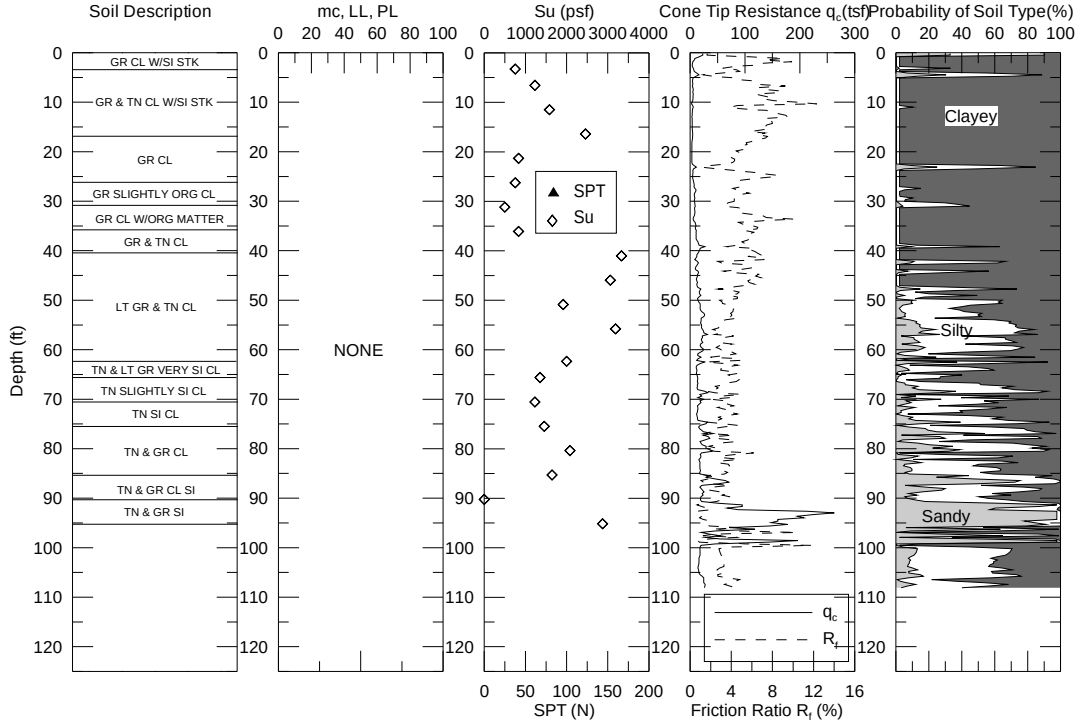


**Figure 81**
**239-01-0080 TP#4**

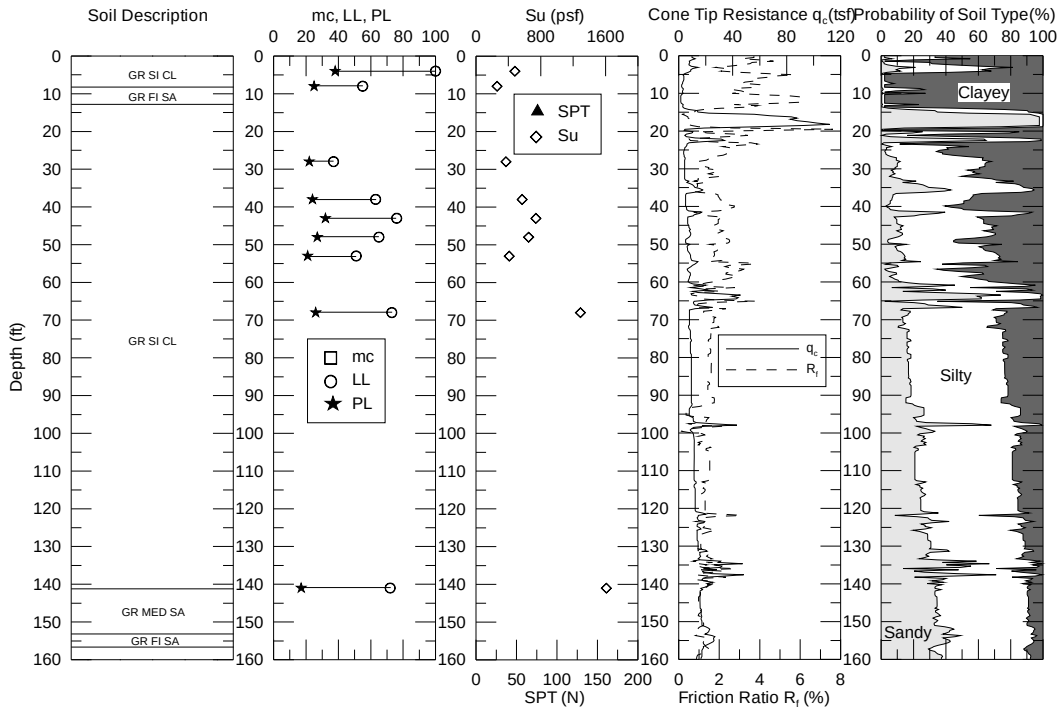


**Figure 82**
**855-14-0036 (Houma) TP#1**

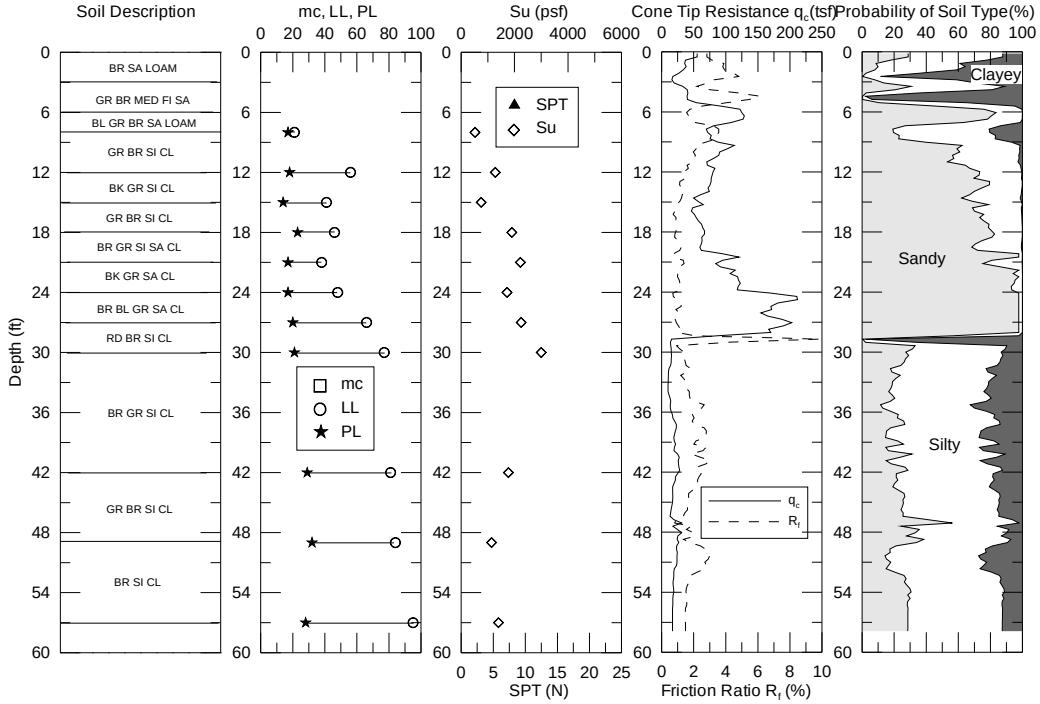


**Figure 83**
**Alexandria TP#1**

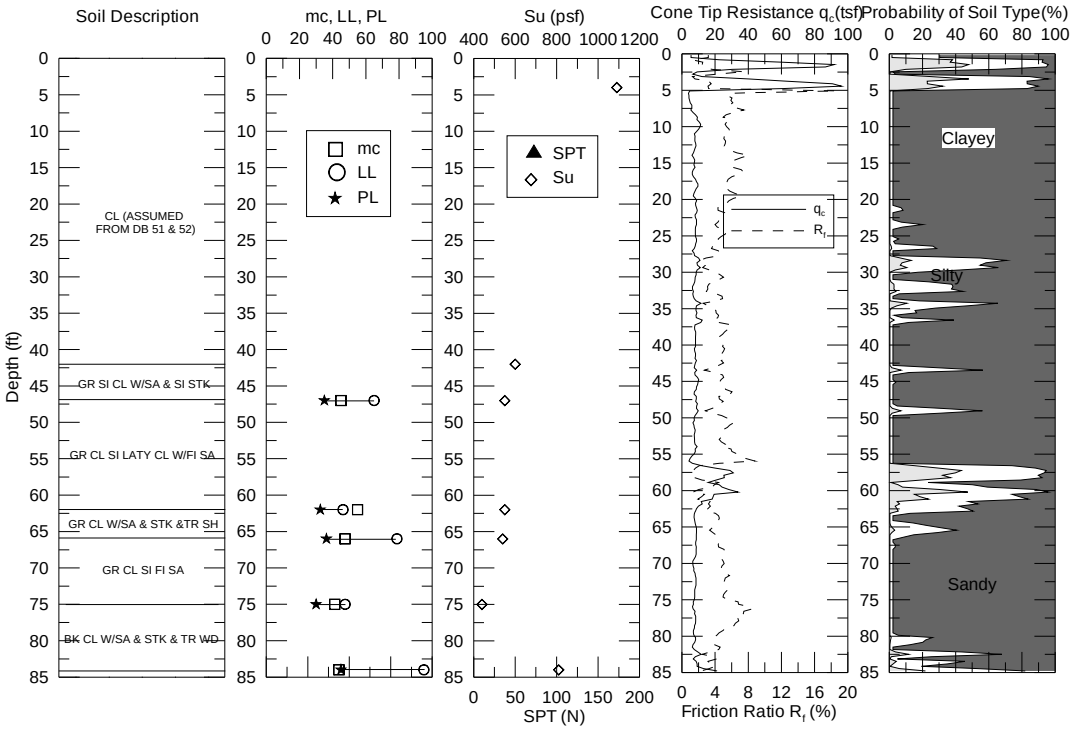


**Figure 84**
**424-06-0005 TP#4**

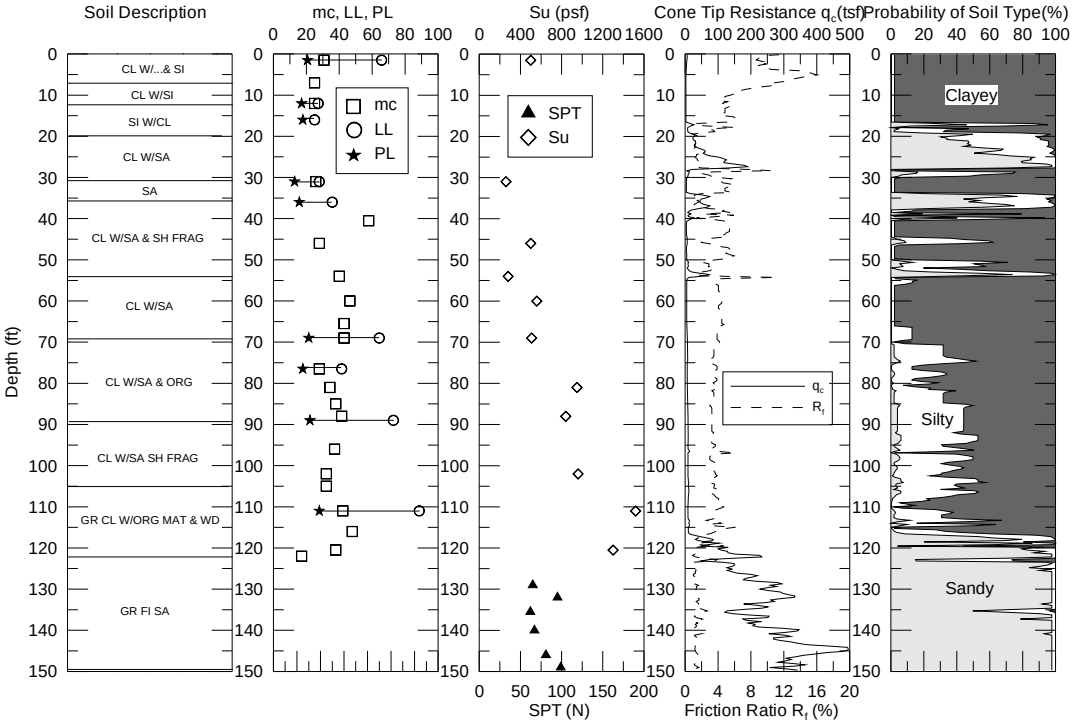


**Figure 85**
**424-07-0009 TP#4 and 4A**

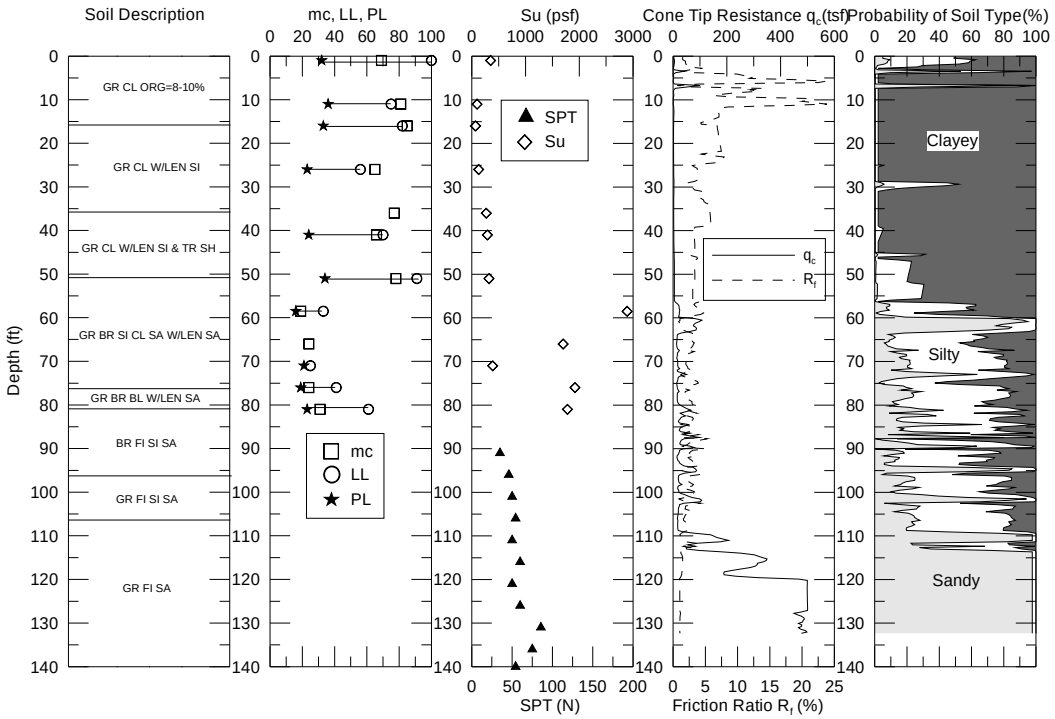


**Figure 86**
**450-36-0002 TP#8**

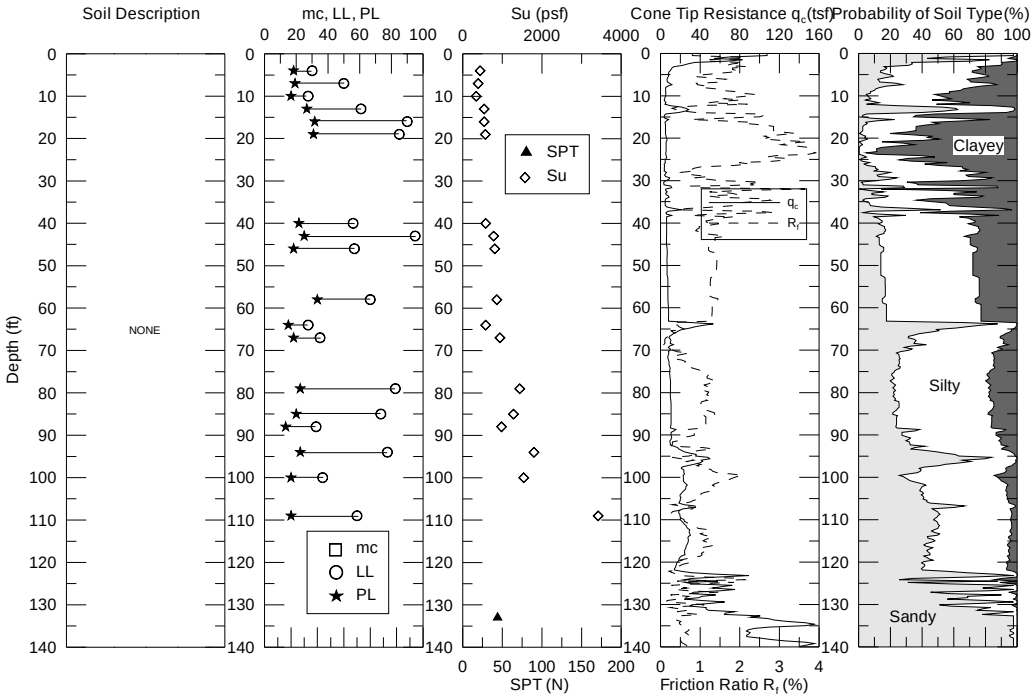


**Figure 87**
**283-03-0052 (New Orleans) TP#1**

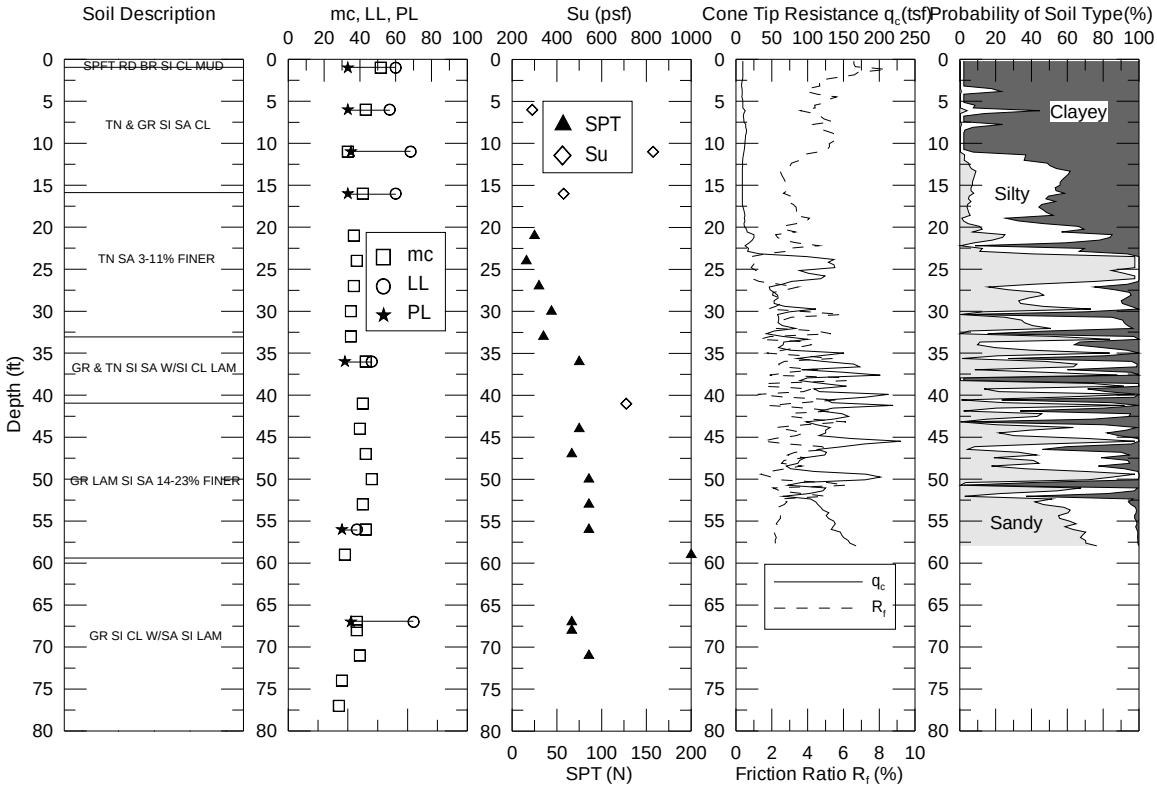


**Figure 88**
**090-01-0015 TP#6**